

Effect of increased vertical stress on the state of grains in tailings

Shane Alexander Aulestia Viscarra

Civil Engineering, master's level (120 credits)
2023

Luleå University of Technology
Department of Civil, Environmental and Natural Resources Engineering

Dedicated to my parents and my brother

Preface

This master thesis is the final part of my Master of Science in Civil Engineering, with specialization in mining and geotechnical engineering at Luleå University of Technology, LTU, funded by the Swedish Institute scholarship. The research has been performed during the spring of 2023 at the Department of Civil, Environmental and Natural Resources at LTU.

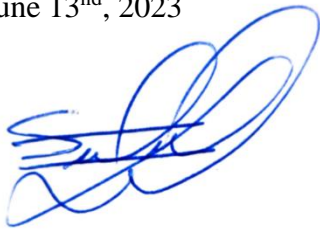
I would like to express my gratitude to my supervisor Viktor Wiklund for the useful remarks, guidance and constant support throughout the whole process. Besides, special thanks to my examiner Jan Laue for his valuable thoughts and assistance during the project. I would also like to thank everyone in Soil Mechanics research subject that belongs to the Division of Mining and Geotechnical Engineering for their advice and support making me feel part of the group since the first day I started this journey.

I would like to thank my friends and relatives back home and the amazing people I have met in Sweden, who helped me to build up my days during these study years, making my time in this Viking land, greatly charming, warming and full of experiences. Last but not least, I would like to express my love and sincere thankfulness to my family for supporting me always in this hard and long adventure away from home being my pillars at every moment to finalize my studies.

I finish a chapter of my life, although I know that it is the beginning of a new and long stig full of many challenges.

Luleå, Sweden

June 13nd, 2023



Shane Alexander Aulestia Viscarra

Abstract

Tailings storage facilities (TSFs) serve as structures for storing tailings, i.e., waste materials generated by the mining industry. In recent years, tailings dam failures and collapse of these constructions have been reduced due to the establishment of regulations to control these structures, nevertheless the consequences are catastrophic when tailings dam failures occur. There are some different construction methods for tailings dams. One common construction method is the upstream method; where the dam is raised by constructing embankments on top of the tailings stored in the impoundment. Thus, it is essential to understand the mechanical and geochemical behavior of deposited tailings to be able to perform safety assessments of tailings dams. Material properties must be assessed for the present time as well as over a longer time since aging and continuous deposition might change the mechanical behavior over time. Continuous deposition leads to continuous increased vertical stress on particles, and there is a need to study if increased vertical stress can lead to a possible change of the mechanical properties of tailings. Therefore, this study has investigated the characteristics of tailings particles after being subjected to vertical stepwise loading.

This study focuses on investigating the impact of particle breakage (or crushing) on tailings by analyzing material recovered from a tailings dam in Sweden. The research was performed on disturbed tailings material from a borehole of approximately 40 m depth. The study was conducted on four samples recovered 10 m apart, developing a characterization of the material and laboratory tests on each of them. The characterization consisted of the determination of intrinsic properties such as particle size distribution, particle shape, and mineralogy before and after testing; while the laboratory tests were conducted by means of the oedometer test. The laboratory tests employed the oedometer test, which applies a vertical load in slow increments under K0 conditions to simulate the behavior of tailings consolidated in the impoundment.

The results obtained from the oedometer tests showed interesting observations regarding changes in particle size distribution (PSD) before and after testing. Based on this study it is hard to conclude if the change in PSD solely is caused by crushing. Three samples show a PSD after oedometer which have slightly more fines than before oedometer, while the last sample has neglectable change in PSD. Theoretically, this small change in PSD indicates that larger tailings particles exhibited a higher susceptibility to some degree of crushing, but since the change is so small it cannot be excluded that the changes origins from the accuracy of determining the PSD.

The samples taken at different depths were prepared using the tamping method, and the oedometer testing indicated minimal differences in their compression characteristics, and since the soil fabric was destroyed under sampling and then reconstituted through tamping this is expected. To investigate the influence of particle arrangement on the compression and potential crushing, one of the samples was tested in a slurry configuration. This test demonstrated that particle arrangement appears to be a contributing factor to crushing, as it showed less deviation in particle size distribution compared to the tamped sample.

To contextualize and validate the findings, the results were correlated, evaluated, and compared with previous studies conducted on tailings from the same tailings storage facility (TSF). Although, future research on crushing in correlation of mineralogy respectively and changes in particle shape are needed, this comparative analysis has provided input that can contribute to enhanced understanding of tailings behavior under increased vertical load.

Keywords: Tailings, Tailings dams, Breakage, Oedometer, Image acquisition analysis

Sammanfattning

Tailings storage facilities (TSFs) fungerar som deponier för att lagra anrikningssand (*eng: tailings*) som genereras av gruvindustrin. I många fall utgör gruvdammar en central del av TSFs, och stabiliteten av gruvdammarna måste vara tillfredsställande för att förhindra dammbrott med förödande konsekvenser. Det finns olika konstruktionsmetoder för gruvdammar. En vanligt förekommande metod är den så kallade "inåt-metoden", där dammen höjs genom att bygga höjningarna ovanpå tidigare deponerad anrikningssand. Det är därför viktigt att förstå det mekaniska och geokemiska beteendet hos anrikningssanden för att kunna utföra beräkna stabiliteten och utföra riskanalyser av inåtdammar. Egenskaperna hos materialet måste bedömas både för nuvarande tidpunkt och över en längre tid eftersom åldrande och kontinuerlig deponering kan förändra det mekaniska beteendet i anrikningssanden över tid. Kontinuerlig deponering medför en kontinuerlig ökning av den vertikala spänningen på anrikningsandens korn, och det finns ett behov av att undersöka om ökad vertikal spänning kan leda till en möjlig förändring av de mekaniska egenskaperna hos anrikningssanden. Därför har denna studie undersökt de mekaniska egenskaperna hos anrikningssand efter att de har utsatts för vertikal stegvis belastning.

Denna studie fokuserar på att undersöka effekten av krossning eller partikelnedbrytning på avfall genom att analysera material som återhämtats från en TSF i Sverige. Forskningen utfördes på störd anrikningssand från en provtagning till cirka 40 meters djup. Studien genomfördes på fyra prover som återhämtades med 10 meters mellanrum och omfattade en karaktärisering av materialet samt laborietester på varje prov. Karaktäriseringen bestod av bestämning av jordegenskaper såsom partikelstorleksfördelning, partikelform och mineralogi före och efter testningen, medan laborietesterna utfördes med hjälp av ödometerförsök. Ödometerförsök tillämpar en vertikal belastning i långsamma steg under K0-förhållanden för att simulera beteendet hos deponerad anrikningssand under konsolidering i magasinet.

Resultaten från ödometerförsöken visar på intressanta observationer avseende förändringar i partikelstorleksfördelning (PSD) före och efter testning. Baserat på denna studie är det svårt att dra slutsatser om förändringen i PSD enbart orsakas av krossning. Tre prover visar en PSD efter ödometer som har något mer finhalt än före ödometer, medan det sista provet har en försumbar förändring i PSD. Teoretiskt sett indikerar denna lilla förändring i PSD att större sandkorn uppvisar en högre känslighet för någon grad av krossning, men eftersom förändringen är så liten kan det inte uteslutas att förändringarna härrör från noggrannheten vid bestämning av PSD.

Proverna som tagits på olika djup preparerades med försiktig "stampning" (*eng: tamping method*) och ödometerförsöken visade på minimala skillnader i deras kompressionsegenskaper, men eftersom kornens in-situ förhållande förstördes under provtagning och re konstituerades genom stampning är detta ett förväntat resultat. För att undersöka påverkan av sandkornens arrangemang på kompressions egenskaper och potentiell krossning testades ett av proverna även genom preparering i en slurrykonfiguration. Detta försök visade att partikelarrangemang verkar vara en bidragande faktor till krossning, eftersom det visade mindre avvikelse i partikelstorleksfördelning jämfört med det stampade provet. För att kontextualisera och validera resultaten korrelerades, utvärderades och jämfördes resultaten med tidigare studier gjorda på anrikningssand från samma

TSF. Även om framtida forskning om krossning i korrelation mellan mineralogi respektive förändringar i partikelform behövs, bidrar denna studie till underlag som förbättrar förståelsen av anrikningssandens beteende under ökad vertikal belastning.

Nyckelord: Avfall, Avfallsdammar, Brytning, Ödometer, Bildinsamling och analys

Table of contents

Preface.....	i
Abstract	ii
Sammanfattning	iv
List of Figures	viii
List of Tables	ix
Introduction.....	1
1.1 Background	1
1.1.1 Tailings dam failures.....	1
1.1.2 Tailings dams: Construction methods.....	1
1.1.3 Production and characteristics of tailings	3
1.2 Motivation of research	4
1.3 Aim and scope of work	5
1.4 Limitations	5
1.5 Research Methodology.....	6
2. Mechanical behavior of tailings – literature review	7
2.1 Particle size distribution on tailings	7
2.2 Particle shape in tailings.....	10
2.3 Mineralogy in tailings	14
2.4 Literature review conclusions	15
3. Materials and Methods	17
3.1 Site description.....	17
3.2 Tailing samples used in this study.....	17
3.3 Image acquisition and analysis.....	20
3.3.1 Light reflected imaging and SEM analysis	20
3.3.2 Dynamic image analysis	23
3.4 Laboratory tests on tailings	24
3.4.1 Oedometer test	25
4. Results	27
4.1 Initial characterization.....	27
4.1.1 Particle size distribution.....	27

4.1.2	Particle shape analysis	29
4.1.3	Mineralogy analysis	30
4.2	Dynamic Image Analysis	31
4.3	Effect of vertical stress on tailings	34
4.3.1	Oedometer testing	34
4.3.2	Stress-strain deformations.....	37
4.3.3	Void ratio	38
4.3.4	Compressibility and compression index	40
4.4	Particle breakage	41
5.	Discussion.....	48
5.1	Basic properties of tailings.....	48
5.2	Particle breakage and crushing effects	49
5.3	Particle breakage for different particle arrangement.....	50
5.4	Compressibility and stress-strain behavior	50
6.	Conclusions	52
7.	Suggested further work.....	54
8.	Bibliography	55
	Appendices.....	60
A.	Reflected light imaging analysis	60
B.	LVDTs curves for each sample	62
C.	Dynamic Image Analysis Plots	65
D.	Dynamic Image Analysis (Raw Data).....	69

List of Figures

Figure 1. Main construction methods for TSFs. Upstream (a), centre line (b) and downstream (c) construction.....	2
Figure 2. Tailing dam construction in practice for Swedish mines (Jantzer et al., 2008).....	3
Figure 3. Peripheral discharge methods (a) Spigotting, (b)Single-point discharge (Vick, 1990) ..	4
Figure 4. PSD of fine and coarse tailings (Pan et al., 2022).	8
Figure 5. Consolidation curves of tailings samples with different particles sizes (Pan et al., 2022).	9
Figure 6. PSD before and after triaxial tests at different confining stresses: (left) fine tailings particles; (right) coarse tailings particles (Pan et al., 2022).....	9
Figure 7. Particle shape describing sub-quantities (Mitchell & Soga, 2005)	10
Figure 8. Form, roundness and surface texture graphical definition (Barrett, 1980b).....	11
Figure 9. Basic measurements of particle (Yang et al., 2019), (based on Janoo, 1998).....	13
Figure 10. Location of Aitik mine (left) and the tailings dam (right).....	17
Figure 11. Samples schema from the drillhole	18
Figure 12. Slurry sampling – initial conditions (left); after 24 hours settlement (right)	19
Figure 13. Grinding and polishing process (left). Samples after grinding and polishing (right)..	21
Figure 14. Microscope with high resolution digital camera for light reflection imaging analysis	21
Figure 15. ZEISS Sigma 300 VP scanning electron microscope (SEM). Source: LTU.....	22
Figure 16. Internal chamber view for SEM analysis	22
Figure 17. Camsizer XT – equipment (Microtrac Retsch GmbH).....	23
Figure 18. Illustration of Xc min in a particle (Microtrac Retsch GmbH)	24
Figure 19. Particle Size Distribution of samples – Sieving test.....	29
Figure 20. Particle shape on tailings samples using SEM (left: S2 – right: S5)	30
Figure 21. Mineralogy analysis on tailings samples using SEM (left: S2 – right: S5).....	30
Figure 22. Particle Size Distribution of samples – Dynamic Image Analysis.....	31
Figure 23. Pictures during the dynamic image analysis (no scale).....	32
Figure 24. LVDTs curve for sample S5.....	35
Figure 25. Plotting of vertical strain ($\log \epsilon$) vs effective vertical stress ($\log \sigma'_v$) ; Samples S2, S5, S8, S11	37
Figure 26. Plotting of vertical strain ($\log \epsilon$) vs effective vertical stress ($\log \sigma'_v$) ; Samples S11, S11.1, S11.2	38
Figure 27. Plotting of void ratio (e) vs effective vertical stress ($\log \sigma'_v$) ; Samples S2, S5, S8, S11	39
Figure 28. Plotting of void ratio (e) vs effective vertical stress ($\log \sigma'_v$) ; Samples S11, S11.1, S11.2	39
Figure 29. Particle Size Distribution for samples S2, S5, S8 and S11 using D.A after oedometer testing.....	42
Figure 30. Partial retained curve material for samples S2, S5, S8 and S11 using D.A data before and after oedometer testing	45
Figure 31. Particle Size Distribution for tamped and slurry sample S11 before and after oedometer testing.....	47

Figure 32. Partial retained curve material for tamped and slurry sample S11 before and after oedometer testing	47
--	----

List of Tables

Table 1. Roundness qualitative scale (Powers, 1953).....	11
Table 2. Measurements description to determine shape descriptors (Yang et al., 2019)	12
Table 3. Description of tailings material used in this study.....	19
Table 4. Description of slurry material used in this study	20
Table 5. Effective stress conditions within the impoundment to validate oedometer test.....	26
Table 6. Particle density of samples	27
Table 7. Particle Size Distribution - Sieving	28
Table 8. Gradation curve characteristics – Sieving testing.....	28
Table 9. Comparison table for Samples S2 and S5 between sieving and dynamic image analysis	32
Table 10. Comparison table for Samples S8 and S11 between sieving and dynamic image analysis	33
Table 11. Soil classification – comparison table between sieving and D.A.	34
Table 12. Initial sample conditions – Oedometer test.....	36
Table 13. Final sample conditions – Oedometer test.....	36
Table 14. Coefficient of volume compressibility and compression index ($\sigma'_0 = 80$ kPa and $\sigma'_1 = 640$ kPa)	40
Table 15. Comparison table for Samples S2 and S5 before and after oedometer testing.....	43
Table 16. Comparison table for Samples S8 and S11 before and after oedometer testing.....	44
Table 17. Comparison table for tamped and slurry sample S11 before and after oedometer testing	46
Table 18. Particle density comparison with literature review.....	49
Table 19. Compression index according to Bhanbhro (2017) and obtained in this study	51

Introduction

1.1 Background

Mining industry is an important supply on modern life due to the wide range use of their products (e.g., computers, airplanes, ships, etc.) and the employment provided all over the world (Lyu et al., 2019). Nevertheless, the high demand and fast developing has led to an increase of mine waste. One sort of mine waste is tailings which are stored in tailings storage facilities (TSFs) (Villavicencio et al., 2014). This leftover material is commonly stored as impoundments within embankment dams in the surroundings of the mine (Jantzer, Bjelkevik, & Pousette, 2008), which are often constructed by tailings material itself.

TSFs are systems to restrain and confine the deposition of fluids in suspended matter (Witt et al., 2004) having site-specific designs. Due to this fast-growing industry dam collapses have become the dreadful outcome (Halabi et al., 2022). According to Davies et al. (2002), over the last 30 years, environmental issues on tailings dams have grown in importance, meaning both physical (safety and stability) and chemical (contaminants) matters are also a concern for countries all over the world to guaranteeing safe and stable dams in short- and long-term.

1.1.1 Tailings dam failures

Tailings dams failures results in deep socioeconomic and environmental consequences (Halabi et al., 2022) . After a dam failure occurs, the risks and effects could be devastating for downstream areas due to the high potential energy outflow released, developing a fast-moving mudflow (Stark et al., 2022). Between 1965 and 2020, tailings storage facilities (TSFs) present a failure rate close to 1.5%, based on roughly 20,230 infrastructures worldwide (Rana et al., 2022). Meanwhile, water reservoir facilities present a failure rate of 0.01% (Lyu et al., 2019). Since 2000, the failure rate of TSFs have decreased considerably compared with the 1950's, but the size and environmental impact of these constructions are greater and more severe than previous years (Stark et al., 2022).

Tailings dam failures throughout history occurred in developed countries, however, this tendency has shifted during the last century to developing countries (Islam & Murakami, 2021). The most well-known causes of failures in TSFs are slope stability, overtopping, and earthquakes (Halabi et al., 2022). Islam & Murakami (2021) determined that the actual failure rate of tailings facilities cannot be considered tolerable for either industry or society, where 3.45 dam facilities are estimated fail each year. Data on dam failures around the world are valuable for improving the ability of TSFs management, design and construction techniques to effectively decrease the likelihood of tailings dam failures.

1.1.2 Tailings dams: Construction methods

Mine tailings management must be carefully planned in order to protect both humans and environment from hazards produced due to tailings disposal (Adiansyah et al., 2015). Ritcey (2005) highlights that the design of TSFs takes into consideration many factors that will be decisive in determining the optimum storage site and discharging techniques to be used. Current environmental policies force TSFs owners to ensure the long-term stability of these structures.

Hence, retained residues must be stored over geological periods, and usually the construction and treatment process could last over decades even after the mining extraction is over (Witt et al., 2004). Therefore, appropriate selection of tailings disposal placement and techniques are crucial considerations for the mining industry (Engels, 2023) to provide reliability of the whole construction from a technical, economical, environmental, and social point of view in the short-term and also in the long-term (Adiansyah et al., 2015).

Management and construction methods have greatly changed over time. Tailings dams can be built, either to the final height at once or heightened according to the impoundment level and needs (Knutsson, 2018). The latter has traditionally been the most common. Tailings disposal is often developed considering environmental regulations and site-specific factors in the most cost-effective way possible (Engels, 2023). TSFs can be either surface impoundments or underground facilities; however, the most common way to store tailings is by using structures such as dams, embankments, and other types of surface impoundments, which remain the primary disposal method (Vick, 1990). TSFs are site-dependent, implying that their construction and management are unique and different from mine to mine, which must be analyzed carefully.

Tailings dams normally are divided into three main construction methodologies: upstream, centre line and downstream construction (Jantzer et al., 2008), as depicted in Figure 1. Initially, borrowed material is needed for the starter embankment since tailings are not produced at early mining stage (Jantzer et al., 2008). Once mining production starts, tailings are normally discharged as a slurry from the dam's crest and left for sedimentation along the impoundments crest; therefore, when the impoundment is nearly full of material, a second embankment is built over increasing the height of the dam (Vick, 1990).

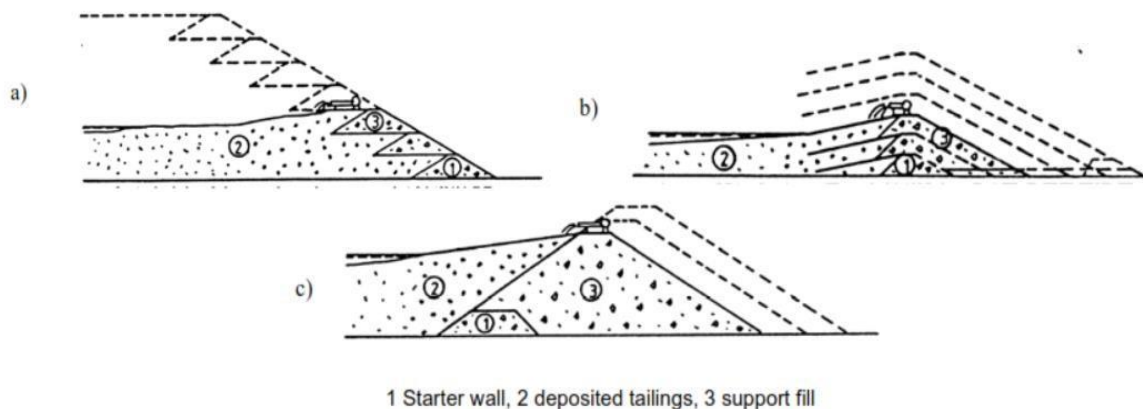


Figure 1. Main construction methods for TSFs. Upstream (a), centre line (b) and downstream (c) construction. (Jantzer et al., 2008)

Upstream methodology has been a trend among industries, with rising embankments over settled and consolidated deposited tailings material. The upstream construction method of tailings dams has been frequently used (Jantzer et al., 2008) due to economical construction processes. This method raises the dam by stepping embankments placed over stored tailings material, implying that the tailings impoundment will eventually become the dam's body and foundation for future

embankments (Bjelkevik & Knutsson, 2005). The understanding of the mechanical behavior for this construction method has become crucial over time due to its high applicability over the world to ensure long-term safety (Vick, 1990).

Nevertheless, construction methodologies for Swedish TSFs have changed over the years in several ways to promise the long-term safety of these prone failure structures. As a result, tailings dam assembly does not follow one construction principle but often becomes a mixture of different construction practices and special adjustments (Jantzer et al., 2008), as shown is Figure 2. Each construction methodology has its pros and cons, and they depend on the planned scope for the mine.

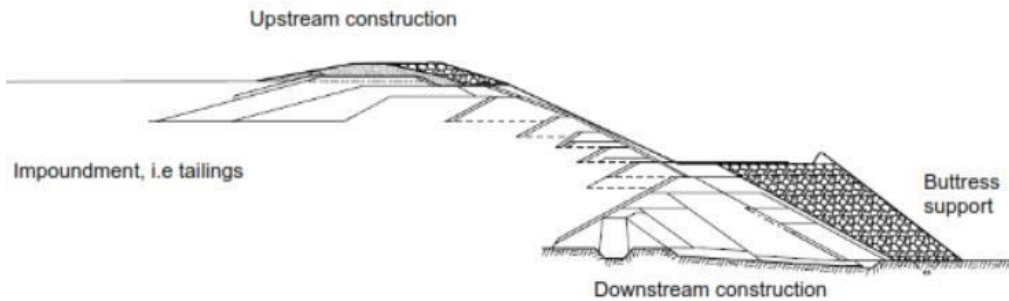


Figure 2. Tailings dam construction in practice for Swedish mines (Jantzer et al., 2008)

Intuitively, for upstream and centerline tailings dams it is crucial to have a great understanding of the mechanical behavior of the tailings in question, and also its performance over time, due to the effects generated on the mechanical properties subjected to different overloads (Bhanbhro, 2017). The design of tailings dams requires not only an assessment of current mechanical and chemical properties of the material but it is also essential to assess the long time perspective behavior of tailings, guaranteeing short- and long-term dam stability (Rodriguez, 2016).

1.1.3 Production and characteristics of tailings

Production of tailings

Tailings are produced after several steps and may differ depending on the mineral value to be extracted. Nevertheless, some essential steps are common for the mineral extraction such as crushing, grinding, concentration, leaching, heating and dewatering (Vick, 1990). Tailings are one of the results of the waste generated due to mining process, with no financial gain (at that particular time) and produced in large quantities. Tailings produced after the crushing, grinding and mineral separation processes can make up roughly 70-99% of the ore production (Bhanbhro, 2017).

Tailings are conventionally transported in slurry form and deposited into TSFs by developing a tailings beach around the dam (Vick, 1990). Slurry tailings are transported as reasonable homogeneous material; nevertheless, this state drops when it is deposited in the impoundment; this is because coarser particles settle more rapidly near the discharging point than finer particles (Blight & Bentel, 1983). Tailings deposition can take place either via spigotting or single-point discharge (Hamade, 2013), as depicted in Figure 3.

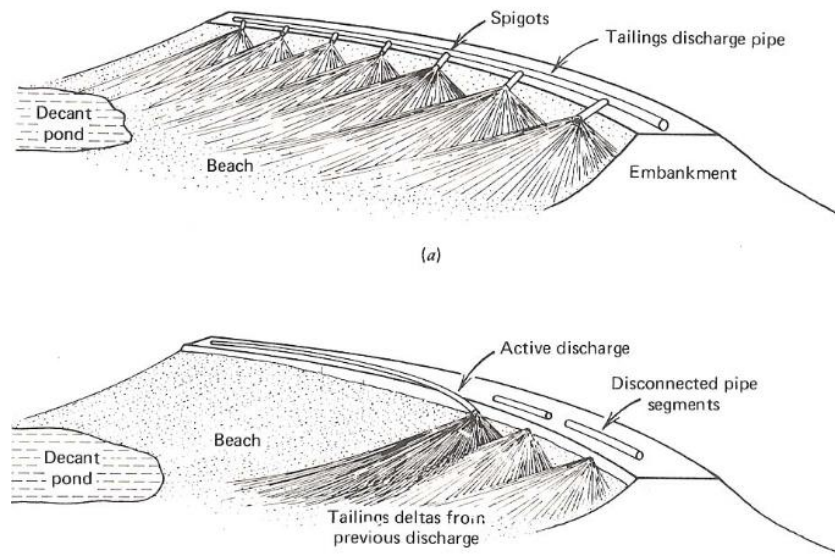


Figure 3. Peripheral discharge methods (a) Spigotting, (b) Single-point discharge (Vick, 1990)

Characteristics of tailings

Tailings geotechnical and geochemical characterization are important for the adequate design and management of TSFs (Knutsson, 2018). Tailings' size range usually varies from sand to silt with an angular-shaped tendency (Rodriguez, 2016) with common particle size varying from 0,01 mm to 1,0 mm, but clay particles can be noticed up to 20%, i.e., 0,002 mm (Jantzer et al., 2008). Due to the angular tailings particles might exhibit different mechanical behavior than natural soils, and since different mines have different production tailings could behave differently from mine to mine (Knutsson, 2018). A study carried out by Bjelkevik & Knutsson (2005) defined the void ratio range for Swedish tailings (within tested samples) between 0.6-1.24. The production process for tailings is different even in the same production plant, which makes its mechanical behavior assessment complex.

1.2 Motivation of research

Tailings dams need to be stable and safe in present time as well as in the long term. For upstream tailings dams, there are many challenges connected to determining and characterizing the mechanical behavior of deposited tailings. There can be several and variable methods used during the mineral separation process, depending on the ore type to be extracted, current available knowledge and technology. Small changes in tailings procedure may alter the characteristics of the tailings, thereby affecting the structure of constructed dams.

The constant deposition of new layers of tailings within the impoundment leads to an increment of stress conditions (Jantzer et al., 2008). Consequently, the conditions in deeper layers change over time due to the increasing overburden stress. Thus, there could be a potential change among some of the intrinsic properties of the material related to long-term behavior, such as particle size distribution (PSD) and particle shape, as they adapt to new state properties (stress state and void ratio). Potentially crushing, particle breakage or degradation can occur which change these

properties. The magnitude of change is in both cases strongly dependent of the mineralogy composition of the tailings.

It is crucial to independently study the intrinsic properties in order to analyze their influence on the mechanical behavior of the tailings (Zhang et al., 2020). Since, the macroscale behavior of soils is a reflection of particle-level features and processes (microscale), i.e., the soil mass behavior results from particle level interactions which are affected by the mechanical properties of the material (Cho et al., 2007) due to increased stress conditions leading to creep-deformations.

Tailings consist of a variety of minerals and is always site specific. These minerals may affect tailings from a mechanical and chemical point of view. Different minerals will result in different tailings mechanical behavior over time, provoking a susceptibility in particles to crushing or weathering effects.

Crushing effects on soils will depend on the mechanical properties: PSD, particle shapes and mineralogy; as well as the soil state properties: stresses, void ratio/density (how particles are packed together)); loading conditions (e.g. shear strains or pure vertical consolidation); and soil fabric (arrangement of particles, micro and macro, including aging effects such as cementation and bonding). It is natural to consider that crushing and particle breakage can occur from shearing, but it is more unclear how pure vertical loading over time effects the particle breakage. There are a couple of factors that must be assessed to comprehend the change in the mechanical and chemical behavior of tailings to guarantee the stability of the structure and its possible influence over time due to increased stress and aging to assure a long-term stability.

Bhanbhro (2017) looked at the crushing for uniform sized tailings material (i.e. tailings sorted out in groups within a particle size range of 0.063 – 0.125 mm, 0.125 – 0.25 mm, 0.25 – 0.5 mm, 0.5 – 1 mm) exposed to stepwise increased vertical stress from oedometer tests making a comparison of the strength parameters, particle shape and breakage analysis. However, there is a need to study the crushing effects for a complete tailings' gradation, since this is the true case in the impoundment and behavior is expected to be different when small grains confine larger grains.

1.3 Aim and scope of work

The aim with this thesis is to characterize and study variances on deposited tailings from different depths (i.e., with different age) and investigate the crushing effects on tailings that arises from increased vertical stress (i.e., from slow and stepwise increased overload due to continued deposition). Based on the main objective, a couple of questions can thus be summarized for this research:

1. How can crushing effects due to increased vertical stress over time be analyzed and isolated from other influencing sources on the characteristics of tailings?
2. How does the stepwise increase in vertical load affect tailing particles?
3. How does particle arrangement influence the effect of vertical load on tailings particles?

1.4 Limitations

It is important to note the study does not take into consideration environmental factors (i.e., frozen tailing layers) or geochemical reactions (e.g. causing degradation, aging or cementation of

particles). Nevertheless, this investigation will provide insight into how mechanical properties are affected due to increased vertical stress.

1.5 Research Methodology

This study has been developed on tailings material at different depths of a tailings dam. The assessing materials have been collected from a borehole with a depth of 38.8m from the Aitik tailings dam in north Sweden. The performance of this study will be determined by analyzing the intrinsic properties of tailings (PSD, particle shape, and mineralogy) and subjecting them to stepwise vertical loading to different state properties (stress state and void ratio). The study was designed to characterize the samples at different depths and understand the breakage generated in the samples.

To develop and accomplish the outcomes of the research, below methodology has been adopted:

- Literature review to comprehend basic fundamentals on tailings and their mechanical properties (PSD, particle shape, and mineralogy).
- Tailings material is recovered from Aitik Dam and consists of samples from different depths (varying from 4 to 34 meters) e.g., particle density, PSD. The sample analyses have an estimated separation length of 10 meters between them.
- Tailings intrinsic parameters were determined at each depth i.e., PSD, particle shape, mineralogy.
- Disturbed samples are subjected to pure uniaxial consolidation test through oedometer testing to compare compression characteristics and potential crushing effect.
- A new characterization took place to determine possible crushing effects on intrinsic properties of the sample, mainly PSD.
- Comparison and findings between experimental data results and a literature review.

2. Mechanical behavior of tailings – literature review

Granular materials' mechanical behavior is essentially influenced by their structure and the applied effective stresses (Vick, 1990). Particle arrangement, density, and anisotropy all affect soil structure. The soil fabric is made up of the sizes, distributions, and shapes of the particles as well as the placement of the particles and their interactions (Mitchell & Soga, 2005).

Tailings are deposited heterogeneously in the impoundment, whereas physical and chemical characteristics vary greatly (Nikonow et al., 2019). There are a couple of factors that influence the mechanical behavior of tailings, which include tailings particle size, bulk density (or void ratio), flow rate, ore drawing method, water level in the reservoir and atmospheric precipitation (Pan et al., 2022). PSD, particle shape and mineralogy of tailings are fundamental parameters to measure, due to their great influence on tailings mechanical behavior.

2.1 Particle size distribution on tailings

Tailings are the result of crushed rock with particle sizes between silt and sand. The particles range from 0.002 mm, in the case of silt particles, and between 0.01 mm and 1.0 mm, in the case of sandy particles (Jantzer et al., 2008). Tailings composition is very complex due to different substances that may show corrosive, volatile, and acidic hazards that can be harmful to people and the environment in combination with water and air (Zhen et al., 2022).

Geotechnical properties of tailings are necessary to design and construct tailings dams, particularly for the construction type where deposited tailings become a part of the structural zone. Results demonstrated by Bhanbhro (2014) showed that deposited tailings in several Swedish mines have a dry density from 1.18 t/m³ up to 1.65 t/m³, a bulk density between 1.66 t/m³ and 2.12 t/m³, a particle density of 2.83 t/m³, and void ratio from 0.71 to 1. During experimental testing, Bhanbhro (2017) indicated that fine content of tailings material increases greatly from the upper layers while the depth increases. In the study, the author explains that this phenomenon could probably be experienced in TSFs due to the effect of distance from the discharge point.

The consolidation reached by a material will depend on factors such as bulk density, which is related to void spacing. Bulk density is a measure of how dense a specific soil is, i.e., the total mass of the element over the total volume. Void ratio is also a measure of how dense a certain soil is, but it measures the pore volume in relation to volume of solids (not in relation to the weight of the particles). By this, it is worth mentioning that consolidation is affected by the PSD since the void ratio under high stresses of fine tailings is smaller than those of coarse tailings (Pan et al., 2022). Pan et al. (2022) looked at coarse and fine tailings with same specific gravity and same void ratio and stated that when soil is subjected to high stresses, the particles tend to get broken and only the pores are compressed. Tailings generally have high water content and porosity, low to moderate hydraulic conductivity and low plasticity when compared to soil (Jantzer et al., 2008).

Particle crushing is a phenomenon where particle failure occurs when subjected stresses are higher than the particle strength (Lade et al., 1996a), and particles break into two or more pieces under an external load. Particle crushing according to Lv et al. (2020), is affected by the mineral composition, particle gradation, particle size, particle roughness, relative density, and stress

conditions. The PSD could be affected by the crushing effect along the depth due to the compressibility they experience by increasing the breakage into different-sized particle. In addition, Russell (2011) asserts that the compressibility on coarse tailings is higher due to severe particle crushing under high confining stress, whereas fine tailings need to store more strain energy in crushed particles.

A study performed on tailings by Pan et al. (2022) demonstrated the influence of the particle size on the mechanical properties of tailings material under high stress. The material used for the investigation had a specific weight of 2.8 t/m^3 with dry density of 1.7 t/m^3 , parameters that are rather similar to tailings described by Bhanbhro (2014). The study performed oedometer tests and triaxial tests for particles with a particle size greater than 0.063 mm , splitting the sample in two groups: fine and coarse particles. Figure 4 shows the PSD curves determined for each sample.

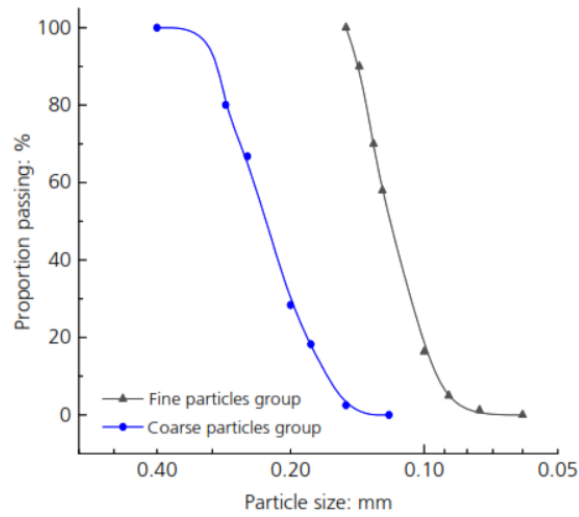


Figure 4. PSD of fine and coarse tailings (Pan et al., 2022).

A one-dimensional compression test was performed for in each tailings group (fine and coarse particles sizes). Figure 5 plots the consolidation curves derived from the analyzed data. Pan et al. (2022) mention that the void ratio decreases slowly initially; however, it decreases rapidly for both samples when stresses are increased. Thus, the soil compression indexes obtained were 0.19 and 0.24 for fine and coarse particles, respectively. This could be mainly due to the void space being filled with fine particles which confirms the state described by Li & Coop (2019), since more severe crushing effects are developed in coarser particles when they are confined under high confining stresses (Russell, 2011).

According to Lade et al., (1996b) a large number of experimental studies involving geotechnical materials subjected to high stresses show considerable particle crushing. This state is once again confirmed through the investigation developed by Pan et al. (2022), where triaxial tests on both group of tailings, fine and coarse particles, were subjected to different stresses. Thus, analyzing the crushing effects on the samples before and after they were loaded and demonstrating that the particle crushing phenomenon will ineluctably bring changes in the PSD where the more severe crushing effect was developed under a high stress for both samples, see Figure 6.

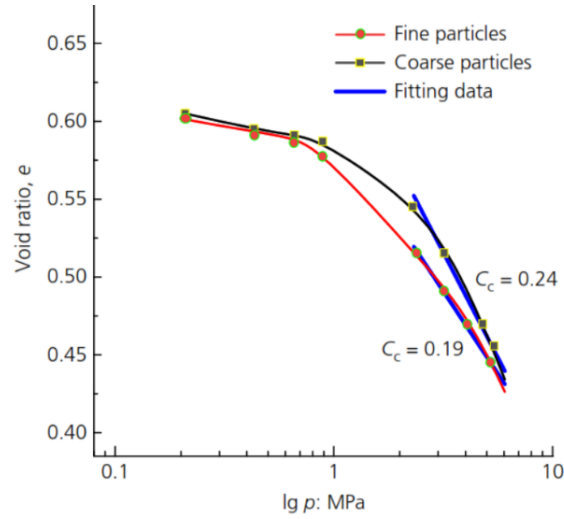


Figure 5. Consolidation curves of tailings samples with different particles sizes (Pan et al., 2022).

Assessing the results of Figure 6, it can be mentioned that coarse tailings PSD curves are more dispersed than fine tailings PSD curves at low stress. The PSD curves show that the breakage in coarse particle tailings increased at a higher rate with increasing confining stress. Nevertheless, the PSD curves will get closer to each other under high stress, meaning the crushing ratio reduces significantly tending to be smoother with increasing confining stress. At the same time the PSD curves do not experience further change under extremely high stress.

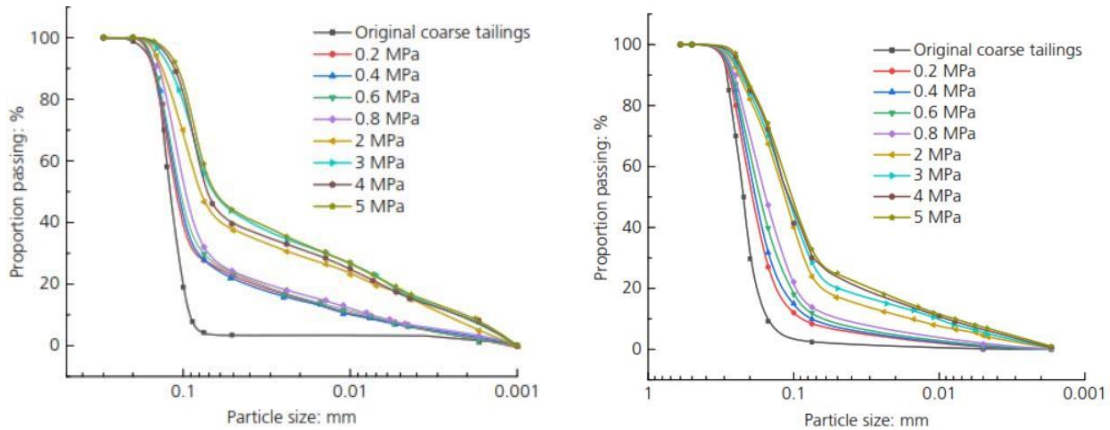


Figure 6. PSD before and after triaxial tests at different confining stresses: (left) fine tailings particles; (right) coarse tailings particles (Pan et al., 2022).

Based on this analysis it can be mentioned that while the particle size increases, the crushing effect also increases. This phenomenon might be due to the fact that bigger or larger particles have a higher probability of failure since more flaws or defects are contained in the structure of the particle. This hypothesis confirms what Lade et al. (Lade et al., 1996a) stated about the particle crushing effects for granular materials. At the same time, the smaller the particle becomes, fewer defects are contained, making fracturing effect less likely.

2.2 Particle shape in tailings

The mechanical behavior of soils is greatly influenced by the particle shape, which is an inherent soil characteristic (Mitchell & Soga, 2005). Therefore, particle shape has a great influence in tailings behavior, although, the contribution of the particle shape on mechanical behavior is not easy to distinguish since can be confused with mineralogy composition (Zhang et al., 2020). Investigations have been carried out to describe and compare the shape of sands and tailings, such as by Altuhafi et al. (2013), Yang et al. (2019); however, their results are aligned on what Zhang et al. (2020) reached out to lately, where the precise effects of particle shape on mechanical behavior remain unknown.

Particle shape could be defined as “the envelope formed by all the points on the surface of the particle” (ISO 9276-6, 2008). The packing ability of granular soils depends not only on the PSD but also on the particle shape (Altuhafi et al., 2016). To properly describe the particle shape, there are a couple terms, quantities and definitions that may vary depending on the scale of consideration (Rodriguez, 2012). The scale term analysis will vary from morphology, roundness and surface texture for large, intermediate, and small scales, respectively, based on Mitchell & Soga (2005); see Figure 7.

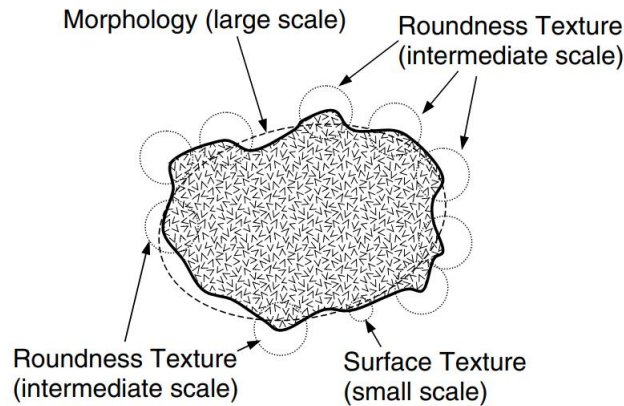


Figure 7. Particle shape describing sub-quantities (Mitchell & Soga, 2005)

The scale dependence will determine the quantity shape descriptor. According to Mitchell & Soga (2005), at large scale particle analyses, diameters in different directions are considered and its shape descriptor will be sphericity (antonym: elongation); at intermediate scale, the description will be based on the presence of irregularities (corners and edges are identified) where its quantity is named roundness (antonym: angularity); at small scale irregularities analysis is applied on an even smaller scale permitting the identification of the surface texture, which can be quantified as roughness (antonym: smoothness).

The scale shape descriptors can be confusing if the relationship within them is not clear. Several authors as Barret (1980a), Bowman et al. (2001), and Rodriguez (2012), have collected information to describe shape descriptors, but until today, there has not been a universal language established to use shape descriptors and avoid misinterpretations.

Sphericity is directly related to the “form” of the particle, meaning an evaluation of the overall configuration of the particle; roundness is related to the angularity or sharpness of the perimeter and surface texture is a property to assess the particle surface between corners. Figure 8 sums up what was mentioned previously.

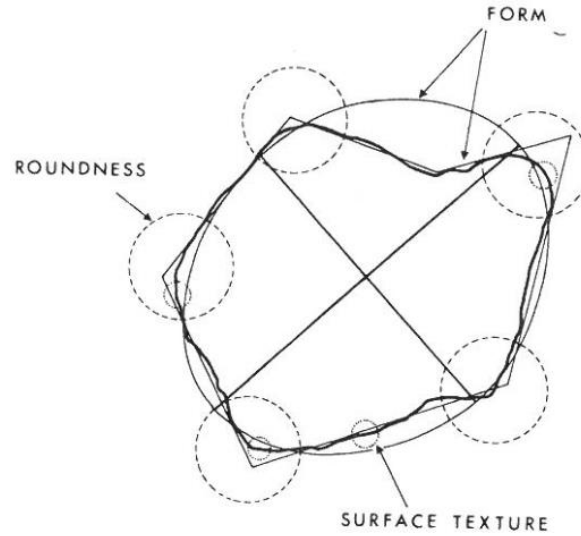


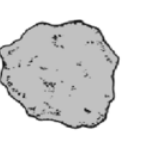











Figure 8. Form, roundness and surface texture graphical definition (Barrett, 1980b)

A graphic scale to measure qualitatively the roundness of a particle was developed by Powers (Powers, 1953), see Table 1. Folk (1955) provided a study in which the risk of errors is low for sphericity yet substantial for roundness when using a chart for categorization. To conclude, it can be emphasized that any comparison chart used to explain the characteristics of particles is highly subjective (Rodriguez, 2012).

Table 1. Roundness qualitative scale (Powers, 1953)

High Sphericity						
Low sphericity						
	Very Angular	Angular	Subangular	Subrounded	Rounded	Well Rounded

It is particular that tailings can be denominated as crushed soil, however, it is certainly different from a natural soil. There are certain features (shape descriptors) that enables tailings particle shape

to be assessed. There are several shape descriptors to describe particles shape related to large, intermediate, and small-scale dependence. An emphasis into four parameters will be emphasized within this report regarding the scale dependence. These parameters are described as: elongation (ant: sphericity), roundness, convexity and roughness, correspondingly to each scale dependence. Yang et al. (2019) determined each parameter, previously described, through Eq. (1)-(4). In the same study, the authors state that elongation reflects the elongation properties, which evaluate the overall shape particles; the degree of similarity between the perimeter of circle with the same area as the particle outline and the particle perimeter is determined by roundness; while convexity and roughness indicate the angularity and the fluctuation of projected outline of particles, respectively. Figure 9 illustrates a scheme for determining the basic measurements.

$$\text{Elongation: } e = F_{max}/F_{min} \quad (1)$$

$$\text{Roundness: } R = \sqrt{4\pi S_1}/P_1 \quad (2)$$

$$\text{Convexity: } C = S_1/S_2 \quad (3)$$

$$\text{Roughness: } r = (S_1/S_2)^2 \quad (4)$$

Table 2. Measurements description to determine shape descriptors (Yang et al., 2019)

Magnitude	Method of measurement
Particle area, S_1	Area of the particle outline
Particle perimeter, P_1	Perimeter of the particle outline
Maximum Feret diameters, F_{max}	Maximum distance between two tangents on opposite sides of the particle
Minimum Feret diameters, F_{min}	Minimum distance between two tangents on opposite sides of the particle
Convex hull area, S_2	Area of the convex hull
Convex hull perimeter, P_2	Perimeter of the convex hull
Equivalent diameter, d	Diameter of a circle with an area equal to that of the particle outline

As mentioned previously, particle shape could be considered as important as the particle size to describe the characteristics of particles, as long as granular materials are considered (Ulusoy et al., 2003). Consequently, the physical and mechanical properties could be affected by the particle shape mentioned by Yang et al. (2019), implying that it is fundamental to determine the effect of particle shape.

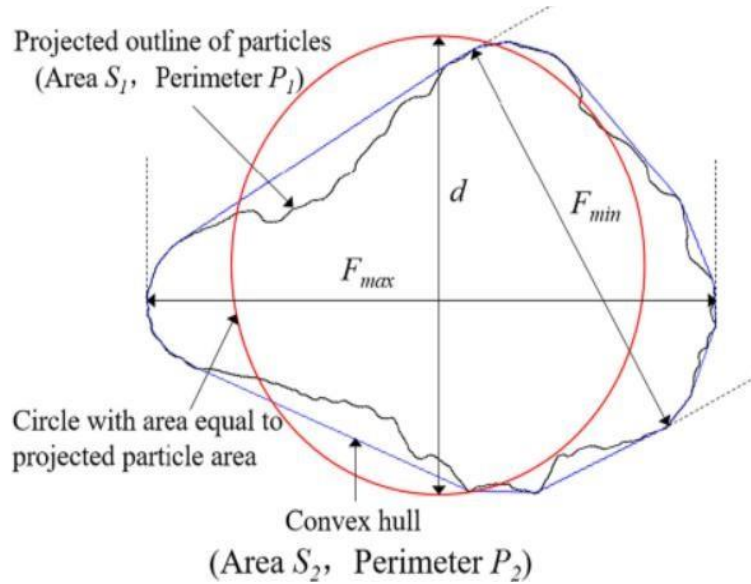


Figure 9. Basic measurements of particle (Yang et al., 2019), (based on Janoo, 1998)

Yang et al. (2019) carried out an investigation to analyze tailings using digital image processing. It showed that particle shape descriptors within tailings have great relationship with particle size. The decrease in particle size leads to an increase in the elongation of tailings, and thus the formation of columnar or needle-like particles. Tailings roundness also increases and produces more circular particle shapes. On the other hand, both the convexity and roughness of tailings grow with larger particle size. Analyzing and detailing the results obtained by Yang et al. (2019) more in depth and connecting them to the scale dependency, it can be stated:

1. From a large-scale dependence (morphology):
 - Elongation of tailings decreases with increasing particle size, which means that the shape of tailings tends to become needle-like or columnar with decreasing particle size.
2. From an intermediate-scale dependence (roundness texture):
 - Roundness could be defined as the ratio of the surface area of a sphere to the surface area of the particle, quantifying the degree of similarity between a particle and a sphere. The results show that tailings roundness decreases with increasing particle size, which means that tailings tend to form round shapes with decreasing particle size.
3. From a small-scale dependence (surface texture):
 - Convexity is the ratio between the particle area and the area of the convex hull. The convexity of tailings increases with the increment of particle size, which indicates that the angularity of tailings decreases with the increment of particle size.
 - Roughness is obtained through the difference between the particle perimeter and the perimeter of the convex hull used to characterize the fluctuation of the projected particle contour. The roughness of tailings increases with increasing particle size.

Based on what has been mentioned the particle shape certainly could influence the soil's behavior. Soil classification systems do not take shape factors into account, and it has been shown how much

they do differ between them; therefore, its true role within the soil structure remains ambiguous (Cho et al., 2007). A better understanding on shape descriptors and their influence could help determine more accurate soil mechanical behavior.

2.3 Mineralogy in tailings

Tailings have a variety of minerals that are not extracted after the grinding process since they are not economically profitable, such as mica, quartz, feldspar, plagioclase, etc., as in the Aitik tailings dam reported by Lindvall (2005) and Rodriguez (2016). Nevertheless, the analysis of residual minerals in tailings will always be mine site-specific since different types of ores are mined at different mine sites (Zhang et al., 2022). Thus, mineralogy of tailings should be considered an important parameter to be assessed; nevertheless, it is not thought as a primary consideration in the literature (Perumal et al., 2020).

For geotechnical purposes, there is a huge field that has to be investigated regarding the effects of mineralogy in soils due to the great influence on particle sizes, shapes, and surface properties. Moreover, minerals within soil particles control the interaction with fluids. By saying this, Mitchel & Soga (2005) highlight the importance of understanding mineralogy due to the close relationship and influence of soil particle mechanical behavior on its plasticity, swelling, compression, strength, and fluid conductivity.

The mineralogy effects in soils are a vast area that must be studied for geotechnical purposes. There are couple of studies such as developed by Zhen et al. (2022), Song & Hong (2020) and, Ni & Huang (2020) where they demonstrated the sensitivity and influence of minerals within samples on the mechanical properties of soils, highlighting the importance of the assessment for mineral composition. Moreover, many TSFs have unrecovered precious and rare metals in them, which can be a valuable resource for secondary exploitation and use (Zhang et al., 2022).

A study carried out by Zhang et al. (2020) measured separately mica and feldspar by single particle crushing tests using the unconfined compression apparatus in a completely decomposed granite (CDG). The study measured the strength of mica and feldspar under same conditions and with the same particle size. It was found that mica with a small particle size (0.6 – 1.18 mm) has a strength particle of 94.8 MPa, which is more than 2.5 times feldspar strength resistance which is 38.1 MPa. On the other hand, when the particle size is bigger (1.18 – 2.00 mm) both feldspar and mica strength reduce significantly, however, the feldspar strength resistance (16.8 MPa) is 4.5 times lower than mica's resistance (79.5 MPa). Nevertheless, the authors state that besides mineralogy, particle shape and texture are also factors that seem to have an effect on the particle strength and particle breakage among tested samples. In addition, it is stated that there could be a possibility that the mineral composition plays a minor role in particle strength and particle breakage.

Analyzing the data obtained by Zhang et al. (2020), it can be observed that particle strength is inversely proportional to particle size. By this, it implies that the particle strength decreases as the particle size increases and a possible reason could be due to the structure of the mineral directly influencing the mineral strength. Meaning that larger particles (larger minerals) have more faults and microcracks and therefore are weaker than smaller intact particles. Nevertheless, further

research needs to be done in this area to determine how minerals affect tailings mechanical behavior and make them more susceptible to crushing effects.

The effects of minerals within tailings remains vague, and research within tailings is limited. It is difficult to determine and distinguish direct effects of mineralogy and they can be confused with other mechanical properties. Moreover, it is also essential to be knowledgeable about the risks that could result from reworking old TSFs (Ljungberg & Öhlander, 2001). Therefore, since mineralogy is one of the intrinsic parameters of tailings, it becomes crucial to have a better insight into them.

2.4 Literature review conclusions

Based on the literature review and investigations shown previously, a couple of conclusions can be drawn regarding the intrinsic properties of tailings (PSD, particle shape and mineralogy) that may be affected and influence changes in mechanical behavior due to crushing of the tailings. It should be emphasized that these conclusions are based on the specific tailings found in this literature review, other conclusions can be expected if moving to tailings with origin that differs from those.

Particle Size Distribution

- Tailings with coarser particles are more susceptible for crushing under high stresses since they can be more easily compressed than finer particles. This could be due to flaws or defects contained in the structure of the particle.
- Coarser tailings particles will suffer more crushing effects under low confining stresses than fine tailings particles. Meaning that the deviation for coarser tailings particles from its original PSD, after being subjected to low confining stresses, will be greater than the deviation experienced with fine tailings material. Implying that more fine material is produced in coarser tailings particles. Nevertheless, under high confining stresses (once particles have crushed enough) the influence of crushing gets gentler for both fine and coarse tailings particles. As a result, a marginal deviation when analyzing the PSD for higher stresses is obtained. Therefore, less fines are produced in both cases with increasing stresses. This behavior can be attributed to a more severe packing effect between coarser particles.

Particle Shape

- To analyze the particle shape and its influence on the mechanical properties, different scale evaluations must be performed. A large-scale dependence analysis will be done assessing the elongation (ant: sphericity); while an intermediate scale analysis is done through roundness (ant: angularity) assessment; and roughness and convexity evaluation will be used for a small-scale dependence analysis.
- The decrease in tailing particle size increases the elongation and roundness of tailings.
- The increment in the tailing particle size increases the convexity and roughness of the particle.

Mineralogy

- The strength of the mineral particles in tailings may vary depending on their size, with finer particles potentially exhibiting higher strength compared to coarser particles. This difference in strength could be due to the influence of the mineral structure on its overall strength. Consequently, larger particles tend to have more microcracks or flaws within their structure, making them more prone to breakage when compared to smaller particles.

3. Materials and Methods

3.1 Site description

The tailings material used to perform this study originates from Aitik mine which is owned by Boliden AB. The mine is located about 100 km north of the Arctic Circle, near Gällivare in the northern Sweden; see Figure 10. The mine was opened in 1968 and has deposited more than 500 Mt of waste rock in waste rock dumps (McKeown et al., 2015), and the mine lifespan is expected to be at least 25 years as of today (Boliden, 2023). The milled material is deposited in a TSF surrounded by tailing dams, which covers an estimated area of 13 km² (Rodriguez, 2016). Boliden (2023) described in the last annual and sustainability report an annual ore production of 43.2 Mt, where more than 79,000 t of copper, almost 28 t of silver and 2.4 t of gold were produced in 2022.



Figure 10. Location of Aitik mine (left) and the tailings dam (right)

The average temperature in the area is +1 °C, which corresponds to a subarctic environment. Lindvall (2005) states that temperatures in the winter may occasionally reach -40 °C, but in the summer, +25 °C or higher have been reported; moreover, there is approximately 500 mm of precipitation each year, with a considerable portion falling as snow. As today, tailings deposition at Aitik is maintained by the “spigot”-method (ICOLD 1996), where quartz, feldspar, plagioclase and mica are the main gangue minerals within tailings (Lindvall, 2005; Rodriguez, 2016).

3.2 Tailing samples used in this study

Disturbed samples were used for laboratory testing. The samples analyzed are from a borehole in Aitik tailings impoundment down to a depth of 38.8m. Sampling was conducted during 2020, before this thesis, and brought to LTU as dry disturbed samples during 2022. A total of 11 samples, at different depths, from the borehole were brought to LTU. The lab work in this study was carried out on 4 of the 11 samples, with a separation depth of approximately 10 meters between them. The

samples are named S2 (4.2 – 4.5 m), S5 (15.0 – 15.4 m), S8 (24.5 – 25.0 m), and S11 (33.5 – 34.0 m). The first sample from the borehole, S1 (1.0 – 1.5 m), was not taken into account since the spigots cause tailings to flow constantly towards the impoundment and may be subject to disturbing processes that alter tailing's properties, and its analysis is not representative, i.e., erosion upon deposition could affect the properties in upper layers. It is estimated the deepest sample in analysis S11 was deposited in 2001 while the most superficial layer in analysis was placed in 2019.

A previous characterization of the borehole allowed the material to be defined within a range of sand and silt, which correlates with previous studies conducted at Aitik tailings dam by Rodriguez (2016) and Bhanbhro (2017). Figure 11 illustrates the depth of each sample, year deposition and the soil classification defined when the borehole was drilled.

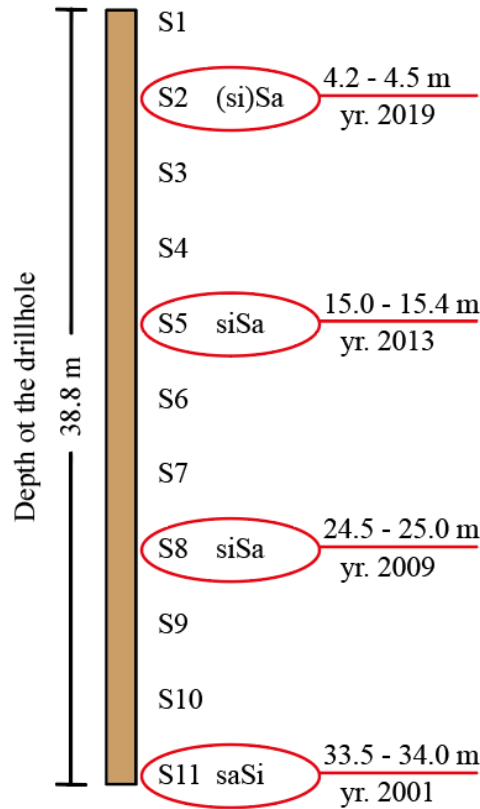


Figure 11. Samples schema from the drillhole

The samples for oedometer testing were constructed in sample tubes of 170 mm in height and 50 mm diameter. A filter in the bottom of the tube was placed to avoid particle loss, and each layer was compacted between 20 to 30 mm height until the tube was filled. The non-linear undercompaction method proposed by Jiang et al. (2003), which is based on Ladd (1978) was used to ensure the homogeneity of the samples because some of the compaction energy will be transferred to lower layers. This tamping procedure was performed with all constructed samples, later used in oedometer testing. Studies performed on Aitik tailings dam Bhanbhro (2017) and Bjelkevik & Knutsson (2005) have shown dry density values between 1.18 – 1.64 t/m³ and 1.55 – 1.65 t/m³, respectively. Thus, the trial dry density for constructed samples was defined as 1.60

t/m^3 . The basic properties for each constructed sample i.e., dry density, moisture content, particle density, bulk density, void ratio and saturation degree, are shown in Table 3.

Table 3. Description of tailings material used in this study

Sample	Depth (m)	Dry Density (t/m^3)	Moisture Content Average (%)	Particle density Average (t/m^3)	Bulk Density Average (t/m^3)	Initial void ratio	Degree of Saturation (%)
S2	4.2 – 4.5	1.62	6.2	2.80	1.72	0.728	23.8
S5	15.0 – 15.4	1.63	6.9	2.73	1.74	0.675	27.9
S8	24.5 – 25.0	1.61	6.7	2.81	1.72	0.745	25.3
S11	33.5 – 34.0	1.61	6.7	2.90	1.71	0.813	23.9

To determine and differentiate the structure and arrangement effects (i.e., effects of soil fabric), slurry samples were constructed and tested to uniaxial compression loading in oedometer. The samples were assembled using material from sample 11. These samples were assembled in order to reproduce a slurry consolidation process without inducing tamping effects. This testing was done since a different particle arrangement could be obtained and to determine whether any major change occurred regarding the samples prepared by tamping process. The samples were prepared in tubes of 50 mm diameter. A filter was placed at the bottom of the tube to allow excess water to flow out, avoiding as much as possible the loss of soil particles, followed by a settlement process of the sample without covering the top face for 24 hours.



Figure 12. Slurry sampling – initial conditions (left); after 24 hours settlement (right)

Material from sample S11 was chosen due to the availability of material. The average water content which samples were prepared was 36.0 %. The basic properties of the slurry sample were determined based on the sample conditions after 24 hours, the average results are presented in Table 4. The outer part of the samples was discarded since it has been exposed and drier material must be found. Therefore, between 5 mm to 8 mm were taken out. Figure 12 displays a slurry sampling prepared before and after 24 hours settlement.

Table 4. Description of slurry material used in this study

Sample	Depth (m)	Dry Density (t/m ³)	Moisture Content Average (%)	Particle density Average (t/m ³)	Bulk Density Average (t/m ³)	Initial void ratio	Degree of Saturation (%)
S11	33.5 – 34.0	1.50	28.1	2.90	1.92	0.933	87.3

3.3 Image acquisition and analysis

Image acquisition and analysis are used to evaluate the intrinsic parameters of the tailings. Imaging through reflected light and Scanning Electron Microscopy (SEM) analysis were executed to evaluate the particle shape and mineralogy of the tailings; meanwhile, dynamic image analysis was carried out to determine the PSD both at the initial stage (which was correlated with sieving tests) and after laboratory testing of the samples. Traditionally particle size distribution is determined through sieving analysis, but in order to be able to compare PSDs before and after oedometer testing this methodology was determined as appropriate for this study case.

3.3.1 Light reflected imaging and SEM analysis

Image analysis using reflected light helped to obtain an overview of the whole sample analysis surface and to determine the areas of interest to proceed later with a more objective SEM analysis. The advantage of these analyses is the possibility of capturing the physical properties of a single particle, which are processed and evaluated by software. It is important to note that the samples for these testing were prepared taking into account tailings particles larger than 0.063 mm.

In preparation for image acquisition, the samples were separated through wet sieving and dried for 24 hours at 105° Celsius. The wet sieving procedure was performed twice in order to avoid as much as possible the attachment of fine particles (< 0.063 mm) to coarser particles that may either interfere with or produce confusion when analyzing the samples. The samples were prepared using fixed forms of 25 mm diameter, where the dry sample was mixed with an epoxy-resin mixture, followed by a vacuum process to take out air content within the samples. After 24 hours, when the examples had solidified, the pieces were cut into sections, continuing with another epoxy-resin curing application. Once samples have solidified, grinding is staged in each sample using resin-bonded diamond discs to create even surfaces. To finalize the samplings, they were polished using a fabric where a mixture of diamond suspension with DP lubricant was applied. The diamond suspension employed for polishing had a size of 9 µm, 3 µm, and 1 µm. The grinding and polishing were developed using semi-automatic equipment (LaboForce 100). Figure 13 shows a view during the grinding and polishing process and the samples used for the imaging and SEM analysis.

Reflected light imaging analysis was performed in 2 dimensions through a microscope (Axioscope 7) with a high-resolution digital camera (Axiocam 305). In so doing, a macro-mapping of the samples could be obtained, followed by an evaluation process to simplify and objectify the SEM analysis beforehand. Figure 14 depicts the equipment used for imaging analysis. The camera has a resolution of 5 megapixels and a magnification of 5x was used since it supplies a good image

acquisition, which is supported by the findings provided of Rodriguez et al. (2012), where an optimal magnification range is between 4x and 10x.



Figure 13. Grinding and polishing process (left). Samples after grinding and polishing (right)

SEM analysis was done by using ZEISS Sigma 300 VP equipment which provides a quantitative mineralogy analysis and enables the evaluation of particle shape within tailings. For SEM analysis, the samples used were the same constructed for image sampling. Prior testing, it is important to clean the samples with ethanol to remove all possible contamination over the surface of interest, i.e., dust or fingerprints. It is not recommended to use water due to the minerals it may contain during the purification process, which could affect the analysis.



Figure 14. Microscope with high resolution digital camera for light reflection imaging analysis

The zones of interest for SEM analysis were chosen based on the macro-mapping obtained through light reflection imaging which are shown in Appendix A. The magnification resolution for each

sample was 113x since the equipment offers a resolution analysis up to 1.2 μm pixels and gives a mineralogical overview among samples. Figure 15 illustrates the equipment used for this investigation.



Figure 15. ZEISS Sigma 300 VP scanning electron microscope (SEM). Source: LTU

The SEM analysis will be done using a variable pressure (VP) allowing the surface characterization of non-conductive materials, with a 30 μm aperture which is standard since we are interpreting in image quality rather than laser analysis, and an electron high tension (EHT) of 20.0 kV while the working distance is set in 8.5 mm based on the EHT used. Figure 16 shows an internal view of the chamber SEM equipment. Elements will be identified using an overview sight of the particle; however, to determine the mineral composition, specific set points will be established in each sample.

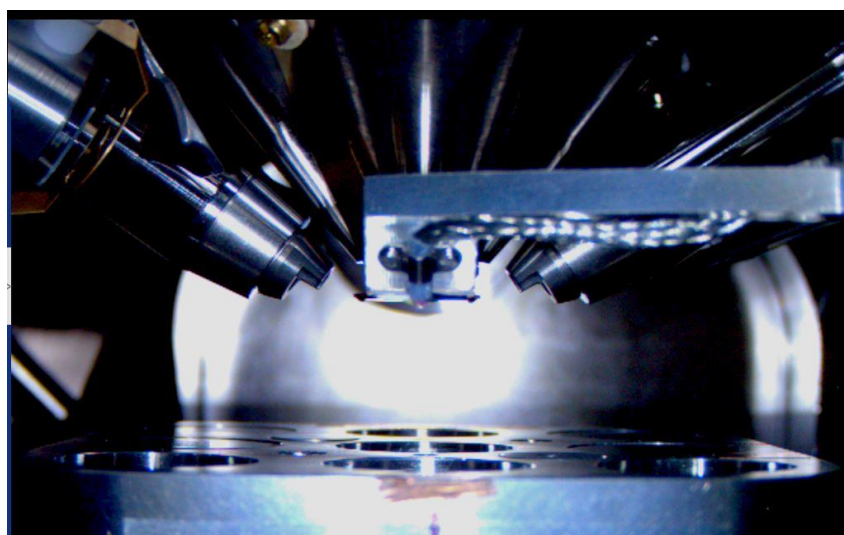


Figure 16. Internal chamber view for SEM analysis

3.3.2 Dynamic image analysis

Dynamic image analysis was developed by using a particle size and shape analyzer (Camsizer® XT), see Figure 17. This methodology is useful due to the precise particle size and shape information of powders and granules. The analysis is performed by scanning using LED light sources in a particle collective. For this test, tailings particles used in this investigation of all range-size were used both before and after laboratory testing.

Samples should be completely dry prior analysis where the measuring particle range of the equipment goes from 3 mm to 0.8 μm . The alternative dispersion method chosen for this study is a dry measurement through air pressure dispersion with “X-Jet”. The material is poured in the feeder hopper where a vibrating feed chute carries the material to a free-fall chamber where compressed air is injected to break up possible agglomerations and where two high-resolution cameras are located physical characteristics of the material in question. The measuring time depends on the desired measuring statistics, but it can last between 2 and 5 minutes, consequently, the results are achieved in real-time. The digital images are processed by the built-in software, resulting in PSD based on the captured images of particle geometry.



Figure 17. Camsizer XT – equipment (Microtrac Retsch GmbH)

The advantage of this method analysis is the simultaneous acquisition of information on size and shape characteristics. The PSD is evaluated by measuring the length, width, equivalent diameter, and circumference. In the meantime, the shape description is assessed through sphericity, roundness, aspect ratio, and convexity.

The Camsizer XT analysis was used in this investigation mainly to determine PSD of tailings samples. As mentioned before, several parameters can be described using this methodology. Nevertheless, the characteristic used to compare the results and relate them to sieving analysis is the particle width ($X_{c \min}$), which is determined from the narrowest of all measured chords in the particle (see Figure 18).

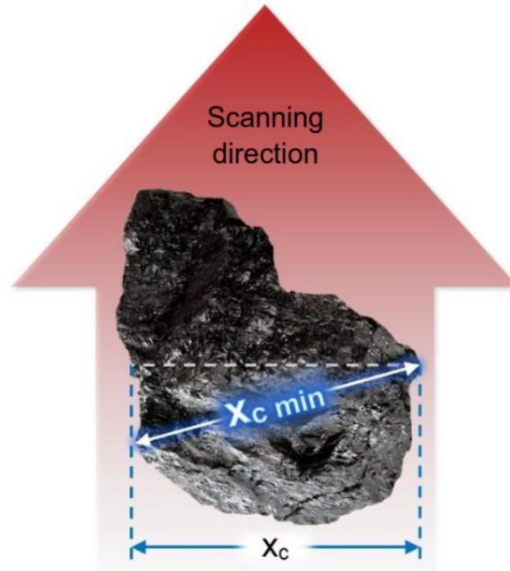


Figure 18. Illustration of $X_c \min$ in a particle (Microtrac Retsch GmbH)

This test method was used to evaluate and compare its accuracy in determining the PSD with that of sieving, which will serve as a backup before proceeding to use the dynamic image analysis method to evaluate the physical properties after laboratory testing. For laboratory testing, the oedometer test was considered suitable. Due to the small amount of material, sieving testing was going to present some issues where sparse values and high uncertainty could have been obtained since the material used for oedometer samples weighs 60 gr approximately, which is not enough to be used for sieving testing, at least under current laboratory conditions.

It is important to highlight that sieving testing and dynamic image analysis have different approaches. Wet sieving followed by sedimentation test was used to determine the PSD of the material, and a sample of 600 gr was characterized. The advantage of this methodology is that enables the washing out of as many finer particles as possible that are lumped in larger particles; nevertheless, an important drawback of this method after oedometer testing is the small amount of material obtained after laboratory testing; meanwhile, dynamic analysis enables the analysis for the amount of material obtained after oedometer testing. However, there is downside with this methodology as well. Even though the samples were dried beforehand for testing and pressured air was injected to the samples during the dynamic image analysis, there are fine particles that will remain attached to coarser particles that will not be detached and may affect the outcome PSD. Besides, it is highly dependent on the batch sampling, considering that the material taken must be representative during the evaluation. Several calibration tests were performed with tailings material to correlate the deviation between sieving and dynamic imaging analysis.

3.4 Laboratory tests on tailings

To analyze the consolidation process and possible crushing effects, oedometer tests were performed. The advantage of using this methodology is that enables the representation of consolidation under K_0 conditions (zero lateral strains). For this reason, triaxial testing was not considered as a first choice based on the scope of this investigation. The oedometer test was performed to obtain the

deformation and compressibility of the material and to study a possible “crushing” by analyzing the PSD after exposing the samples to a uniaxial load.

The oedometer methodology was chosen over other compression tests (i.e., unconfined compression test, soil compression test), whereas higher loads could be achieved as it could generate a gentler crushing on the particles. This is due to the possibility of a gradual load increase that allows time for the particles time to sort themselves out and settle at the same moment, replicating a “similar” behavior as in a tailings impoundment, considering that tailings are stored along the lifespan of the mine, increasing the loading over tailings already deposited. Meanwhile, other compression tests could induce a more severe and sudden crushing that would not be representative of field conditions.

3.4.1 Oedometer test

Disturbed remolded and slurry samples were performed through oedometer test. The test was performed according to ASTM D2435 under saturated and drained conditions. The aim of this type of consolidation is to prevent the lateral strain of the soil mass, simulating K0 conditions as in tailings impoundment some distance away from the crest.

The analyzed samples had two different arrangement conditions. The first arrangement condition corresponds to samples at different depths (S2, S5, S8, S11) which were assembled by tamping while, the second sample preparation was in form of slurry material. This last sample condition was manufactured with material of deepest layer in analysis (S11) to determine if any change may be produced due to a different particle arrangement.

Before running the test, the initial sampling conditions for the assembled samples were determined to ensure the results. Oedometer samples were acquired from the remolded sampling tubes with dimensions of 20 mm high and 40 mm diameter. When extracting the sample from the remolded tube, part of the material was taken to determine water conditions prior to testing. Both the upper and bottom sides of the oedometer were covered with filters to avoid losing mass and guaranteeing drained conditions. The samples were submerged in water, where constant monitoring by LVDT was carried out, enabling to analyze the settlements continuously.

The samples were subjected to different weight conditions starting from 10 kPa, doubling the load stepwise until 640 kPa was reached. It is important to highlight, since the samples are subjected to saturated and drained conditions, they will be subjected to effective stresses. According to the findings provided by Bhanbhro (2017), the bulk density at Aitik tailings dam is within the range of 1.66 t/m^3 and 2.12 t/m^3 . By saying this, the worst scenario of loads applied in the impoundment will be whether tailings from the surface of the impoundment are saturated bearing a bulk density of 2.12 t/m^3 . Taken into consideration this estimation, it can be likely that sample S11 have been subjected to an effective stress of 378 kPa which is less than the maximum load applied with oedometer testing, which is 640 kPa. Consequently, possible crushing effects may be experienced among samples. Furthermore, the soil fabric is different from the samples previous in situ conditions and the fact that particles now have contact in another way will also influence on the potential crushing during compression. Table 5 shows an estimation of the effective vertical

stresses determined for this test assuming saturated conditions in the impoundment, supporting the use of this testing.

Table 5. Effective stress conditions within the impoundment to validate oedometer test

Sample	Initial depth (m)	Final depth (m)	Mean depth (m)	γ_{sat} (kN/m ³)	σ'_v (kPa)
S2	4.20	4.50	4.35	21.20	48.72
S5	15.00	15.40	15.20	21.20	170.24
S8	24.50	25.00	24.75	21.20	277.20
S11	33.50	34.00	33.75	21.20	378.00

4. Results

4.1 Initial characterization

The initial properties of the four samples in question were determined in order to assess and compare them. The intrinsic properties of each sample that were evaluated are:

- Particle size distribution
- Particle shape
- Mineralogy

The average particle density of the samples was estimated to be 2.81 t/m^3 . Slight changes between samples were observed in the data at each depth, which are summarized in Table 6.

Table 6. Particle density of samples

Sample	Depth (m)	Particle density Average/Depth (t/m^3)	Particle density Average/Total (t/m^3)
S2	4.2 – 4.5	2.80	2.81
S5	15.0 – 15.4	2.73	
S8	24.5 – 25.0	2.81	
S11	33.5 – 34.0	2.90	

The variations in the particle density may be due to diverse gangue minerals within tailings, although, the gap between samples is not massive. It is clear that tailings material are composed by several elements which may have a different density than others and this deviation may be influenced due to different percentual mineral composition between them. By saying so, sample S5 and S11 set the outer boundaries within the samples by being the minimum (2.73 t/m^3) and maximum (2.90 t/m^3) particle density in this study, respectively. Meanwhile, S2 and S8 have the same particle density.

4.1.1 Particle size distribution

Sieve analysis was performed on disturbed samples and the PSDs are plotted in Figure 19. Tailings materials are typically classified between the range of sand and silt, which is quite common to find in tailings itself, with a null and low amount of gravel and clay particles, correspondingly. The material passing at each sieve size is shown in Table 7, where the similarity between the particle size distribution between samples S5 and S8 slightly differ from samples S2 and S11. For particle sizes below 0.063 mm , sedimentation test was performed.

There are a couple of characteristics can be marked between samples by assessing Figure 19. The gradation curves of samples S5 and S8 are relatively similar for both coarse and fine material. On the other hand, samples S2 and S11 have different approximations having more fines within the example, being S11 the finest sample of the four tested. The different behavior in the gradation curve of S11 are likely to be an effect of deposition (e.g. segregation and erosion) or the mineral extracting process. Potentially it could also be due to possible particle crushing effects in the

particles due to higher initial stress conditions than upper layers, chemical reactions, or creep effects, that have developed an effect on the sample, therefore more fines are produced. However, sample S2 also shows more fines than S5 and S8 despite being the shallowest layer analyzed and thereby it is a clear indicator that the processing and deposition have great influence.

Table 7. Particle Size Distribution - Sieving

Sieve size (mm)	Passing material (%)			
	S2	S5	S8	S11
2	99.99	99.99	99.99	99.99
1	99.96	99.82	99.99	99.99
0.5	98.29	94.00	99.25	99.79
0.25	86.90	79.01	85.28	93.88
0.125	54.62	42.58	45.53	63.88
0.063	21.02	10.12	13.01	32.19
0.0304	9.25	5.15	5.16	14.93
0.0163	5.59	2.94	2.99	8.64
0.0079	3.36	1.67	1.51	4.89
0.0035	1.97	0.95	0.84	2.70
0.0018	1.15	0.52	0.48	1.61
Soil Classification				
	silty Sand	Sand	Sand	silty Sand
Sand (%)	79.0	89.8	87.0	67.8
Silt (%)	19.9	9.6	12.5	30.6
Clay (%)	1.2	0.5	0.5	1.6

The tailings material is classified between the range of sands and silts. A qualitative methodology was used to group the soils. As a result, samples S5 and S8 are defined as sands, while S2 and S11 are defined silty-sand material.

Table 8. Gradation curve characteristics – Sieving testing

Sample	D10 (mm)	D30 (mm)	D50 (mm)	D60 (mm)	D90 (mm)	C_u	C_c
						$C_u = \frac{D_{60}}{D_{10}}$	$C_c = \frac{D_{60}^2}{D_{10} \times D_{90}}$
S2	0.032	0.080	0.116	0.146	0.318	4.49	1.34
S5	0.062	0.101	0.150	0.185	0.433	2.98	0.89
S8	0.051	0.095	0.139	0.170	0.334	3.38	1.06
S11	0.019	0.059	0.098	0.117	0.234	6.07	1.52

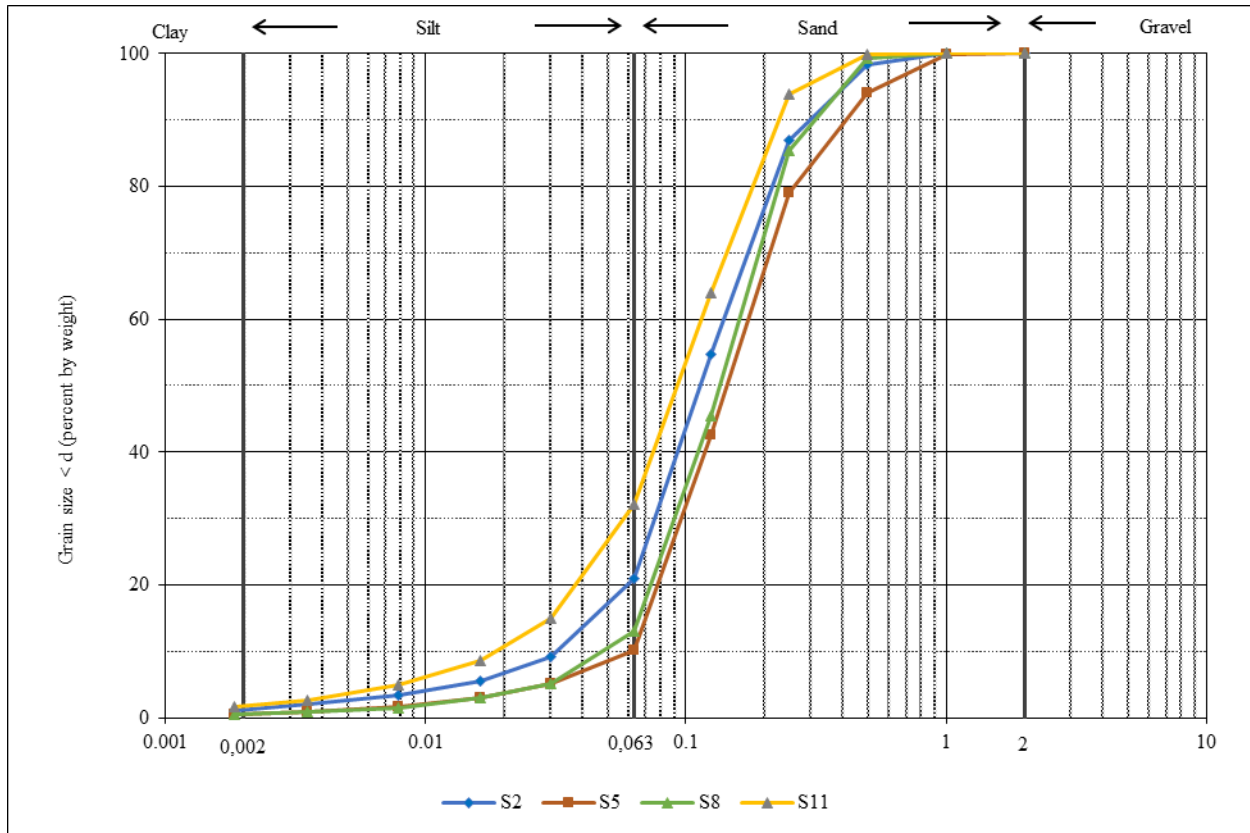


Figure 19. Particle Size Distribution of samples – Sieving test

An evaluation of particle sizes (D_{10} , D_{30} , D_{50} , D_{60} , D_{90}), coefficient of uniformity (C_u) and coefficient of curvature (C_c) was performed to better understand the gradation curves. The results are presented in Table 8. The coefficient of uniformity of the samples analyzed ranges from 2.98 to 6.07, where samples S5 and S8 have comparable C_u , while S2 and S11 have more scattered values. The coefficient of curvature is between 0.89 to 1.52, where once again the similarity of S5 and S8 is reiterated. The likeness of these samples (S5 – S8) is reflected among most analyzed particle sizes, which are intermediate layers, and differ from superficial (S2) and deeper (S11) layers.

4.1.2 Particle shape analysis

Tailings particle shape analysis was performed using Powers roundness scale (1953) where bigger particles have a subangular shape meanwhile smaller particles tend to be a variety between subangular and angular shapes. The particle shape analysis was carried out for particles greater than 0.063 mm. The areas of interest were determined based on light imaging captures which are shown in Appendix A, in the same manner the areas will be the base spots for the mineralogy analysis. Figure 20 shows the SEM images with particle shapes of different sizes (0.063 – 1.00 mm) for samples S2 and S5 used in this study.

Results of particle shapes for S8 and S11 are only available from the reflective light imaging (see appendix A. Unfortunately, the SEM broke down during the time period of this study, and a complete analysis of the samples was not possible to conduct in the SEM.

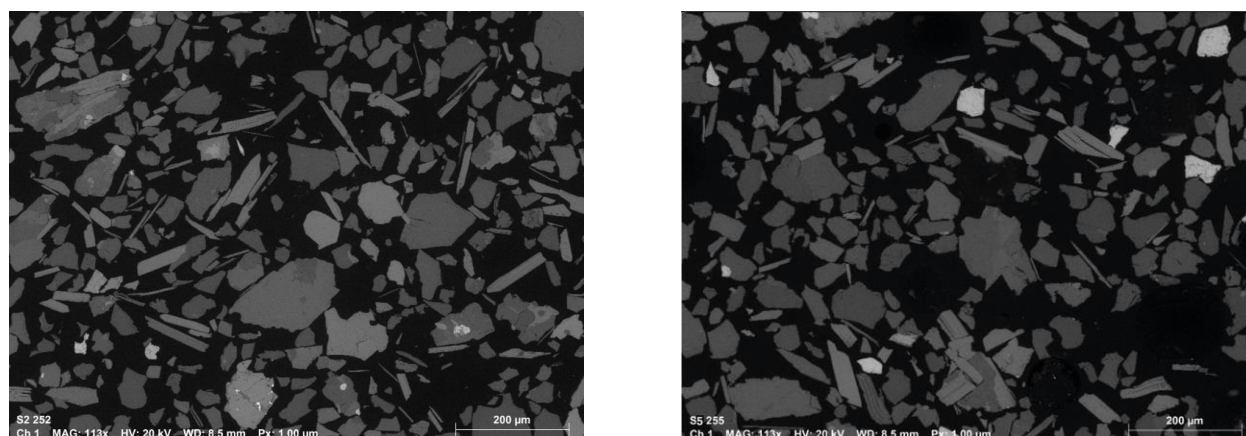


Figure 20. Particle shape on tailings samples using SEM (left: S2 – right: S5)

During this study, it was not feasible to conduct a quantitative assessment. Nonetheless, by qualitatively analyzing the results obtained from reflective light imaging (presented in appendix A), it appears that sample S2 contains a higher concentration of needle-shaped particles compared to samples S5, S8, and S11.

4.1.3 Mineralogy analysis

Analysis of sample mineralogy was unfortunately limited for this study, since the SEM broke down during the time period of study. A complete mineralogy analysis, with automated mapping of all the samples was not possible to conduct in the SEM. Only samples S2 and S5 have results that could manually be interpreted.

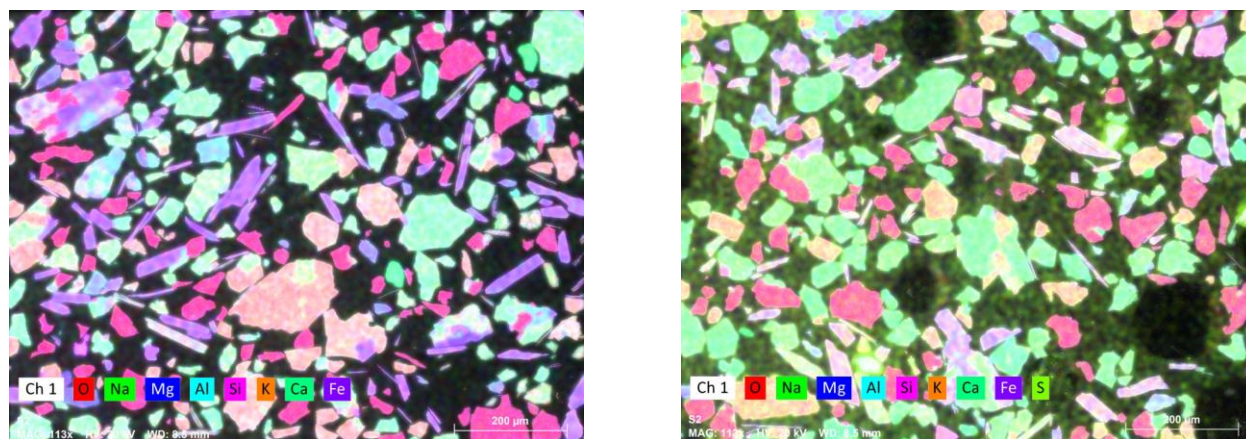


Figure 21. Mineralogy analysis on tailings samples using SEM (left: S2 – right: S5)

Mineralogy composition within particles is rather similar nevertheless the concentrations in each sample differ among them as can be qualitatively interpreted in Figure 21. To analyze the composition specific set points within the sample are analyzed. The more often minerals found within both samples are mica, feldspar, plagioclase, and quartz. However, each sample contained different residual minerals. Sample S2 exhibited gangue minerals such as sorosilicate, K-feldspar,

and apatite. On the other hand, sample S5 contained minerals such as iron, hematite, pyrite, illite, and biotite.

The minerals contained in tailings samples have different hardness. Among the most common identified minerals, the highest hardness value corresponds to quartz while the lowest is for mica with 8 and 2.5, respectively, according to Mohs hardness scale. Thus, feldspar and plagioclase have an intermediate hardness value of 6 within the same hardness scale.

4.2 Dynamic Image Analysis

Dynamic image analysis using the Camsizer XT was performed on tailings material prior to laboratory testing to check the accuracy of the methodology and to comply with the sieving tests. This was done to compare the accuracy and determine the reliability of this method for future analysis. The size range of the dynamic image analysis was in the range of 3 mm to 0.8 μm . In addition, the median value was considered for plotting where at least 3 measurements were performed for each sample.

The assembled samples S2, S5, S8 and S11 were brought under dynamic image analysis, where their results are presented in Figure 22. The gradation curves are between the range of sand and silt as sieving test results. PSD from the sieving test is presented as the dashed lines in Figure 22. Besides, they show a similar behavior to that of the sieving analyses. However, curves S5 and S11 have a more noticeable change composed with coarser particles than the ones identified by sieving testing. By this, a more detailed analyzed in each gradation curve was performed in order to identify the suitability of this test.

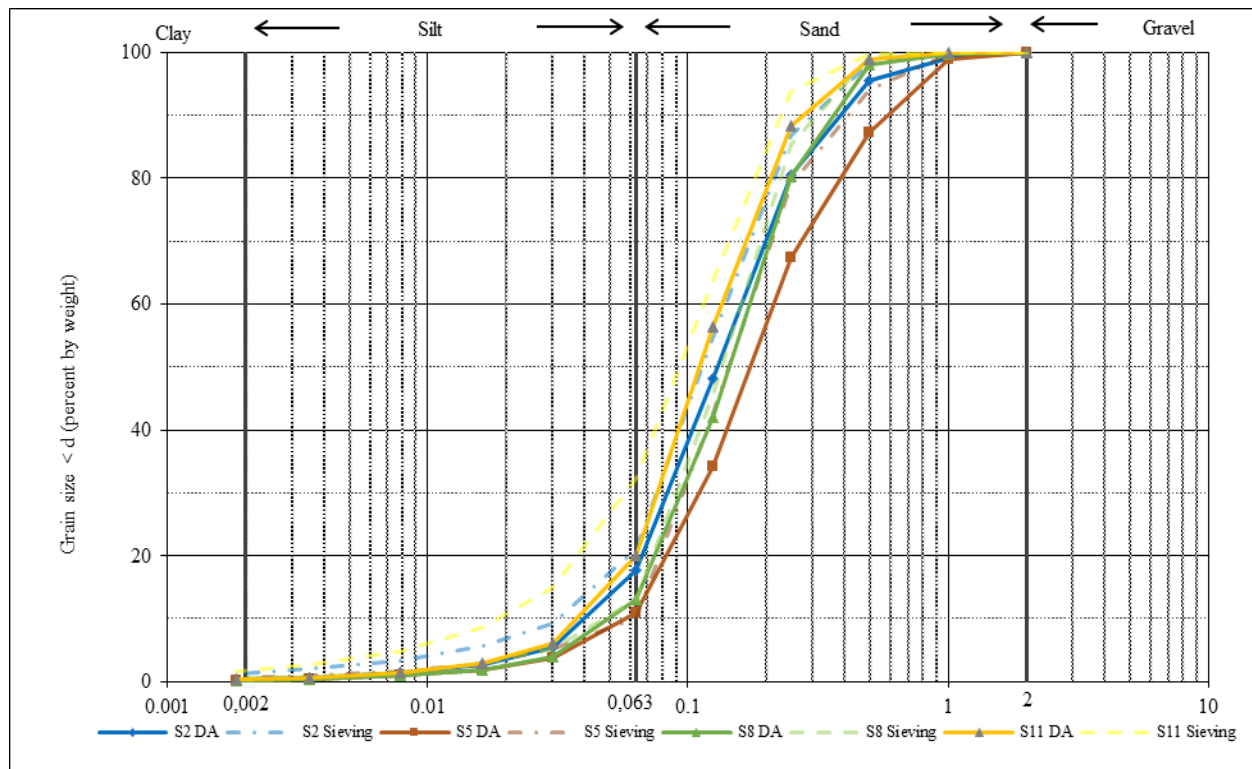


Figure 22. Particle Size Distribution of samples – Dynamic Image Analysis

An evaluation of the overall PSD gradation and partial curves was performed to evaluate the results. Although PSD by sieving and sedimentation offers a wider analysis range down to 0.18 μm , a linear regression for partial retained gradation analysis was performed with the results obtained through the Camsizer XT to get down to 0.18 μm . Thus, a comparison for partial retained material curves both by sieving and dynamic image analysis could be developed and assessed.

The dynamic image analysis uses two LED cameras to evaluate particle characteristics. During testing it could be seen the high resolution it offers, as depicted in Figure 23. It is needed to clean up the equipment previous test in order to avoid a side effect of dust or residual particles alterations in the measurement.

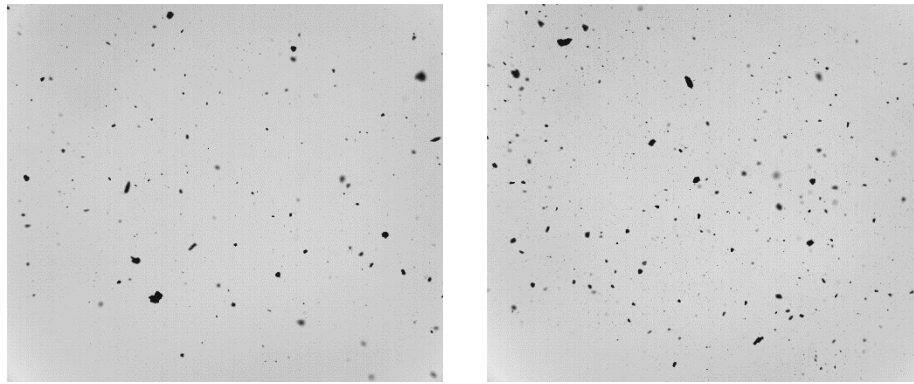


Figure 23. Pictures during the dynamic image analysis (no scale)

To assess the accuracy of the methodology a comparison between data was performed which are described in Table 9 and Table 10 for samples S2 – S5 and S8 – S11 correspondingly. The plots considering the passing volume and retained material at each sieve size for individually samples can be found in Appendix C in this report.

Table 9. Comparison table for Samples S2 and S5 between sieving and dynamic image analysis

SAMPLE S2							SAMPLE S5					
Sieve size	S2 sieving (%)		S2 D. A. (%)		Deviation S2		S5 sieving (%)		S5 D. A. (%)		Deviation S5	
(mm)	Pass. Acc.	Ret. Part.	Pass. Acc.	Ret. Part.	Pass. Acc.	Ret. Part.	Pass. Acc.	Ret. Part.	Pass. Acc.	Ret. Part.	Pass. Acc.	Ret. Part.
2	99.99	0.01	100.00	0.00	-0.01	0.01	99.99	0.01	100.00	0.00	-0.01	0.01
1	99.96	0.03	99.20	0.80	0.76	-0.77	99.82	0.17	98.95	1.05	0.87	-0.88
0.5	98.29	1.67	95.54	3.67	2.75	-2.00	94.00	5.82	87.26	11.69	6.74	-5.87
0.25	86.90	11.39	80.42	15.11	6.48	-3.72	79.01	14.99	67.32	19.94	11.69	-4.95
0.125	54.62	32.28	48.08	32.35	6.54	-0.06	42.58	36.43	34.24	33.07	8.34	3.35
0.063	21.02	33.60	17.65	30.43	3.37	3.17	10.15	32.43	10.91	23.33	-0.75	9.09
0.0304	9.25	11.77	5.44	12.21	3.81	-0.44	5.15	5.00	3.65	7.26	1.50	-2.26
0.0163	5.59	3.66	2.68	2.76	2.90	0.90	2.94	2.21	1.85	1.80	1.09	0.41
0.0079	3.36	2.23	1.40	1.28	1.96	0.94	1.67	1.27	0.96	0.89	0.71	0.38
0.0035	1.97	1.39	0.62	0.78	1.35	0.61	0.95	0.72	0.43	0.54	0.52	0.18
0.0018	1.15	0.82	0.32	0.30	0.83	0.52	0.52	0.43	0.22	0.21	0.30	0.22
D90 (mm)	0.318		0.365		-0.047		0.433		0.575		-0.141	

D60 (mm)	0.146	0.169	-0.023	0.185	0.221	-0.036
D50 (mm)	0.116	0.140	-0.023	0.150	0.183	-0.032
D30 (mm)	0.080	0.091	-0.012	0.101	0.123	-0.022
D10 (mm)	0.032	0.044	-0.012	0.062	0.060	0.002
Cu	4.490	3.810	0.680	2.980	3.710	-0.730
Cc	1.340	1.110	0.230	0.890	1.140	-0.250

Sample S2 has a maximum deviation of 6.54% (sieve size = 0.125 mm) regarding the passing volume and 3.17% (sieve size = 0.25 mm) in retained material. Moreover, the particle sizes between both analyzes are rather close with a maximum variation of 0.047 mm. Meanwhile, Sample S5 presents a higher deviation whereas maximum is 11.69% in the passing volume (sieve size = 0.125 mm) and 9.09% in retained material (sieve size = 0.063 mm). Despite the similarity between particle sizes in both curves from D₁₀ to D₆₀, there is a higher difference in D₉₀ particle size where a variation of 0.14 is showed. Moreover, it can be pointed that particle sizes determined by dynamic image analysis present higher particle size than the ones determined by wet sieving and sedimentation, therefore a change can be sight in Cu and Cc values.

Table 10. Comparison table for Samples S8 and S11 between sieving and dynamic image analysis

SAMPLE S8							SAMPLE S11					
Sieve size	S8 sieving (%)		S8 D. A. (%)		Deviation S8		S11 sieving (%)		S11 D. A. (%)		Deviation S11	
(mm)	Pass. Acc.	Ret. Part.	Pass. Acc.	Ret. Part.	Pass. Acc.	Ret. Part.	Pass. Acc.	Ret. Part.	Pass. Acc.	Ret. Part.	Pass. Acc.	Ret. Part.
2	99.99	0.01	100.00	0.00	-0.01	0.01	99.99	0.01	100.00	0.00	-0.01	0.01
1	99.99	0.01	99.69	0.31	0.30	-0.31	99.99	0.01	99.86	0.14	0.13	-0.14
0.5	99.25	0.74	98.01	1.68	1.24	-0.94	99.79	0.20	98.84	1.02	0.95	-0.82
0.25	85.28	13.97	80.29	17.72	4.99	-3.74	93.88	5.91	88.37	10.47	5.51	-4.56
0.125	45.53	39.75	41.93	38.36	3.60	1.38	63.88	30.00	56.29	32.08	7.59	-2.08
0.063	13.00	32.53	13.02	28.91	-0.02	3.62	32.19	31.69	20.01	36.28	12.18	-4.59
0.0304	5.16	7.84	3.86	9.16	1.30	-1.31	14.93	17.27	6.13	13.89	8.80	3.38
0.0163	2.99	2.17	1.82	2.04	1.17	0.13	8.64	6.29	2.95	3.17	5.69	3.11
0.0079	1.51	1.48	0.90	0.92	0.60	0.56	4.89	3.75	1.50	1.45	3.39	2.30
0.0035	0.84	0.67	0.40	0.50	0.44	0.16	2.70	2.20	0.67	0.84	2.03	1.36
0.0018	0.48	0.36	0.21	0.19	0.28	0.16	1.61	1.08	0.34	0.32	1.27	0.76
D90 (mm)	0.334		0.331		0.003		0.234		0.275		-0.041	
D60 (mm)	0.170		0.183		-0.012		0.117		0.144		-0.027	
D50 (mm)	0.139		0.155		-0.016		0.098		0.121		-0.024	
D30 (mm)	0.095		0.107		-0.011		0.059		0.082		-0.023	
D10 (mm)	0.051		0.054		-0.004		0.019		0.042		-0.022	
Cu	3.380		3.370		0.010		6.070		3.470		2.600	
Cc	1.060		1.150		-0.090		1.520		1.130		0.390	

Sample S8 has a maximum deviation of 4.99% (sieve size = 0.25 mm) and 3.74% (sieve size = 0.25 mm) for passing volume and retained material respectively. Besides, the particle sizes

between both analyzes from D_{10} to D_{90} has a maximum difference of 0.012 mm which is displayed in the ratio for C_u and C_c values. On the other side, Sample S11 presents a higher deviation with a maximum of 12.18% for the passing volume (sieve size = 0.063 mm) and 4.59% for retained material (sieve size = 0.063 mm). The particle sizes in both curves are rather similar with a maximum deviation of 0.041 mm. Although, this variation in particle sizes is minor, it considerably affects the C_u and C_c values.

The dynamic imaging analysis defines the material with coarser particles, where most of these changes are produced between the range of 0.25 mm, 0.125 mm and 0.063 mm. Most of the analyzed particle sizes parameters present a larger size during the dynamic image analysis, which may be produced due to a possible adhesion of fine particles to coarser particles. Thus, a soil classification was developed based on the data obtained by the Camsizer XT to perceive whether any major change is produced due to this fluctuation in the data, which is summarized in Table 11.

Table 11. Soil classification – comparison table between sieving and D.A.

Soil Classification				
Sample	S2	S5	S8	S11
Sieving Classif.	Silty Sand	Sand	Sand	Silty Sand
D.A. Classif.	Silty Sand	Sand	Sand	Silty Sand

Analyzing the presented data, it can be mentioned that there are no significant changes in the analyzed samples within their soil classification comparing the sieving with the dynamic image analysis. Therefore, all samples retained their original classification meaning that the dynamic image analysis was able to accurate enough for soil classification. In this case, it is also viewed accurate enough to study the change of PSD before and after PSD. The alternative of small scale sieving would have resulted in similar, or even greater uncertainties. Based on the above, the analysis will continue taking into account the data obtained with the dynamic image analysis, since it can be used for small samples, as is the case of the amount of material obtained after performing the oedometer test, which may present some uncertainty if it is performed by sieving.

4.3 Effect of vertical stress on tailings

4.3.1 Oedometer testing

The oedometer testing was carried out by loading tailings sample stepwise from 10 to 640 kPa. Samples were loaded by doubling the initial load, resulting in steps of 10, 20, 40, 80, 160, 320 and 640 kPa. The samples were subjected to testing until the consolidation curves showed no significant changes at each load step. The samples in this case behave different from each other, but on average, the consolidation time for initial loadings required a few hours (2-4 hours). However, as the loading increased, the time required for consolidation extended up to 24 hours. Since the samples have a large amount of sand, the consolidation in certain steps was faster than

in others. Figure 24 exemplifies the loading steps and vertical compression of sample S5. Loading steps vs. vertical compression developed for this study are illustrated in Appendix B.

In order to determine the effects that the particle arrangement can produce in the tailings, tamping and slurry samples were tested. Thus, a comparison was made between samples S2, S5, S8 and S11 which were constructed by tamping. However, from sample S11 slurry samples were produced to compare the samples under two different arrangement setups. The slurry material will be referred to as S11.1 and S11.2 from now on.

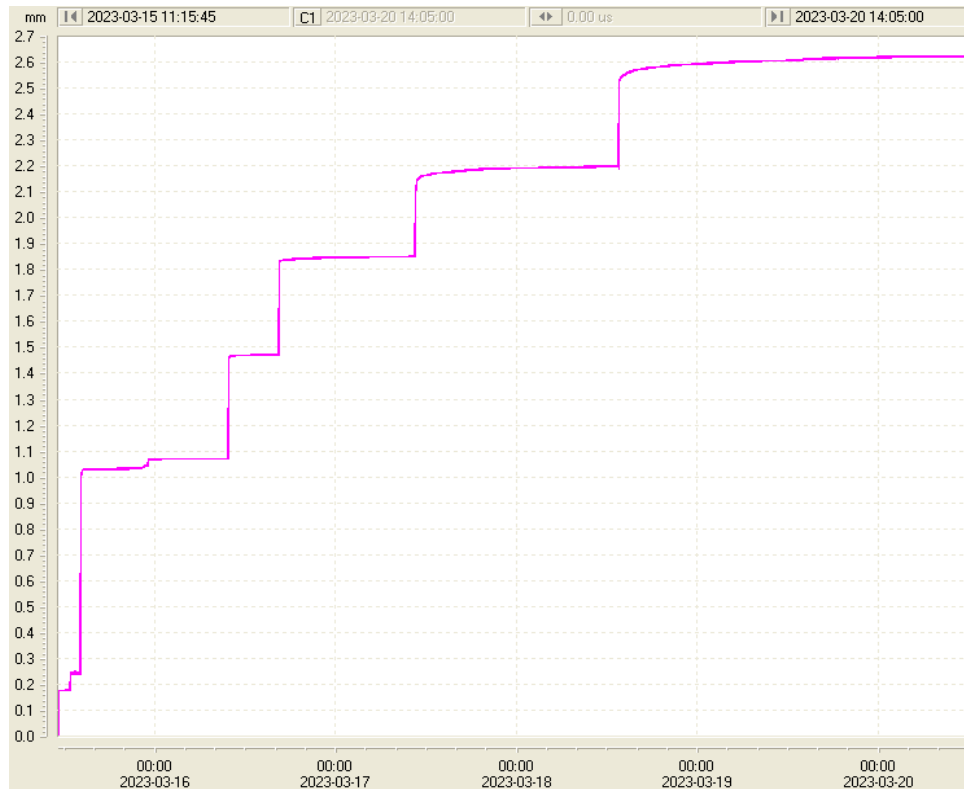


Figure 24. LVDTs curve for sample S5

The characteristics of the samples to be analyzed were determined prior to laboratory testing. The results represented in Table 12 show the initial conditions of the samples in which the dry density for the oedometer test is approaching the 1.60 t/m^3 initially set, being in the range of $1.50 - 1.59 \text{ t/m}^3$. Although, the dry density of the slurry material is slightly higher than tamped samples.

In order to set the prepared void ratios of samples S2 and S11 in context, comparison is done with the findings of Bhanbhro (2017), who also studied tailings from Aitik. Bhanbhro (2017) presented field values of void ratio in the range of $0.72 - 1.41$ which is comparable with the values obtained for samples S2 to S11 of $0.796 - 0.937$. In the same way, the bulk density achieved for slurry samples is 2.00 t/m^3 , which is within the field's values obtained by Bhanbhro (2017) of $1.66 - 2.12 \text{ t/m}^3$.

Table 12. Initial sample conditions – Oedometer test

Sample	Depth (m)	Spec. Gravity (t/m ³)	w (%)	Bulk density (t/m ³)	Dry density (t/m ³)	Void ratio (e)
Tamped samples						
S2	4.2 – 4.5	2.80	6.30	1.60	1.51	0.860
S5	15.0 – 15.4	2.73	6.58	1.62	1.52	0.796
S8	24.5 – 25.0	2.81	6.69	1.64	1.54	0.831
S11	33.5 – 34.0	2.90	6.78	1.60	1.50	0.937
Slurry samples						
S11.1	33.5 – 34.0	2.90	26.10	2.00	1.59	0.827
S11.2	33.5 – 34.0	2.90	30.06	2.00	1.54	0.888

The conditions at the end of the tests were also determined and are shown in Table 13. As expected, the dry density of the samples increased while the void ratio decreases, being in the range of 1.67 – 1.75 t/m³ and 0.560 – 0.742, respectively. For samples S11 larger differences are experienced in tamped sampling rather than slurry samplings.

Table 13. Final sample conditions – Oedometer test

Sample	Depth (m)	Final Dry density (t/m ³)	Dry density variation (%)	Final Void ratio (e)	Void ratio variation (%)	Vertical strain (%)
Tamped samples						
S2	4.2 – 4.5	1.71	13.0	0.641	25.5	11.80
S5	15.0 – 15.4	1.75	15.1	0.560	29.6	13.10
S8	24.5 – 25.0	1.70	11.0	0.650	21.8	9.87
S11	33.5 – 34.0	1.69	12.8	0.713	23.9	11.55
Slurry samples						
S11.1	33.5 – 34.0	1.73	8.6	0.682	17.4	7.89
S11.2	33.5 – 34.0	1.67	8.4	0.742	16.4	7.70

It was observed that shallow samples (S2 – S5) suffered more noticeable changes than deeper layers (S8 – S11). S2 and S5 samples were more susceptible for void ratio reduction with a higher dry density over samples S8 and S11, thus having larger percentual variations on both parameters. On the other side, assessing slurry samples (S11.1 – S11.2) with its corresponding tamped sampling (S11) can be seen that S11 is between the dry density range obtained for slurry samples even when their initial conditions were different, while the void ratio variation for slurry samples is considerably lesser than the average percentual reduction obtained for tamped samples. In addition, the vertical strain at the end of the test for tamped samples is within a range of 9.87% to 13.10%, where these values are greater than the vertical strain decrease obtained for slurry samples

which present an average decrement of 7.80%. It indicates that the particle arrangement is an important factor that influences the compressibility for tailings.

4.3.2 Stress-strain deformations

Vertical strains at each depth were plotted in form of $\log \varepsilon - \log \sigma'_v$ in Figure 25. The strains analyses are considering the linear portion in the plot which are between the interval of 80 – 640 kPa. Nevertheless, the dash lines in the plot show the early vertical strain stage behavior of the samples. Analyzing the linear interval, the strains of all tailing's samples tested were in the range of 4% and 13%. It can be stated that sample S5 presented the highest vertical strains of all samples, meanwhile, samples S11 and S8 have sort of similar conditions, but sample S8 ends up with the lowest strain conditions within all samples. In the case of S2, its initial vertical strain conditions are lower, though, its increasing ratio is higher ending with a vertical strain lower than S8 and S11.

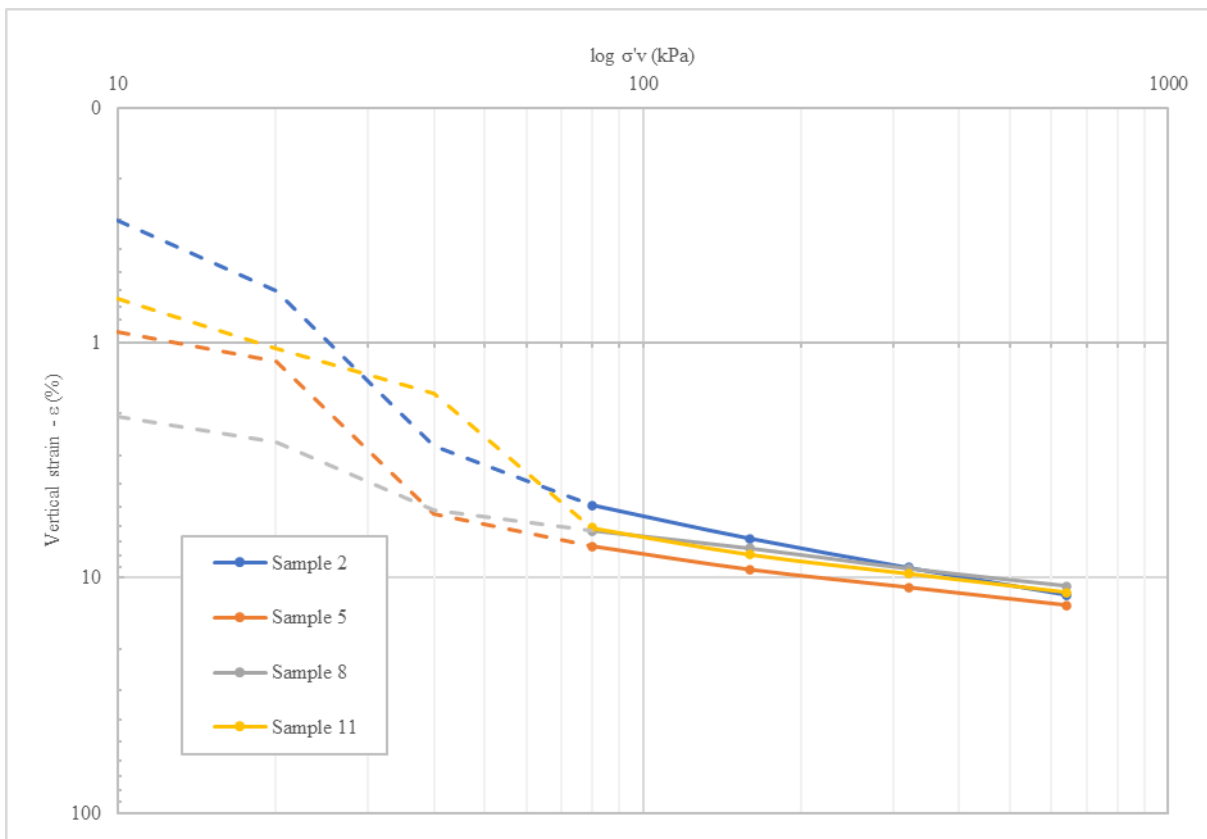


Figure 25. Plotting of vertical strain ($\log \varepsilon$) vs effective vertical stress ($\log \sigma'_v$) ; Samples S2, S5, S8, S11

It can be stated that sample S8 displayed the more stable vertical strain deformation throughout the entire testing period. Meanwhile, sample S2 exhibited the highest vertical strain ratio during the whole test.

The strain-stress behavior for sample S11 for slurry and tamped conditions is represented in Figure 26, which was plotted as $\log \varepsilon - \log \sigma'_v$. The strain development of slurry examples is equal regardless their different initial conditions. Even so, S11.1 and S11.2 curves differ from sample S11 where a steeper vertical strain curve is reached while increasing loading. This could be

attributed to the fact of water dissipation within the slurry material producing a faster vertical strain development in the samples. The strains between these two different particle arrangements are within a range of 2 and 11% whereas slurry have stress ratio between 2 and 7% while tamped samples are between 6 and 11%. Though, between 320 – 640 kPa, slurry prepared samples have curves that starts to have a gentler tendency being likely to S11.

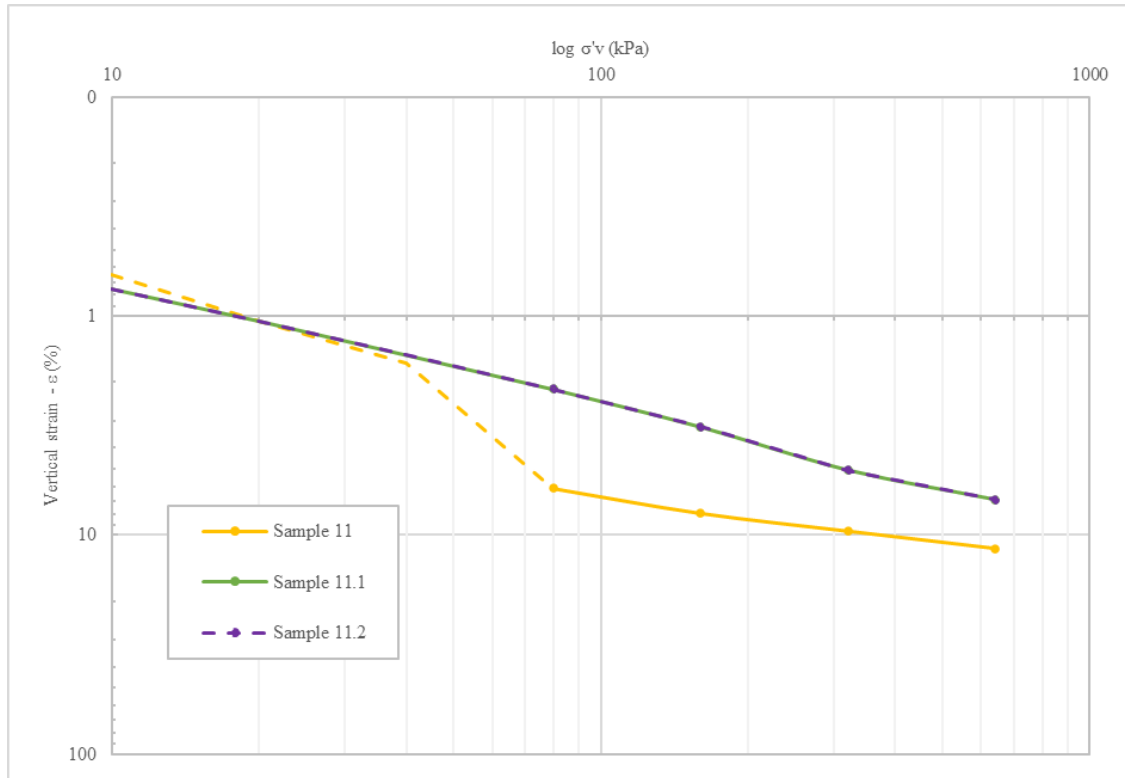


Figure 26. Plotting of vertical strain ($\log \epsilon$) vs effective vertical stress ($\log \sigma'_v$) ; Samples S11, S11.1, S11.2

It can be stated that sample S11 displayed a similar behavior with its slurry samples, but there is a sudden change at 40 kPa that develops a sudden increment of vertical strain for the tamped samples. As a result, slurry samples have more stable vertical strain deformation throughout the whole testing period.

4.3.3 Void ratio

The void ratio against effective vertical stress were plotted in form of $e - \log \sigma'_v$ in Figure 27. It was observed that all samples at initial loading phase showed no significant change until the second (20 kPa) or third (30 kPa) loading step was applied. This behavior may be due to an arrangement of the particles with the surface of the loading cap. By this, the void ratio began to decrease once a “full contact” was reached, and the load evenly applied between the particles and the cap. Though, once this sudden void ratio change occurred in the initial phase, the trend of the void ratio becomes smoother reaching a constant void ratio decrement.

Samples have a void ratio reduction between 21.8% and 29.6%, as earlier shown in Table 13, where the higher variation is presented in sample S5 while the lowest is S8. Evaluating the other samples, it can be stated that S11 and S2 present a reduction of 23.8% and 25.5%, respectively. In

addition, sample S5 depicted the lowest initial void ratio, and holds the same positioning among the samples by being the lowest void ratio at the end of the test.

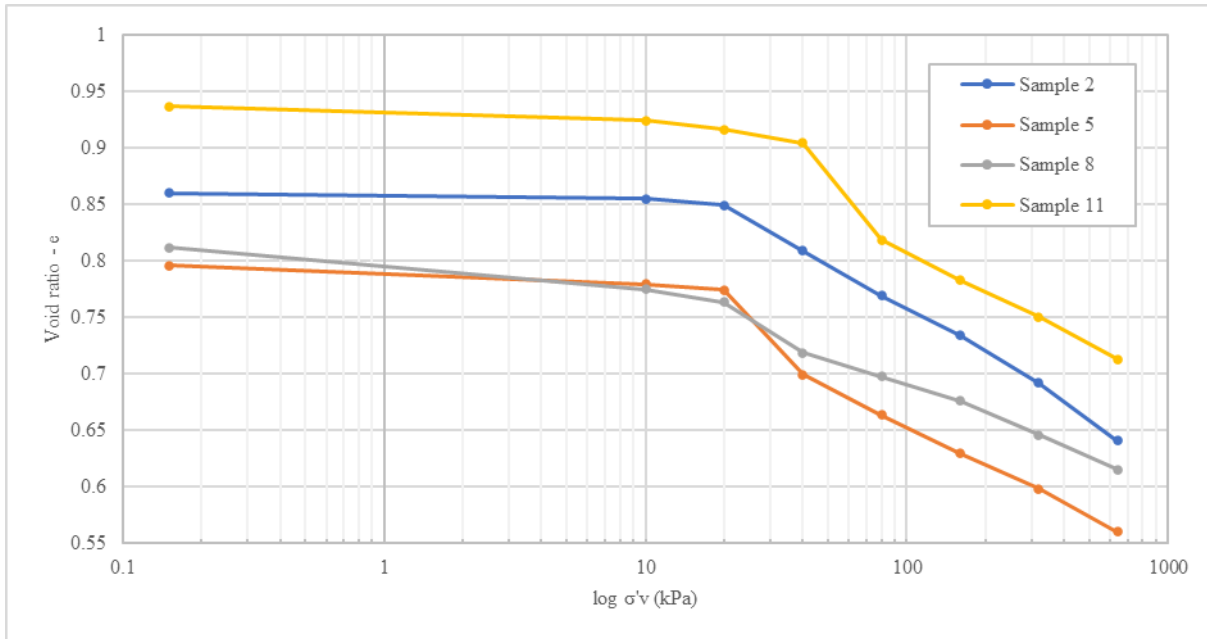


Figure 27. Plotting of void ratio (e) vs effective vertical stress ($\log \sigma'_v$) ; Samples S2, S5, S8, S11

The void ratio-stress behavior was plotted as $e - \log \sigma'_v$ for sample S11 in slurry and tamped conditions in Figure 28. It can be pointed the behavior of slurry samples where there is not a sudden change in the void ratio as the tamped sample, having a constant decrement while the load increases. Moreover, a similar trend between them can be depicted where there is no variance among them being parallel from the first load until the termination of the test.

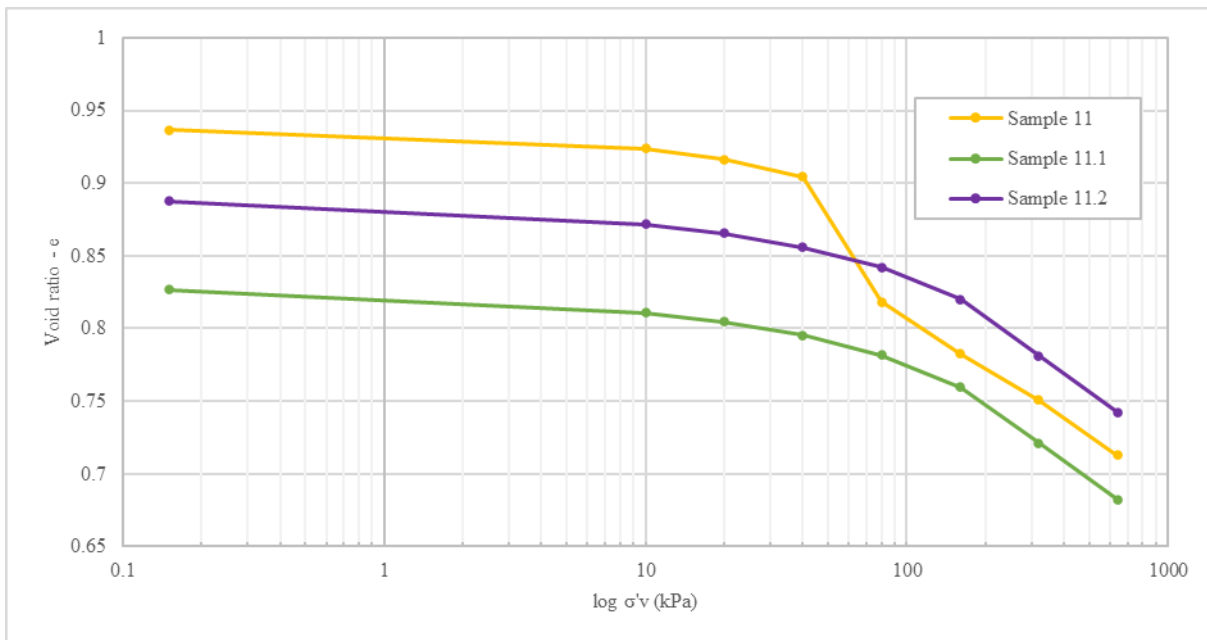


Figure 28. Plotting of void ratio (e) vs effective vertical stress ($\log \sigma'_v$) ; Samples S11, S11.1, S11.2

The void ratio in sample S11 decreases with the same tendency once the sudden decrement of void ratio occurs, adjusting its trend to the behavior of the slurry samples, even though S11 has a different particle arrangement. As the load on sample S11 sample increases, the curve tends to become more likely as S11.1 and S11.2.

4.3.4 Compressibility and compression index

The compressibility of the soil can be derived through oedometer test and can be defined through the coefficient of volume compressibility (m_v) which is defined as volume change per unit volume per unit increase in effective stress (Craig, 2004). Moreover, the compression index (C_c) is the slope of the linear portion of void ratio against effective stress curve, which is extensively used for settlement determination.

The coefficient of volume compressibility and compression index are determined for stress range of $\sigma'_0=80$ kPa and $\sigma'_1=640$ kPa which are shown in Table 14. Both parameters can be determined based on the void ratio (e) and effective stress (σ') at arbitrary points on the normal consolidation line obtained through oedometer testing by using Eq.1 and Eq.2 described below (Craig, 2004).

$$m_v = \frac{1}{1+e_0} \left(\frac{e_0 - e_1}{\sigma'_1 - \sigma'_0} \right) \quad (m^2/MN) \quad \text{Equation 1}$$

$$C_c = \frac{e_0 - e_1}{\log(\sigma'_1 / \sigma'_0)} \quad \text{Equation 2}$$

It was observed that the volume of compressibility for tamped samples is more significant for superficial layers than deeper layers, which is also partly reflected in the C_c value for sample S2. For the chosen stress range of $\sigma'_0=80$ kPa and $\sigma'_1=640$, sample S5 and S2 experienced a higher void ratio reduction resulting in a higher m_v value, while lesser compressibility was experienced in S8 where the minor void ratio was developed. Slurry samples have the same compressibility behavior with its correlated tamped sample even when their initial conditions and void ratio reduction after testing were different.

Table 14. Coefficient of volume compressibility and compression index ($\sigma'_0 = 80$ kPa and $\sigma'_1 = 640$ kPa)

Material	m_v (m ² /MN)	C_c
Tamped samples		
S2	0.0944	0.1421
S5	0.0739	0.1144
S8	0.0527	0.0839
S11	0.0673	0.1168
Slurry samples		
S11.1	0.0703	0.1100
S11.2	0.0684	0.1107

4.4 Particle breakage

Dynamic image analysis (DA) was performed in order to determine the PSD after oedometer testing was completed for later comparison with the initial PSD. The small amount of sample would have introduced many sources of error if conventional sieving would have been used.

For the DA, two different assessments were performed to better visualize the changes occurred in the samples. The first one considers accumulative passing material while the second analysis uses the retained material according to particle size. The advantage of performing the second assessment is due to the range of analysis obtained through DA; the evaluation was done considering a particle size range of 0.01 mm. Three measurements were performed for each sample where the median value was used for comparison. It can be pointed out that the deviation between measurements was certainly minimal.

A comparison between PSD from sieving and DA is done for the initial samples under section 4.1.1. Based on that, DA is considered accurate enough as a tool for comparison PSDs before and after oedometer testing. Therefore, the difference between PSD before and after testing could be considered as a combination of particle breakage (i.e., crushing) and potentially discrepancy within the original sample.

Comparative tables for each sample were structured based on the standard sieve sizes used for sieving analysis. These tables were based on the raw data obtained from the DA measurements, which can be found in Appendix D. In order to maintain a consistent evaluation framework, a linear regression procedure was employed for particle sizes below 0.008 mm, as used in Table 9 and Table 10 (section 4.2). Furthermore, the DA data presented in these tables for each sample will serve as the basis for evaluating the results after oedometer testing.

The DA data will be used in two ways: for plotting graphs and comparative tables before and after oedometer testing. For plotting, the raw data will be used to provide a graphical understanding of particle changes, as used in Figure 29 and Figure 30. Meanwhile, for comparison charts, the data will be accumulated according to the sieve size range, to develop an analytical comparison before and after testing as used in Table 15, Table 16 and Table 17.

Figure 29 shows the PSD curves obtained for each sample. It was observed that, samples tested in oedometer present only a slightly to neglectable difference in PSD compared with initial samples where the greater change is made within the sand range in the samples. Most of the largest deviation between the gradation curves is detected between 0.25 mm and 0.063 mm, where samples S5 and S11 have the largest cumulative deviation of 2.93% and 3.83% respectively. Thus, being the most divergent samples with their original, where both have a similar coefficient of compressibility although it is not the highest within the samples.

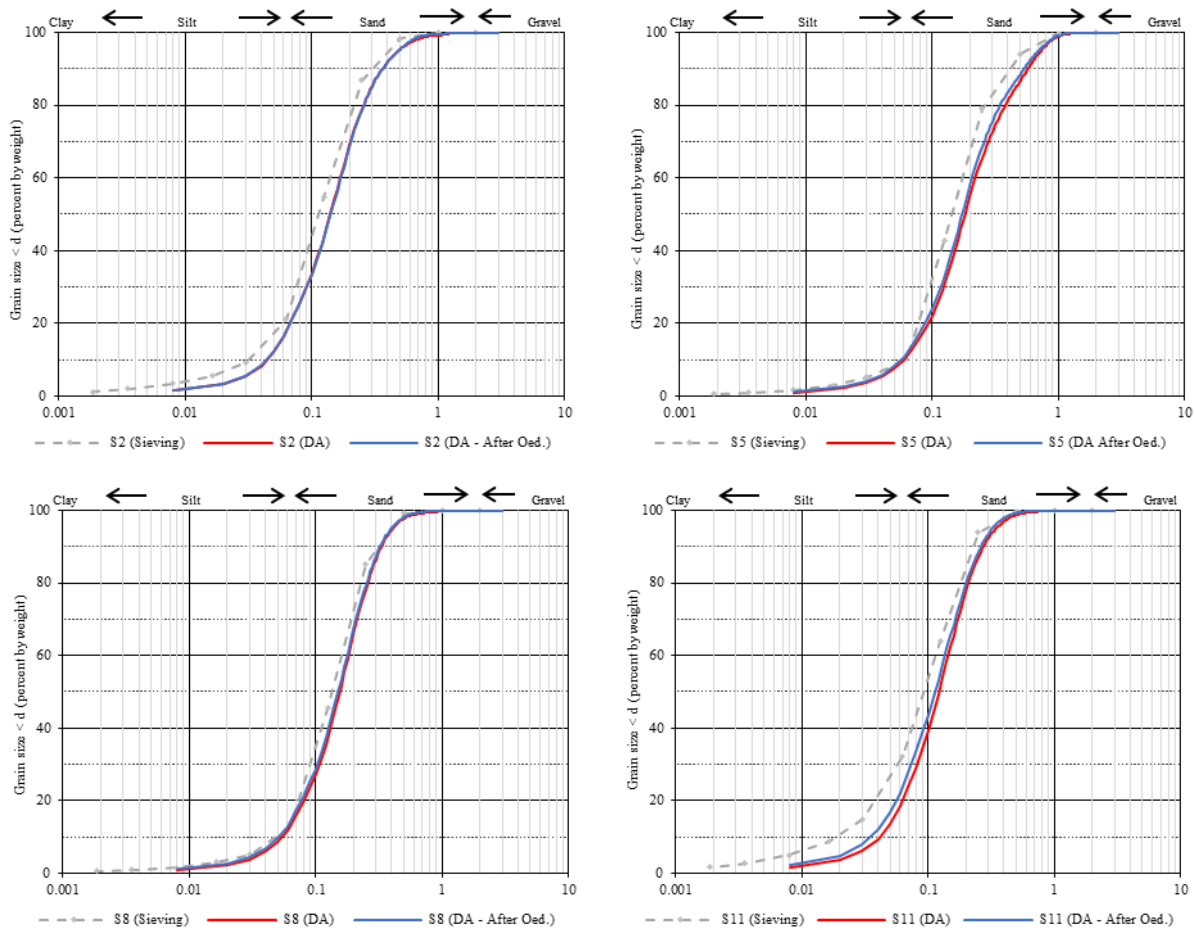


Figure 29. Particle Size Distribution for samples S2, S5, S8 and S11 using D.A after oedometer testing

The analysis for samples S2 and S5 is summarized in Table 15. Regarding sample S2, particles with a diameter greater than 1 mm potentially experienced some crushing effect as the amount of retained material between 0.063 and 0.5 mm increased, meanwhile the amount of fine particles does not considerably differ from original PSD sampling. There is a small indicator of some potential crushing occurrences in coarser particles, although, it is not a large difference. Consequently, the particle size values (i.e., D_{10} , D_{30} , D_{50} , D_{60} , and D_{90}) and the uniformity and curvature coefficients are quite similar. Sample S2 shows a maximum deviation of 0.459% for cumulative passing material and 0.445% for the retained material for the sieve sizes of 0.125 mm and 0.063 mm, correspondingly.

Sample S5 retains less material up to the 0.25 mm size sieve, where from this point the retained material starts to increase. Potentially, this implies that the particles with a diameter greater than 0.25 mm have undergone some crushing, therefore there is an increase in the amount of fine material below this threshold. The greatest deviations for passing material and retained material for sample S5 occur at 0.25 mm (2.935%) and 0.063 mm (1.679%), individually with respect to the initial PSD. The aforementioned distinctions for sample S5 can be seen among the particle size values, where all values have reduced in size by a maximum of 0.038 mm. Nevertheless, the variations between constraints do not affect either the coefficient of curvature or uniformity.

The analysis for samples S8 and S11 is summarized in Table 16. Regarding sample S8, particles with a diameter greater than 0.125 mm potentially experienced some crushing effect since less material is retained but this behavior shifts by increasing the amount of material retained for particles with a particle size as of 0.063 mm. Thus, there might be some crushing effect that can be detected in coarser particles therefore the particle size values somewhat differ while the uniformity and curvature coefficients are similar. Sample S8 shows a maximum deviation with its original PSD by 2.047% and 0.994% for cumulative passing material and retained material, respectively, where both occur at 0.125 mm sieve size.

Table 15. Comparison table for Samples S2 and S5 before and after oedometer testing

SAMPLE S2							SAMPLE S5					
Sieve size	S2 D.A. (%)		S2 D. A. OED (%)		Deviation S2		S5 D.A. (%)		S5 D. A. OED. (%)		Deviation S5	
(mm)	Pass. Acc.	Ret. Part.	Pass. Acc.	Ret. Part.	Pass. Acc.	Ret. Part.	Pass. Acc.	Ret. Part.	Pass. Acc.	Ret. Part.	Pass. Acc.	Ret. Part.
2	100.000	0.000	100.000	0.000	0.000	0.000	100.000	0.000	100.000	0.000	0.000	0.000
1	99.204	0.796	99.631	0.369	-0.427	0.427	98.948	1.052	99.207	0.793	-0.259	0.259
0.5	95.536	3.668	95.590	4.041	-0.054	-0.373	87.257	11.691	88.964	10.243	-1.707	1.448
0.25	80.424	15.112	80.260	15.330	0.164	-0.218	67.316	19.941	70.251	18.713	-2.935	1.228
0.125	48.079	32.345	47.620	32.640	0.459	-0.295	34.244	33.073	36.714	33.538	-2.470	-0.465
0.063	17.650	30.429	17.635	29.985	0.014	0.445	10.909	23.335	11.699	25.014	-0.791	-1.679
0.0304	5.440	12.210	5.508	12.127	-0.068	0.082	3.652	7.257	4.029	7.671	-0.377	-0.414
0.0163	2.685	2.755	2.788	2.720	-0.103	0.035	1.853	1.799	2.077	1.951	-0.224	-0.153
0.0079	1.401	1.283	1.477	1.310	-0.076	-0.027	0.963	0.890	1.086	0.991	-0.123	-0.101
0.0035	0.621	0.780	0.655	0.823	-0.034	-0.042	0.427	0.536	0.481	0.605	-0.055	-0.069
0.0018	0.319	0.302	0.337	0.318	-0.017	-0.016	0.219	0.207	0.248	0.234	-0.028	-0.027
D90 (mm)	0.3647		0.3647		0.0000		0.5746		0.5366		0.0380	
D60 (mm)	0.1691		0.1709		-0.0018		0.2212		0.2080		0.0132	
D50 (mm)	0.1398		0.1413		-0.0015		0.1829		0.1736		0.0093	
D30 (mm)	0.0911		0.0916		-0.0005		0.1225		0.1163		0.0062	
D10 (mm)	0.0444		0.0442		0.0002		0.0597		0.0571		0.0026	
Cu	3.8090		3.8670		-0.0580		3.7050		3.6430		0.0620	
Cc	1.1050		1.1110		-0.0060		1.1360		1.1390		-0.0030	

It can be noted that sample S11 retains less material up to sieve size 0.063 mm, which means that from this instance onwards the retained material starts to increase for smaller sieve sizes. This can indicate that a crushing process is generated for particles with a diameter greater than 0.063 mm, leading to an increase in the amount of fine material below this limit. The largest deviations for the passage material and the retained material for sample S11 occur in the sieves with a size of 0.063 mm (3.831%) and 0.125 mm (2.180%), respectively regarding to the initial PSD. The particle size values for sample S11 differ for larger diameters with a maximum variation of 0.0127 mm. Moreover, this increase in fine particles mainly affects the uniformity coefficient, while the curvature coefficient is quite similar.

Based on the above analysis of PSD with DA, before and after oedometer testing, it is tendency of that coarser particles subjected to vertical loads are more susceptible to changes which is seen in PSD. Most of these particle size variations arise in particles larger than 1 mm, 0.25 mm, 0.125 mm and 0.063 mm for samples S2, S5, S8 and S11, respectively. The largest fluctuations between the original and tested PSD curves are concentrated between the 0.25 mm and 0.063 mm sieve sizes with a higher incidence at the 0.125 mm sieve size. It is important to note that sample S11 is the only test that after laboratory testing did not retain any material with a particle size of 1 mm, followed by S8 which retained some material but in a minimal amount.

Table 16. Comparison table for Samples S8 and S11 before and after oedometer testing

SAMPLE S8							SAMPLE S11					
Sieve size	S8 D.A. (%)		S8 D. A. OED (%)		Deviation S8		S11 D.A. (%)		S11 D. A. OED (%)		Deviation S11	
(mm)	Pass. Acc.	Ret. Part.	Pass. Acc.	Ret. Part.	Pass. Acc.	Ret. Part.	Pass. Acc.	Ret. Part.	Pass. Acc.	Ret. Part.	Pass. Acc.	Ret. Part.
2	100.000	0.000	100.000	0.000	0.000	0.000	100.000	0.000	100.000	0.000	0.000	0.000
1	99.686	0.314	99.937	0.063	-0.251	0.251	99.855	0.145	100.000	0.000	-0.145	0.145
0.5	98.008	1.679	98.298	1.639	-0.291	0.040	98.838	1.017	99.314	0.686	-0.476	0.331
0.25	80.291	17.717	81.344	16.954	-1.053	0.762	88.372	10.466	89.768	9.546	-1.396	0.920
0.125	41.930	38.361	43.977	37.367	-2.047	0.994	56.293	32.079	59.869	29.899	-3.576	2.180
0.063	13.020	28.910	14.121	29.857	-1.101	-0.946	20.013	36.280	23.844	36.025	-3.831	0.255
0.0304	3.862	9.158	4.371	9.749	-0.509	-0.592	6.127	13.886	8.093	15.751	-1.966	-1.865
0.0163	1.823	2.039	2.090	2.281	-0.267	-0.242	2.954	3.172	3.986	4.107	-1.031	-0.935
0.0079	0.901	0.922	1.052	1.038	-0.151	-0.116	1.505	1.449	2.051	1.935	-0.546	-0.485
0.0035	0.399	0.502	0.466	0.586	-0.067	-0.084	0.667	0.838	0.909	1.142	-0.242	-0.304
0.0018	0.205	0.194	0.240	0.226	-0.034	-0.032	0.343	0.324	0.467	0.441	-0.124	-0.118
D90 (mm)	0.3311		0.3243		0.0068		0.2748		0.2621		0.0127	
D60 (mm)	0.1825		0.1780		0.0045		0.1441		0.1353		0.0088	
D50 (mm)	0.1553		0.1505		0.0048		0.1214		0.1129		0.0085	
D30 (mm)	0.1066		0.1026		0.0040		0.0821		0.0739		0.0082	
D10 (mm)	0.0541		0.0514		0.0027		0.0415		0.0351		0.0064	
Cu	3.3730		3.4630		-0.0900		3.4720		3.8550		-0.3830	
Cc	1.1510		1.1510		0.0000		1.1270		1.1500		-0.0230	

Figure 30 illustrates the plot of the dynamic image analysis using partially retained material before and after the oedometer test, where a variation occurs for all samples. As a result, more fine particles can be found in each gradation curve for the samples tested in oedometer.

Two comparisons were carried out with the slurry sample S11.1/2 after testing which are summarized in Table 17. The first comparison was performed regarding the original sample, while the second comparison considered the tamped tested sample. The second comparison will provide an understanding whether the particle arrangement affects or not, and to quantify this probable divergence. The median value was used for both analytical analysis and plotting the gradation curves. The plots will show the data for the original sample and the tamped sample to visualize the behavior due to different particle arrangement that can be seen in Figure 31.

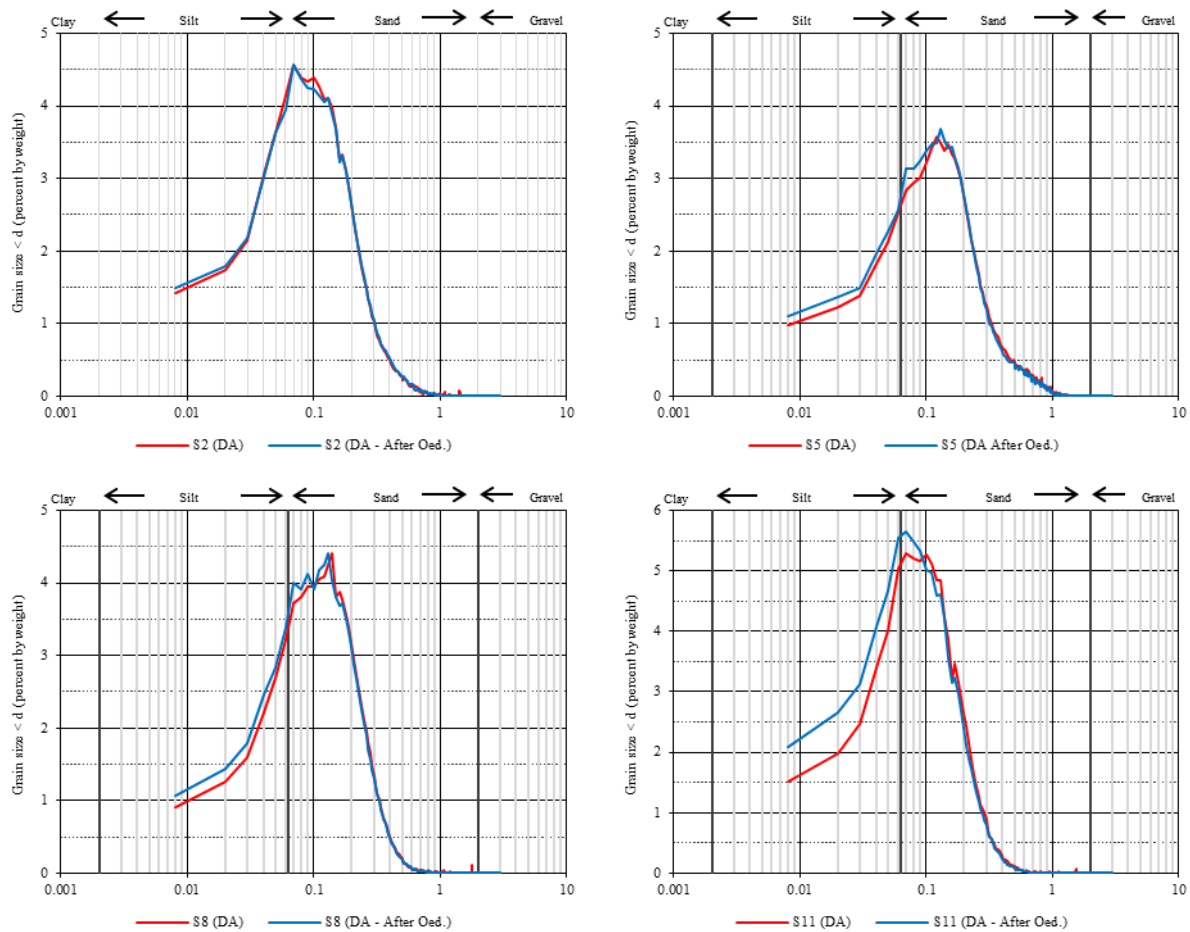


Figure 30. Partial retained curve material for samples S2, S5, S8 and S11 using D.A data before and after oedometer testing

Regarding the first comparison, it can be stated that the slurry samples potentially also show crushing effects, although the percentage of deviation is less substantial concerning tamped samples. By saying this, the slurry samples are less retained up to the 0.063 mm sieve size, changing this retention behavior after this instance. As the case of tamped sample, this behavior indicates that crushing occurs for particles with diameter greater than 0.063 mm, resulting in an increase in the number of fine particles. Slurry sample S11 shows a maximum fluctuation with its original PSD of 1.314% for the accumulated material passing and 1.376% for retained material. The particle size values have decreased in size with a maximum of 0.0038 mm. Due to this size variation the coefficient of curvature and uniformity also differ from the original PSD.

Table 17. Comparison table for tamped and slurry sample S11 before and after oedometer testing

SAMPLE S11.1/2										
Sieve size	S11 (%)		S11 OED (%)		S11.1/2 OED (%)		Deviation S11 – S11.1/2 (%)		Deviation S11 OED – S11.1/2 OED (%)	
(mm)	Pass. Acc.	Ret. Part.	Pass. Acc.	Pass. Acc.	Pass. Acc.	Ret. Part.	Pass. Acc.	Ret. Part.	Pass. Acc.	Ret. Part.
2	100.000	0.000	100.000	0.000	100.000	0.000	0.000	0.000	0.000	0.000
1	99.855	0.145	100.000	0.000	100.000	0.000	-0.145	0.145	0.000	0.000
0.5	98.838	1.017	99.314	0.686	99.216	0.784	-0.378	0.233	0.098	-0.098
0.25	88.372	10.466	89.768	9.546	88.710	10.507	-0.337	-0.041	1.059	-0.961
0.125	56.293	32.079	59.869	29.899	56.231	32.479	0.063	-0.400	3.639	-2.580
0.063	20.013	36.280	23.844	36.025	21.327	34.904	-1.314	1.376	2.517	1.121
0.0304	6.127	13.886	8.093	15.751	6.765	14.561	-0.639	-0.675	1.327	1.190
0.0163	2.954	3.172	3.986	4.107	3.276	3.490	-0.321	-0.317	0.710	0.617
0.0079	1.505	1.449	2.051	1.935	1.655	1.621	-0.150	-0.171	0.396	0.314
0.0035	0.667	0.838	0.909	1.142	0.733	0.922	-0.067	-0.084	0.175	0.221
0.0018	0.343	0.324	0.467	0.441	0.377	0.356	-0.034	-0.032	0.090	0.085
D90 (mm)	0.2748		0.2621		0.2710		0.0038		-0.0089	
D60 (mm)	0.1441		0.1353		0.1442		-0.0001		-0.0089	
D50 (mm)	0.1214		0.1129		0.1202		0.0012		-0.0073	
D30 (mm)	0.0821		0.0739		0.0791		0.0030		-0.0052	
D10 (mm)	0.0415		0.0351		0.0391		0.0024		-0.0040	
Cu	3.4720		3.8550		3.6880		-0.2160		0.1670	
Cc	1.1270		1.1500		1.1100		0.0170		0.0400	

Concerning the second case, it can be testified that after oedometer testing there is a deviation between samples, thus the particle arrangement seems to have an influence for crushing. Even though the potential crushing behavior between them is similar regarding the untested sample, there a couple of differences among them. The slurry sample material is more retained within sieves with a particle size larger than 0.063 mm, changing this behavior from this point onwards substantially, meaning that slurry samples were less susceptible for crushing than tamped samples. Nevertheless, both samples do not have the presence of particles with a diameter greater than 1 mm. The largest deviations among samples for the passage material and the retained material for sample S11 occur in the sieve with a size of 0.125 mm, showing a variation of 3.639% and 2.580% respectively. The particle size values for sample S11 differ for larger diameters with a maximum variation of 0.0089 mm, showing a different behavior for Cu and Cc values. Although, slurry sample presents lower values than tamped sample.

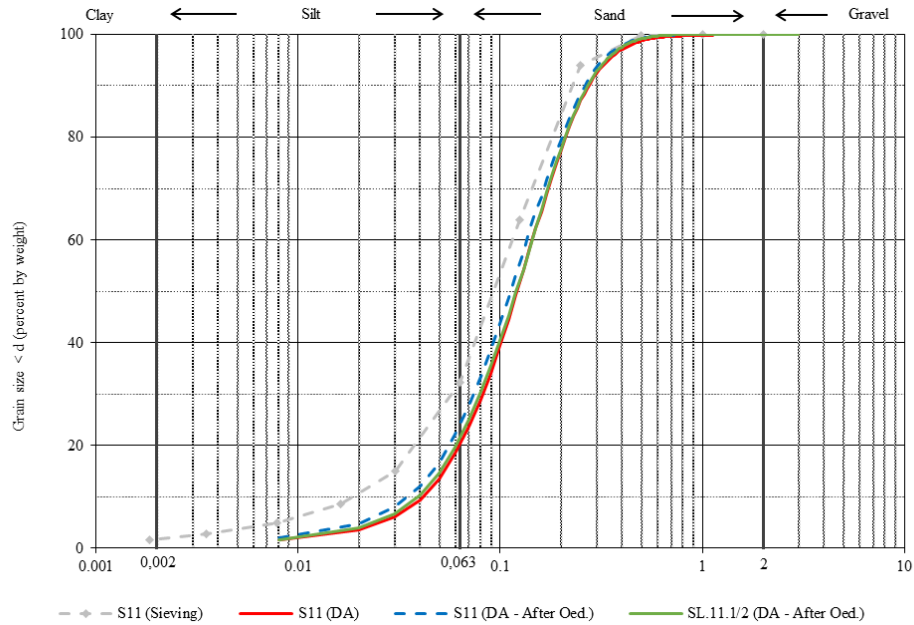


Figure 31. Particle Size Distribution for tamped and slurry sample S11 before and after oedometer testing

The different retained material curves based on raw data showed in Appendix D, are plotted in Figure 32. It can be seen that a gentler change in PSD is developed for slurry samples rather than tamped samples; nevertheless, the increment of fines is detected in both cases. Highlighting the inputs mentioned previously it can be seen that particle arrangement indeed affects somehow the crushing on particles. This may be due to an attachment of fines to coarser particles that could protect larger particles to the crushing exposure, while tamped samples do not have this attachment when they were constructed.

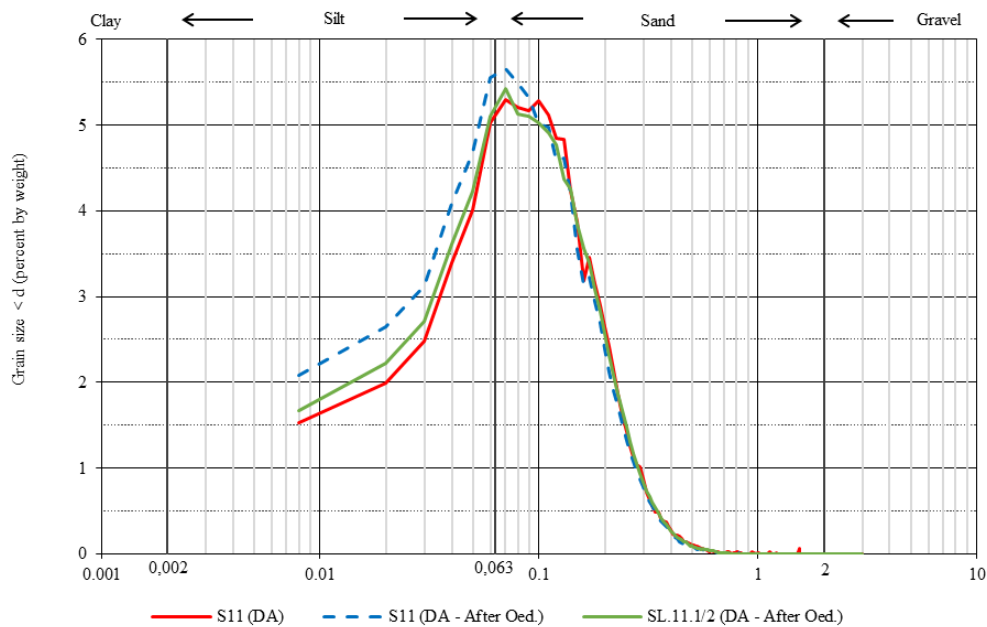


Figure 32. Partial retained curve material for tamped and slurry sample S11 before and after oedometer testing

5. Discussion

Within this thesis, some aspects related to the state of particles in tailings at different depths under vertical stresses have been studied. Tailings is a broad topic which studies have been carried out during the last half century. Nevertheless, the main objective with this discussion is to highlight certain aspects that may provide a better insight of the mechanical behavior within tailings particles answering the questions raised in chapter 1.

The literature review showed that PSD, particle shape and mineralogy are determinants of mechanical behavior within tailings particles. Studies have shown that these intrinsic parameters can greatly affect tailings behavior. Coarser particles could have internal flaws that can make them more susceptible to crushing effects than finer particles. Therefore, the crushing effects could be more severe when the material starts to be loaded for a coarse-grained tailings compared to a fine-grained. Lower stresses will root more crushing than higher stresses since most of the particle defects will break away at early loading stages. Thus, when higher stresses are reached, the particle will have less particle defects and finer material is made up due to this detachment varying the initial PSD. Meanwhile, particle shape and mineralogy are also aspects that matter and determine particle performance, as the soil fabric will largely depend on the particle arrangement, which will be influenced by surface roughness and particle shape (rounded or elongated). A rough surface has more contact points where particles may be susceptible to crushing or degradation, as stresses can effectively occur at these contact points than particles with smoother surfaces. Although it also depends on minerals within the particle where hardness minerals will be less prone to crushing than soft particles. As can be seen, crushing of tailings is a complex issue that needs to be carefully considered to ensure long-term stability and safety.

5.1 Basic properties of tailings

The results showed that there is a variation between samples along with depth which probably mainly is due to deposition and different discharge processes through time. The particles are within the range of silt and sand, similar to Bhanbhro (2017) and Rodriguez (2016) who also studied tailings from Aitik. The material is classified as silty sand up to a depth of 10 m, when it turns into sand up to a depth of 30 m, and from this depth, it reverses back to silty sand. This behavior of the particle size distribution can be attributed to several reasons, such as the deposition and location of the discharging points, different production processes, construction methods, etc. It was observed that tailings particles (> 0.063 mm) have a variety of shapes where the larger particles are mostly subangular and as the particle size reduces the particle shape also changes emerging a combination between subangular and very angular shapes according to Powers (1953) roundness scale. The statement for fine particles partially agrees with the findings obtained by Bhanbhro (2017) where fine particles are very angular. However, it agrees with the statement provided by Rodriguez (2016) where the tailings material is classified as very angular to subangular. In addition, the tailings samples have varying mineral composition, however, the most frequently found minerals were mica, feldspar, plagioclase and quartz. These minerals are consistent with the findings provided by Lindvall (2005) and Rodriguez (2016).

The particle density of each sample was determined and compared to investigations conducted at the Aitik tailings dam. Table 18 shows a comparison of the particle density at each depth for this study with values observed in other investigations for Aitik's tailings material. The average particle density found in this investigation coincides with previous findings in this tailings dam. However, it has been observed that the particle density between layers slightly differs. This could be due to the presence or absence of minerals in the samples, which in turn is related to the procedures used during their deposition.

Table 18. Particle density comparison with literature review

Sample	Depth (m)	Year deposition	Particle density Present study (t/m ³)	Particle density (Bhanbhro, 2017) (t/m ³)	Particle density (Bjelkevick & Knutsson, 2005) (t/m ³)
S2	4.2 – 4.5	2019	2.80		
S5	15.0 – 15.4	2013	2.73		
S8	24.5 – 25.0	2009	2.81	2.83	2.81 - 2.84
S11	33.5 – 34.0	2001	2.90		
			2.81 (Avg.)		

The year of deposition for the deepest and shallowest layers in analysis were deposited in 2001 and 2019, respectively. Therefore, there is an 18-year production period between samples. This implies that changes may have occurred over time as the deposition of tailings management and production may have varied. As a result, it is expected that the particle density differs slightly from layer to layer. However, the mean value agrees well with the results of other studies previously conducted in the impoundment.

5.2 Particle breakage and crushing effects

In this thesis, the effect of incremental overloading and the effects of crushing have been studied using the oedometer test. The vertical load produced by the oedometer test reproduces the K-zero conditions that occur in the impoundment on a tailing's embankment.

The particle size distribution (PSD) was examined at various sieve sizes to analyze the differences before and after conducting oedometer testing using dynamic image analysis. It could be observed that a deviation from the original PSD occurs after subjecting the sample to vertical loading, where the greatest change occurs in the coarser particles increasing the fines. A common factor among all samples is that most of the gradation curves experience a change between sieves with an aperture of 1.00 mm and 0.063 mm, where the largest cumulative deviations are reflected in samples S5 and S11 with a variation of 2.93% and 3.83% with respect to their original PSD, correspondingly. However, the largest fluctuations between the gradation curves in each sample are concentrated in the sieve size with an aperture of 0.125 mm. Meanwhile, a lower amount of fines is developed in sample S2 with a cumulative variation of 0.459%. There may be variation in the extent of crushing between different samples, but all samples experience a physical change when subjected to vertical stepwise loads. In addition, another factor to be considered is the fact

that creep effects could be generated within the particles, as structural strength and inter-particle contacts can be reduced with time (Fedda, 2003). However, the generation of fines depends largely on the mineral composition of the tailings (mineralogy, hardness, structure, etc.), but also on environmental conditions (Wentworth, 1923).

Thus, it is clear that larger particles are more likely to undergo physical alteration after being subjected to vertical loading, which correlates with the findings obtained by Bhanbhro (2017). This could be due to possible internal fractures within particles that are more susceptible to breakage and contact points as higher stresses could be developed at the edges of the particle. Bhanbhro (2017) studied the effects of crushing on tailings material with different sizes where coarser particles showed more breakage compared to finer particles and is related to the statement reported by Lee & Farhoomand (1967) where larger particles are more susceptible to particle breakage. The influence of the particle shape highly affects the inter-particle contact, nevertheless, it also depends on the mineralogy that each particle is composed of since the crushing is more severe for particles with low hardness such as mica rather than particles with quartz.

A comparison between sieving and DA was carried out in this study in order to find an alternative to determine the PSD before and after oedometer testing due to certain laboratory limitations. Although, the findings were accurate enough in this study, it cannot be assured the method is 100% reliable. Three out of four samples analyzed through DA had similar values with the sieving test; nevertheless, the fourth sample threw odd results that could bring out the idea about uncertainties in the method. Further research must be done in order to compare the accuracy and reliability of DA with sieving method, which is the most traditional method used to determine PSD.

5.3 Particle breakage for different particle arrangement

The crushing effect was analyzed in samples that were constructed with slurry tailings material to determine whether a major incidence occurs due to a different particle arrangement. The discussion in this section is carried out considering sample S11 based on two different scenarios. The first case was based on the original PSD of the sample and the slurry sample after being tested, while the second instance was a comparison between both assembling tailings conditions (tamping and slurry).

Particle arrangement was observed to influence the mechanical behavior of tailings samples, as the crushing effect is lower in slurry samples. This implies that slurry material might have developed a different interlocking behavior between particles, where finer particles might protect larger particles from crushing exposure. This could be due to the initial void ratio which is lower for slurry samples than in the tamped samples, meaning that inter-particle bonding is greater and that finer particles could bind to coarser particles filling the voids and making the soil fabric stiffer than tamped samples.

5.4 Compressibility and stress-strain behavior

The compressibility coefficient of the samples is within a range of 0.094 and 0.1698, which when related to the findings obtained by Bhanbhro (2017) corresponds to a compressibility developed at particle size within a particle size range of 0.125 mm and 1.00 mm. However, there is a higher incidence with particles within a range of 0.5 mm and 0.25 mm. Coarser particles are more

susceptible to crushing, which means that greater compressibility may develop in these particles (Lee & Farhoomand, 1967). Therefore, the tailings samples in both scenarios (tamped and slurried) developed higher compressibility in the coarser particles than in the fine particles, which relates to Mitchell and Soga's (2005) statement that coarser particles have a greater chance of breaking, resulting in higher compressibility. Table 19 summarizes a comparison of the compression ratios obtained in this study and Bhanbhro (2017).

Table 19. Compression index according to Bhanbhro (2017) and obtained in this study

Material (Particle size range) mm	Cc range Bhanbhro (2017)	Cc Sample S2	Cc Sample S5	Cc Sample S8	Cc Sample S11	Cc Slurry Sample S11
1 – 0.5	0.174 – 0.138	0.142				
0.5 – 0.25	0.101 – 0.121		0.114		0.117	0.113
0.25 – 0.125	0.080 – 0.103			0.084		
0.125 – 0.063	0.054 – 0.060					

The compression index of the samples is clearly reflected in the stress-strain behavior of the samples (ref. Figure 25), where the highest and lowest stress-strain behavior corresponds to samples S2 and S8 correspondingly. Meanwhile, slurry samples have a similar stress-strain trend to that of the tamped samples (ref. Figure 26), which is also likely as their compression ratio. This implies that larger particles undergo greater breakage compared to finer particles, therefore, an arrangement of particles may occur due to a loose skeleton with overlapping particles (Bhanbhro, 2017).

6. Conclusions

The aim with this thesis was to characterize and determine variances on tailings material at different year deposition and investigate the crushing effects on tailings that arises from increased vertical stress. The research questions that have been raised in section 1.3 are answered below.

1. *How can crushing effects due to increased vertical stress over time be analyzed and isolated from other influencing sources on the characteristics of tailings?*

Tailings can be analyzed by characterizing and study the variances on deposited tailings located at different depths in an impoundment and assessing the intrinsic properties of the material (i.e., PSD, particle shape and mineralogy) before and after subjecting the samples to increased vertical stress. In this study, it could be noticed that PSD, particle shape and mineralogy are determinants factors within the mechanical behavior of tailings that may respond in a different manner during consolidation depending on the stress conditions and the void ratio.

This is clearly seen in the different PSD of the samples taken into consideration, where an 18-year interval is evaluated. The particles are within a range of sand and silt; however, the surface and bottom layers in the analysis are classified as silty-sand, while the middle layers are categorized as sand. In addition, the particle density varies slightly between layers, which means that the mineralogy between layers could differ, although the most common gangue minerals found among the samples are quartz, feldspar, mica and plagioclase. On the other hand, the shape of the particles between them is quite similar, with the larger particles being mostly subangular, while the smaller ones tend to be a combination of subangular and very angular. The mineralogy and particle shape effect on tailings need to be studied to fully understand if tailings undergo crushing or not.

The compressibility coefficient obtained in this investigation corresponds to particles within a range size of 0.125 mm and 1.00 mm, which means that coarser particles are more susceptible to crushing effects rather than fine particles. By this, the compressibility of the material is also reflected in its stress-strain behavior. Hence, the higher coefficient of compressibility implies a higher stress-strain behavior on the material.

2. *How does the stepwise increase in vertical load affect tailing particles?*

This study indicates that vertical loading on tailings particles potentially induces particle breakage in all samples. However, this conclusion is limited to small observations in change of PSD before and after oedometer and it is unclear if those changes solely depend on crushing. Theoretically the change in PSD agrees well with expected behavior for particles exposed to crushing, since the change occurs mainly in coarser particles, larger than 0.063 mm, which are within the sand range. Thus, the percentage of fines increases where the variations between gradation curves, between the original and after being subjected to a maximum load of 640 kPa, reach up to 3.83% in the

accumulated passing material. In addition, the largest fluctuations are reflected in the sieve size with an aperture of 0.125 mm. Coarser tailings are more susceptible to possible crushing due to the fact that they may have more internal flaws that they may break apart from the main particle.

3. *How does particle arrangement influence the effect of vertical load on tailings particles?*

Particle arrangement does affect potential particle breakage based on the findings of this study. Tamped samples are more susceptible to change in PSD than slurry samples, implying that tamped samples have a more prone soil fabric, and this could be due to a lack of attachment of fines to coarser particles that could protect them from being crushed, even when the compressibility ratio for both arrangement conditions is similar. Although the largest particles are most affected by a potentially crushing in both scenarios.

7. Suggested further work

The mechanical behavior of tailings is complex which makes essential to understand this material from a geotechnical and geochemical point of view to guarantee an adequate design and management of TSFs. In this thesis, vertical loading under K_0 conditions was applied on tailings samples from different depths to study crushing effects. Furthermore, different particle arrangement was simulated in the preparation phase to see how crushing effects could be influenced.

During this thesis, several additional questions was raised which are suggested as further work and are described below:

- Perform an extensive comparison of the effects of particle arrangement (tamping or slurry) on the compressibility and crushing from increased vertical stress.
- Quantify the mineral content within samples since it may help to comprehend why some samples are more susceptible to crushing rather than others.
- Analyze the tailings particle shape after being subjected to vertical loading and identify the role of mineralogy in change of particle shape. This could help to understand how large particles are affected and which shape particles are developed after crushing occurs.

8. Bibliography

- Adiansyah, J. S., Rosano, M., Vink, S., & Keir, G. (2015). A framework for a sustainable approach to mine tailings management: Disposal strategies. *Journal of Cleaner Production*, 108, 1050-1062.
- Altuhafi, F., O'sullivan, C., & Cavarretta, I. (2013). Analysis of an image-based method to quantify the size and shape of sand particles. *Journal of Geotechnical and Geoenvironmental Engineering*, 139(8), 1290-1307.
- Altuhafi, F. N., Coop, M. R., & Georgiannou, V. N. (2016). Effect of particle shape on the mechanical behavior of natural sands. *Journal of Geotechnical and Geoenvironmental Engineering*, 142(12), 04016071.
- Barrett, P. J. (1980a). The shape of rock particles, a critical review. *Sedimentology*, 27(3), 291-303.
- Bhanbhro, R. (2014). *Mechanical properties of tailings: Basic description of a tailings material from sweden* (Doctoral dissertation). <https://www.diva-portal.org/smash/record.jsf?pid=diva2%3A989943&dswid=-5886>
- Bhanbhro, R. (2017). Mechanical behavior of tailings: Laboratory tests from a swedish tailings dam. *Licenciature Thesis: Luleå University of Technology*,
- Bjelkevik, A., & Knutsson, S. (2005). Swedish tailings: Comparison of mechanical properties between tailings and natural geological materials. Paper presented at the *International Conference on Mining and the Environment, Metals and Energy Recovery: 27/06/2005-01/07/2005*, 117-129.
- Blight, G. E., & Bentel, G. M. (1983). The behaviour of mine tailings during hydraulic deposition. *Journal of the South African Institute of Mining and Metallurgy*, 83(4), 73-86.
- Boliden, A. B. (2023). *Boliden annual and sustainability report 2022*.
(<https://www.boliden.com/investor-relations/reports-and-presentations/annual-reports>
Hämtad från <https://www.boliden.com/investor-relations/reports-and-presentations/annual-reports>
- Bowman, E. T., Soga, K., & Drummond, W. (2001). Particle shape characterisation using fourier descriptor analysis. *Geotechnique*, 51(6), 545-554.
- Cho, G., Dodds, J., & Santamarina, J. C. (2007). Closure to “particle shape effects on packing density, stiffness, and strength: Natural and crushed sands” by gye-chun cho, jake dodds,

- and J. carlos santamarina. *Journal of Geotechnical and Geoenvironmental Engineering*, 133(11), 1474.
- Craig, R. F. (2004). *Craig's soil mechanics* (7th Edition uppl.). London, GBR: CRC press.
- Davies, M. P., Lighthall, P. C., Rice, S., & Martin, T. E. (2002). Design of tailings dams and impoundments. *Keynote Address, Tailings and Mine Waste Practices SME, AGM Phoenix*, , 1-18.
- Engels, J. (2023). What are tailings? från <https://www.tailings.info/basics/tailings.htm>
- Feda, J. (2003). Irregular creep in granular materials. *Acta Technica ČSAV*, 48(4), 395-410.
- Folk, R. L. (1955). Student operator error in determination of roundness, sphericity, and grain size. *Journal of Sedimentary Research*, 25(4), 297-301.
- Halabi, A. L. M., Siacara, A. T., Sakano, V. K., Pileggi, R. G., & Futai, M. M. (2022). Tailings dam failures: A historical analysis of the risk. *Journal of Failure Analysis and Prevention*, 22(2), 464-477. Hämtad från <https://doi.org/10.1007/s11668-022-01355-3>
- Hamade, T. (2013). Geotechnical design of tailings dams-a stochastic analysis approach.
- Islam, K., & Murakami, S. (2021). Global-scale impact analysis of mine tailings dam failures: 1915–2020. *Global Environmental Change*, 70, 102361.
- ISO 9276-6. (2008). Representation of results of particle size analysis—part 6: Descriptive and quantitative representation of particle shape and morphology. *Iso 9276–6: 2008*,
- Janoo, V. C. (1998). Quantification of shape, angularity, and surface texture of base course materials.
- Jantzer, I., Bjelkevik, A., & Pousette, K. (2008). (2008). Material properties of tailings from swedish mines. Paper presented at the *Nordiska Geoteknikermötet: 03/09/2008-06/09/2008*, 229-235.
- Jiang, M. J., Konrad, J. M., & Leroueil, S. (2003). An efficient technique for generating homogeneous specimens for DEM studies. *Computers and Geotechnics*, 30(7), 579-597. 10.1016/S0266-352X(03)00064-8 Hämtad från <https://www.sciencedirect.com/science/article/pii/S0266352X03000648>
- Knutsson, R. (2018). On the behaviour of tailings dams: Management in cold regions. *Licenciature Thesis: Luleå University of Technology*,

- Ladd, R. S. (1978). Preparing test specimens using undercompaction. *ASTM Geotechnical Testing Journal*, 1(1)
- Lade, P. V., Yamamuro, J. A., & Bopp, P. A. (1996a). Significance of particle crushing in granular materials. *Journal of Geotechnical Engineering*, 122(4), 309-316.
- Larsson, R. (2008). *Jords egenskaper* Statens geotekniska institut (In Swedish).
- Lee, K. L., & Farhoomand, I. (1967). Compressibility and crushing of granular soil in anisotropic triaxial compression. *Canadian Geotechnical Journal*, 4(1), 68-86.
- Li, W., & Coop, M. R. (2019). Mechanical behaviour of panzhihua iron tailings. *Canadian Geotechnical Journal*, 56(3), 420-435.
- Lindvall, M. (2005). Strategies for remediation of very large deposits of mine waste: The aitik mine, northern sweden.
- Ljungberg, J., & Öhlander, B. (2001). The geochemical dynamics of oxidising mine tailings at laver, northern sweden. *Journal of Geochemical Exploration*, 74(1), 57-72. 10.1016/S0375-6742(01)00175-3 Hämtad från <https://www.sciencedirect.com/science/article/pii/S0375674201001753>
- Lv, Y., Li, X., & Wang, Y. (2020). Particle breakage of calcareous sand at high strain rates. *Powder Technology*, 366, 776-787.
- Lyu, Z., Chai, J., Xu, Z., Qin, Y., & Cao, J. (2019). A comprehensive review on reasons for tailings dam failures based on case history. *Advances in Civil Engineering*, 2019, 1-18.
- McKeown, M., Christensen, D., Taylor, T., & Mueller, S. (2015). (2015). Evaluation of cover system field trials with compacted till layers for waste rock dumps at the boliden aitik copper mine, northern sweden. Paper presented at the *10th International Conference on Acid Rock Drainage & IMWA Annual Conference*,
- Mitchell, J. K., & Soga, K. (2005). *Fundamentals of soil behavior* John Wiley & Sons New York.
- Ni, H., & Huang, Y. (2020). Rheological study on influence of mineral composition on viscoelastic properties of clay. *Applied Clay Science*, 187, 105493. 10.1016/j.clay.2020.105493 Hämtad från <https://www.sciencedirect.com/science/article/pii/S0169131720300582>

- Nikonow, W., Rammlmair, D., & Furche, M. (2019). A multidisciplinary approach considering geochemical reorganization and internal structure of tailings impoundments for metal exploration. *Applied Geochemistry*, 104, 51-59.
- Pan, Z., Zhang, C., Guo, X., Ma, C., Ma, L., & Gan, S. (2022). Influence of particle size scale on mechanical properties of tailings under high pressure. *Proceedings of the Institution of Civil Engineers - Geotechnical Engineering*, 175(2), 200-213. 10.1680/jgeen.20.00216 Hämtad från <https://doi.org/10.1680/jgeen.20.00216>
- Perumal, P., Niu, H., Kiventerä, J., Kinnunen, P., & Illikainen, M. (2020). Upcycling of mechanically treated silicate mine tailings as alkali activated binders. *Minerals Engineering*, 158, 106587. 10.1016/j.mineng.2020.106587 Hämtad från <https://www.sciencedirect.com/science/article/pii/S0892687520304076>
- Powers, M. C. (1953). A new roundness scale for sedimentary particles. *Journal of Sedimentary Research*, 23(2), 117-119.
- Rana, N. M., Ghahramani, N., Evans, S. G., Small, A., Skermer, N., McDougall, S., & Take, W. A. (2022). Global magnitude-frequency statistics of the failures and impacts of large water-retention dams and mine tailings impoundments. *Earth-Science Reviews*, 232, 104144. 10.1016/j.earscirev.2022.104144 Hämtad från <https://www.sciencedirect.com/science/article/pii/S0012825222002288>
- Ritcey, G. M. (2005). Tailings management in gold plants. *Hydrometallurgy*, 78(1-2), 3-20.
- Rodriguez, J. (2012). Particle shape quantities and influence on geotechnical properties: A review.
- Rodriguez, J. (2016). Effect of physical weathering on mechanical properties of tailings. *Licenciature Thesis: Luleå University of Technology*,
- Rodriguez, J., Johansson, J., & Edeskär, T. (2012). Particle shape determination by two-dimensional image analysis in geotechnical engineering. Paper presented at the *Nordic Geotechnical Meeting: 09/05/2012-12/05/2012*, 207-218.
- Russell, A. R. (2011). A compression line for soils with evolving particle and pore size distributions due to particle crushing. *Géotechnique Letters*, 1(1), 5-9.
- Song, Y., & Hong, S. (2020). Effect of clay minerals on the suction stress of unsaturated soils. *Engineering Geology*, 269, 105571. 10.1016/j.enggeo.2020.105571 Hämtad från <https://www.sciencedirect.com/science/article/pii/S0013795219306222>

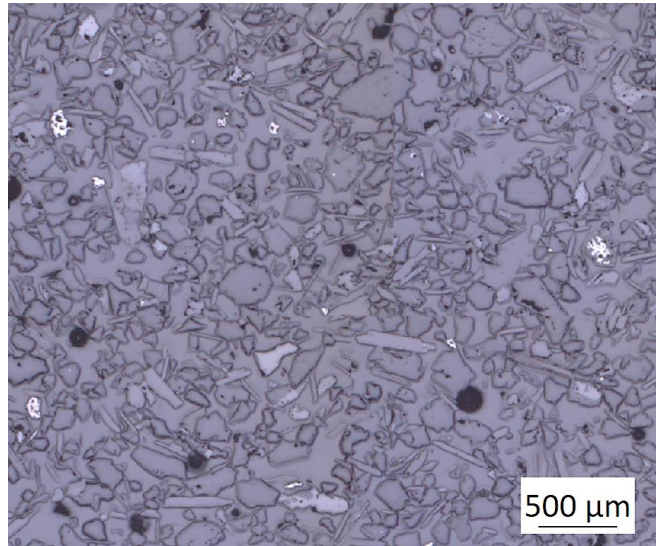
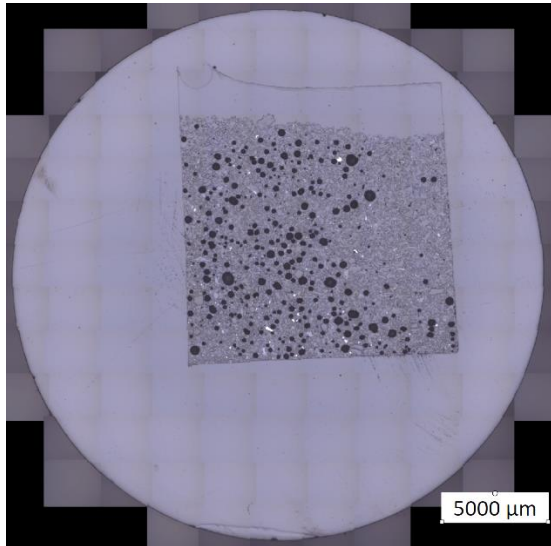
- Stark, T. D., Moya, L., & Lin, J. (2022). Rates and causes of tailings dam failures . *Advances in Civil Engineering*, 2022, 1-21. Hämtad från <https://doi.org/10.1155/2022/7895880>
- Ulusoy, U., Yekeler, M., & Hiçyılmaz, C. (2003). Determination of the shape, morphological and wettability properties of quartz and their correlations. *Minerals Engineering*, 16(10), 951-964.
- Vick, S. G. (1990). *Planning, design, and analysis of tailings dams* BiTech Publishers Ltd.
- Villavicencio, G., Espinace, R., Palma, J., Fourie, A., & Valenzuela, P. (2014). Failures of sand tailings dams in a highly seismic country. *Canadian Geotechnical Journal*, 51(4), 449-464.
- Wentworth, C. K. (1923). *Method of measuring and plotting the shapes of pebbles* (Volume 730C uppl.). Washington, US: US Geological Survey Bulletin.
- Witt, K. J., Schönhardt, M., Saarela, J., Frilander, R., Csicsak, J., Csövari, M., . . . Zlagnean, M. (2004). Tailings management facilities—risks and reliability. *Sustainable Improvement in Safety of Tailings Facilities TAILS SAFE*, Eds. Witt, KJ, Schönhardt, M.A European Research and Technological Development Project, Contract Number: EVG1-CT-2002-00066,
- Yang, Y., Wei, Z., Fourie, A., Chen, Y., Zheng, B., Wang, W., & Zhuang, S. (2019). Particle shape analysis of tailings using digital image processing. *Environmental Science and Pollution Research*, 26(25), 26397-26403.
- Zhang, C., Pan, Z., Yin, H., Ma, C., Ma, L., & Li, X. (2022). Influence of clay mineral content on mechanical properties and microfabric of tailings. *Scientific Reports*, 12(1), 1-17.
- Zhang, X., Baudet, B. A., & Yao, T. (2020). The influence of particle shape and mineralogy on the particle strength, breakage and compressibility. *International Journal of Geo-Engineering*, 11(1), 1-10.
- Zhen, Z., Wu, X., Ma, B., Zhao, H., & Zhang, Y. (2022). Propagation network of tailings dam failure risk and the identification of key hazards. *Scientific Reports*, 12(1), 5580.

Appendices

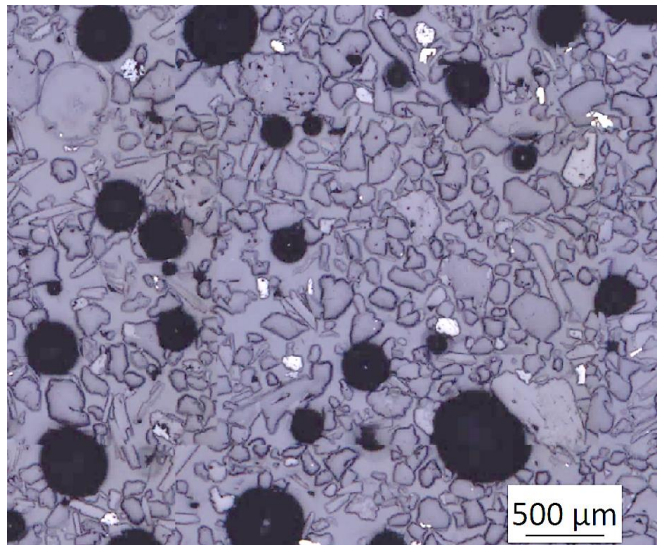
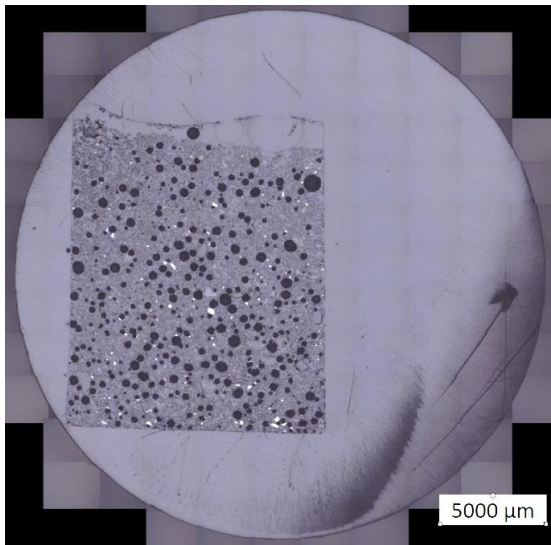
A. Reflected light imaging analysis

NOTE: Black bubbles are trapped air voids from the epoxy resin used for the sample preparation

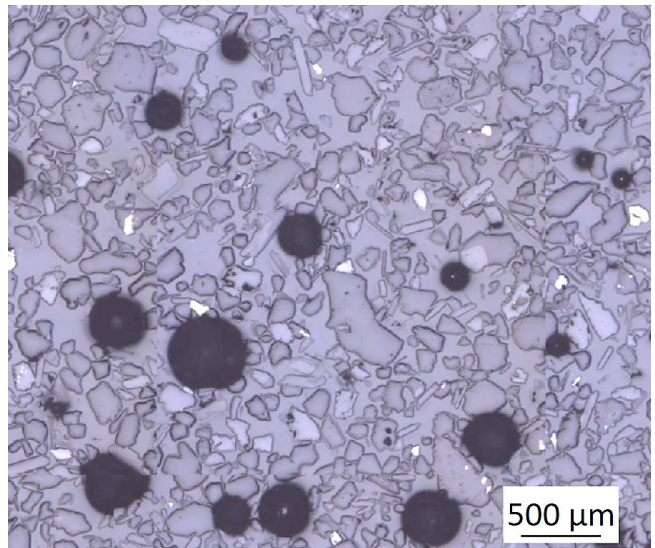
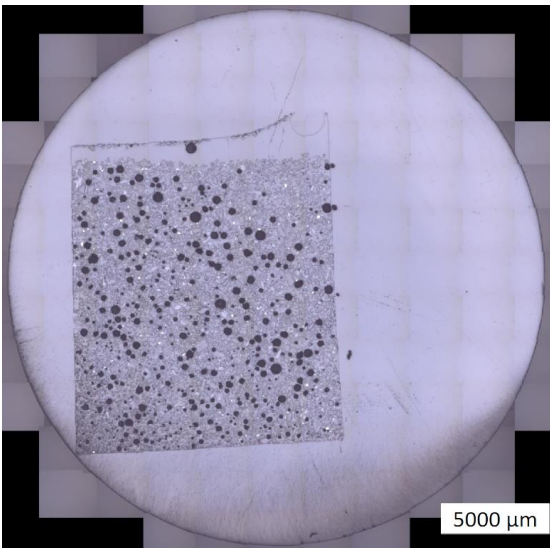
Sample 02



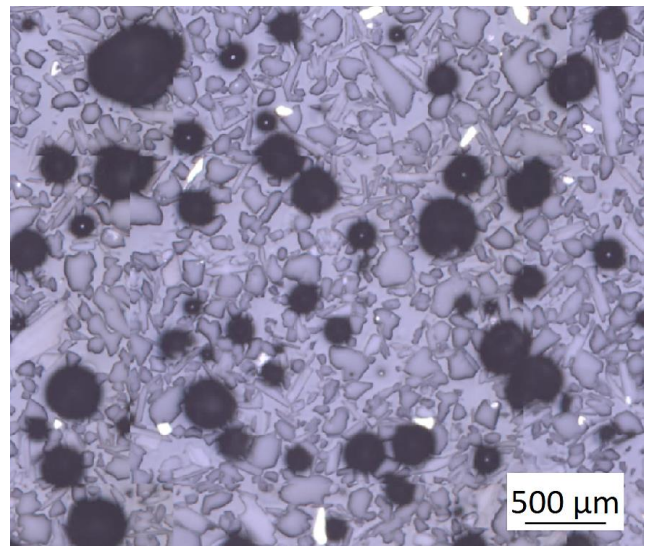
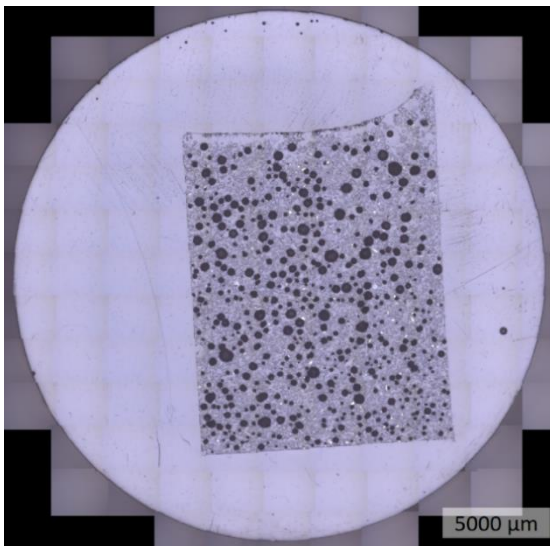
Sample 05



Sample 08

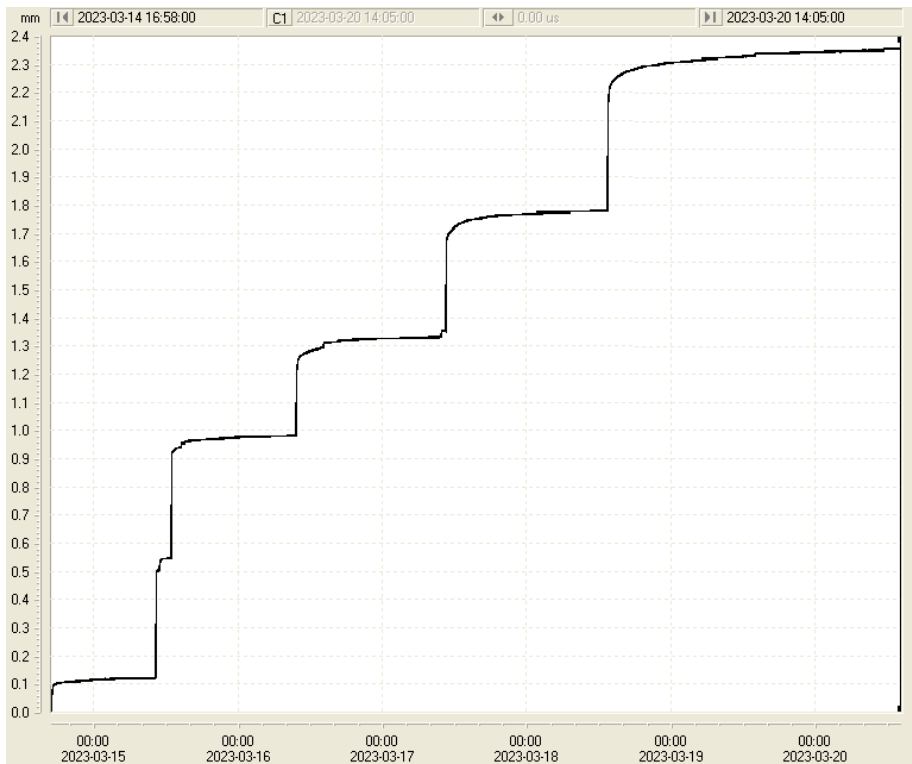


Sample 11

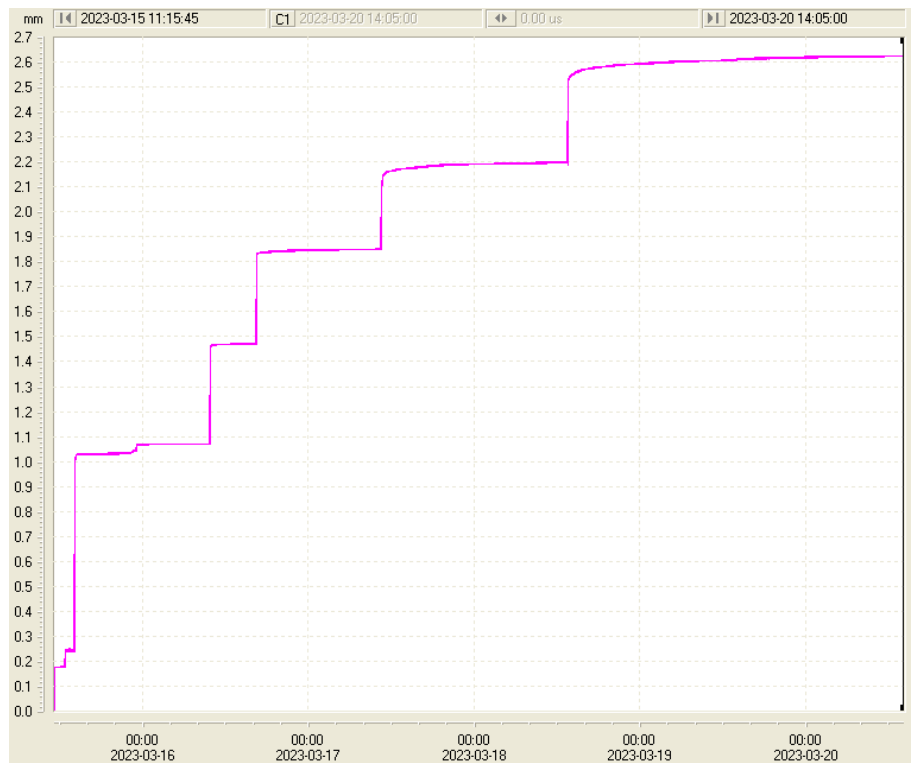


B. LVDTs curves for each sample

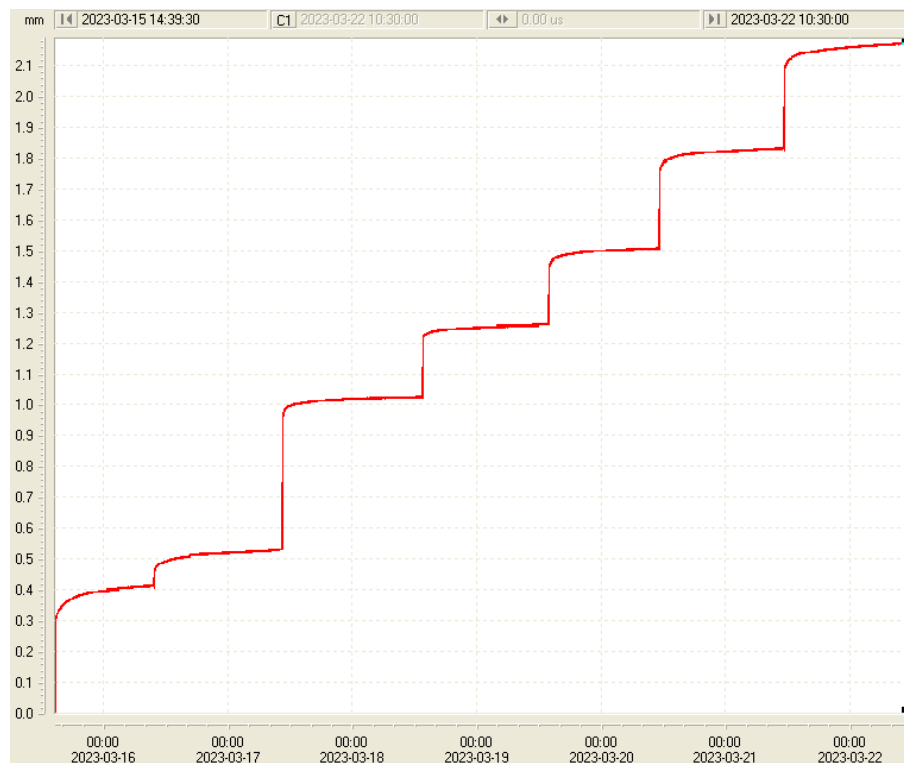
Sample 2



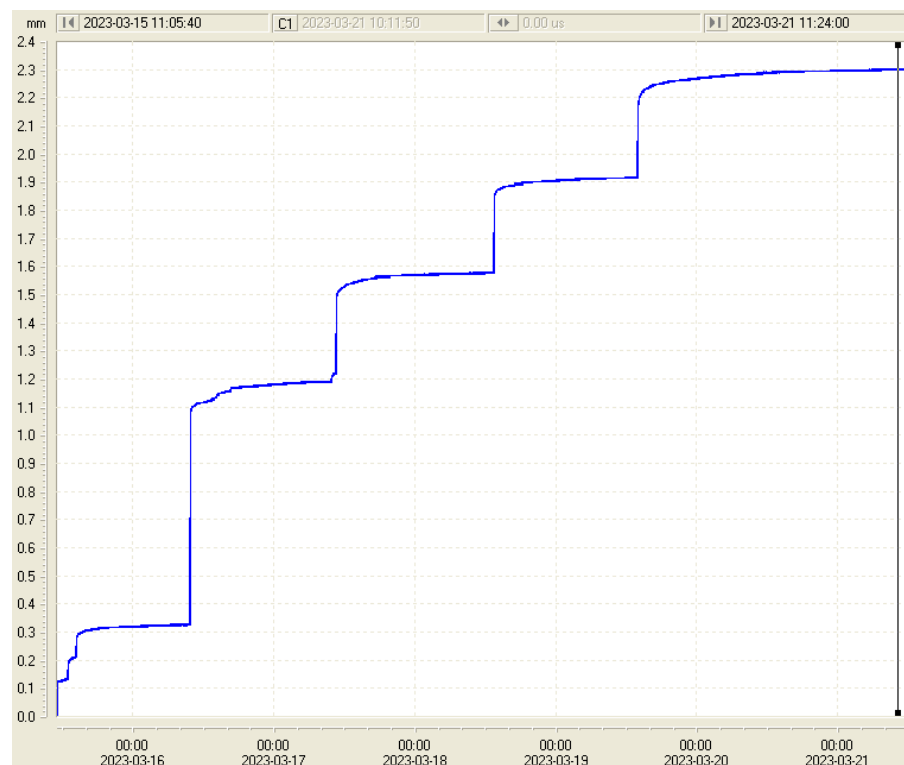
Sample 5



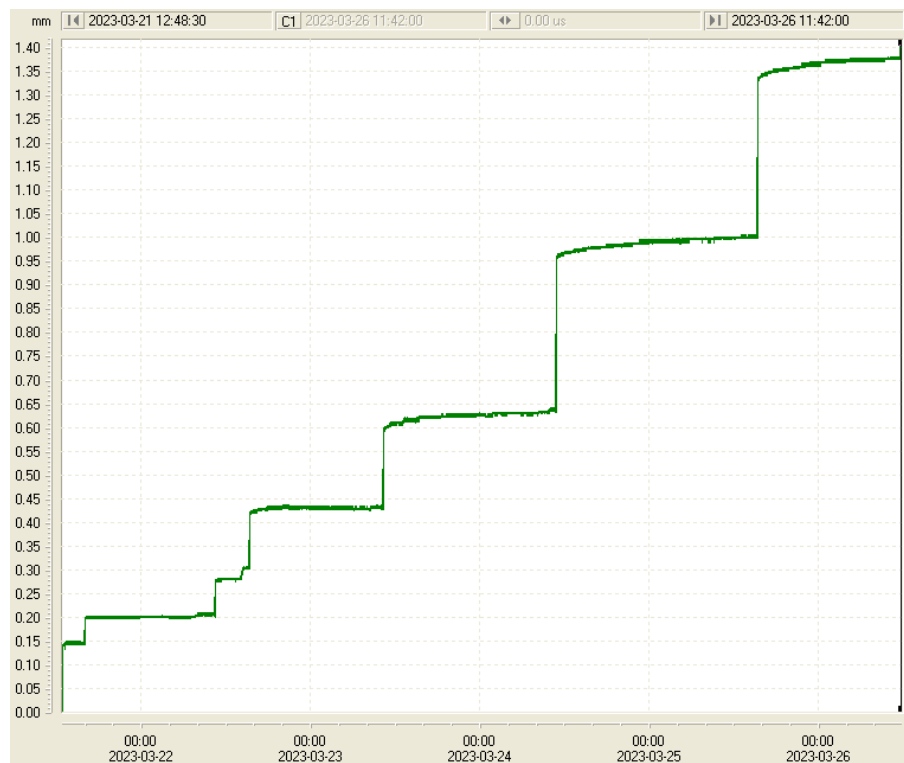
Sample 8



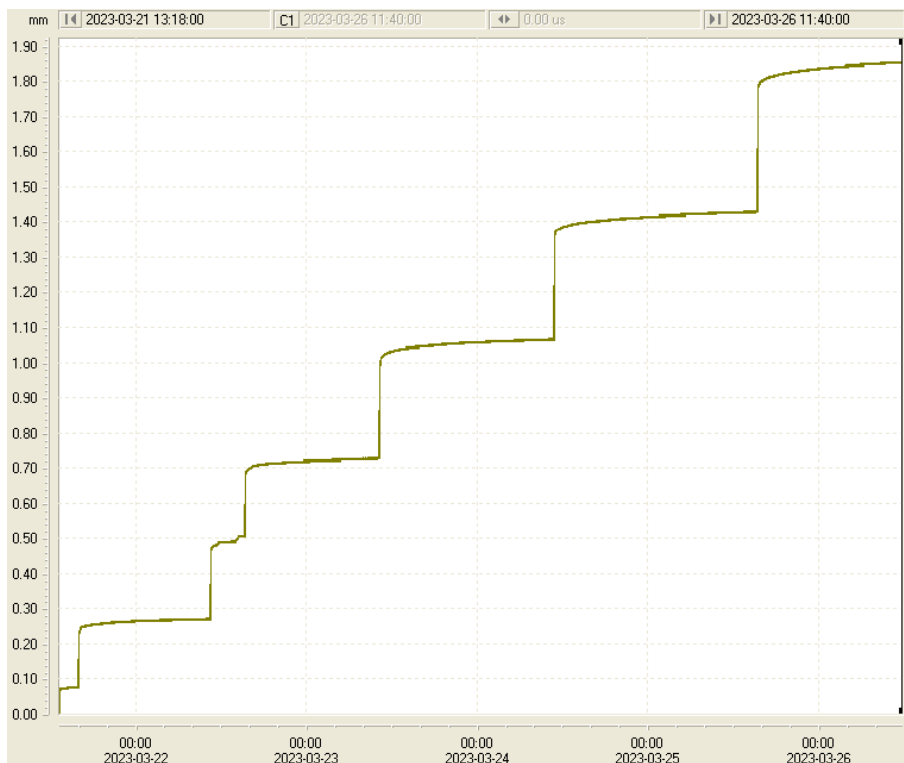
Sample 11



Slurry - Sample 11.1

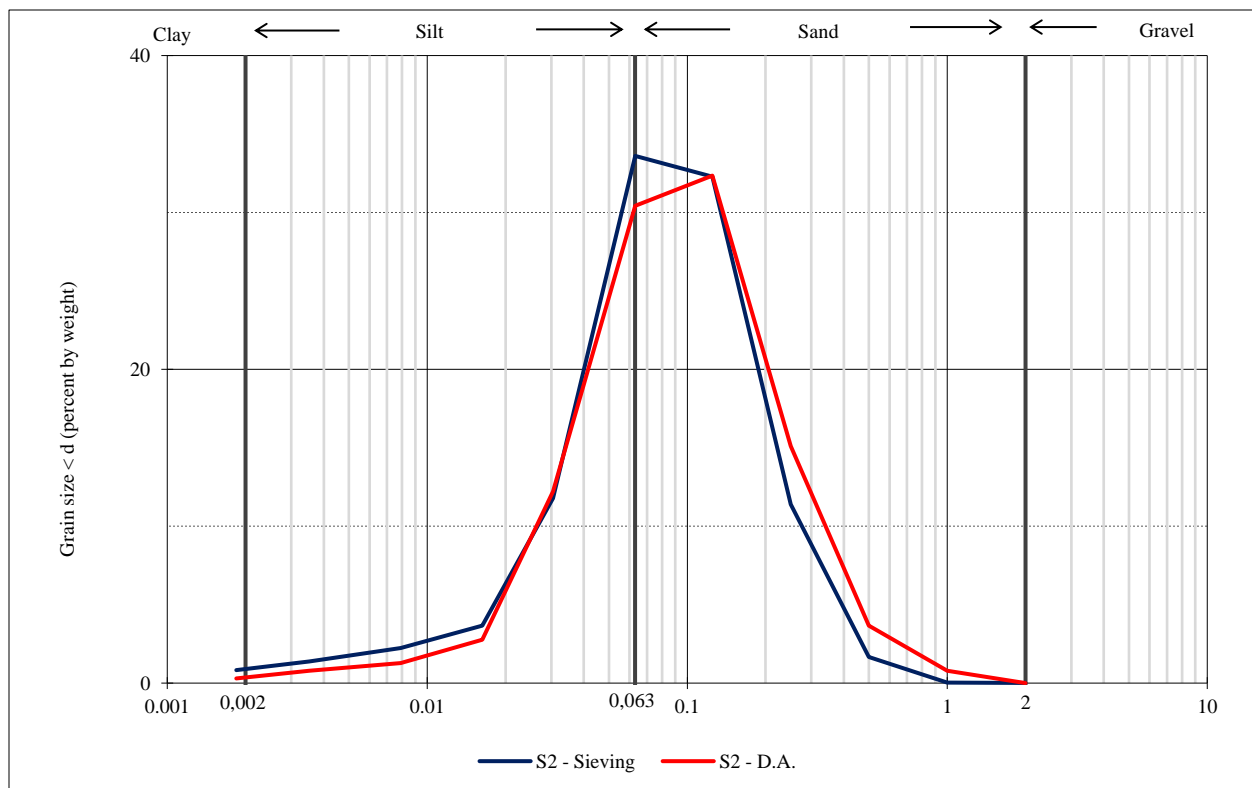
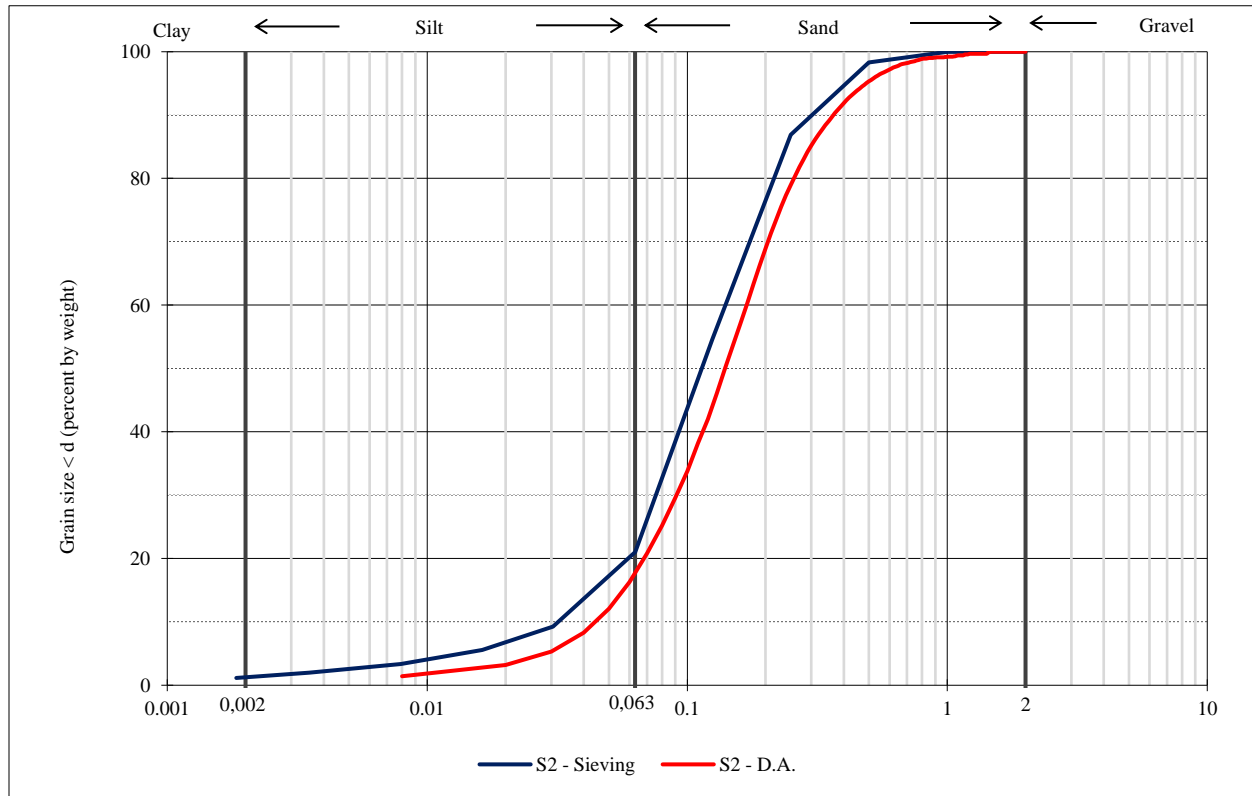


Slurry - Sample 11.2

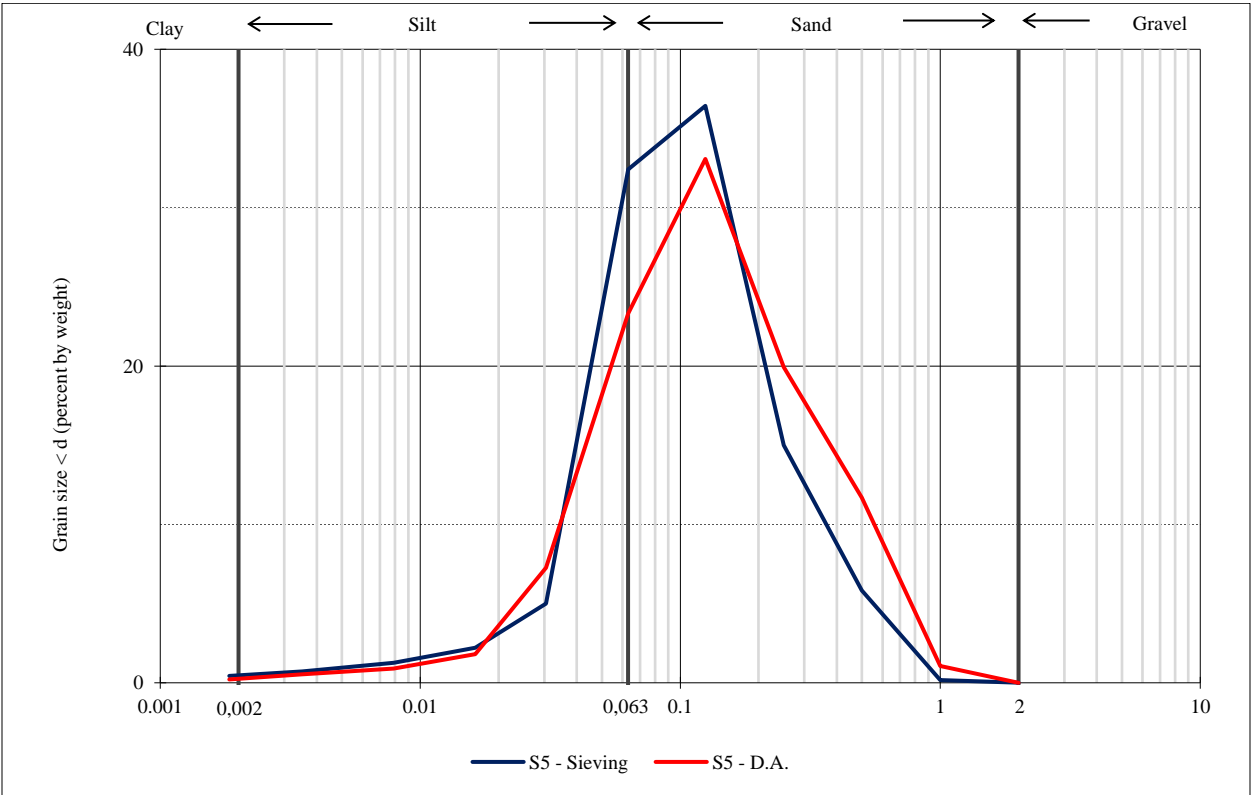
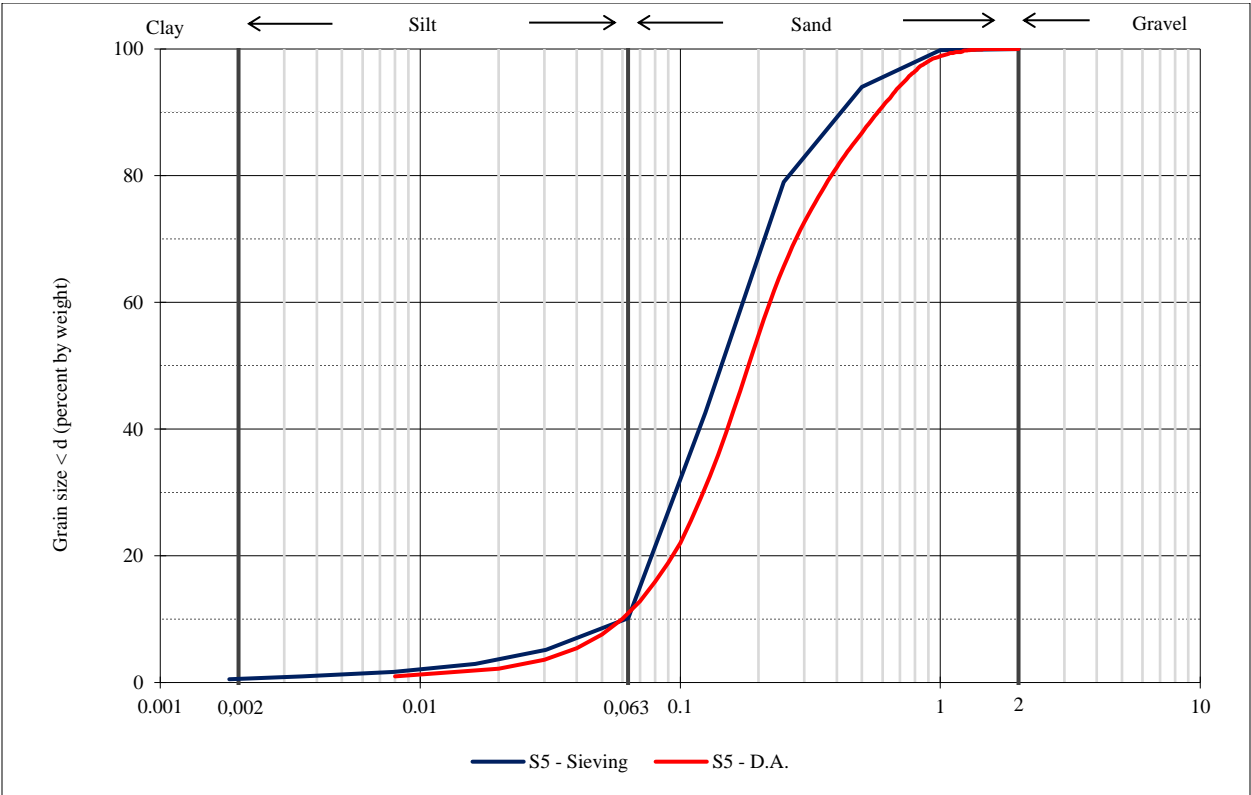


C. Dynamic Image Analysis Plots

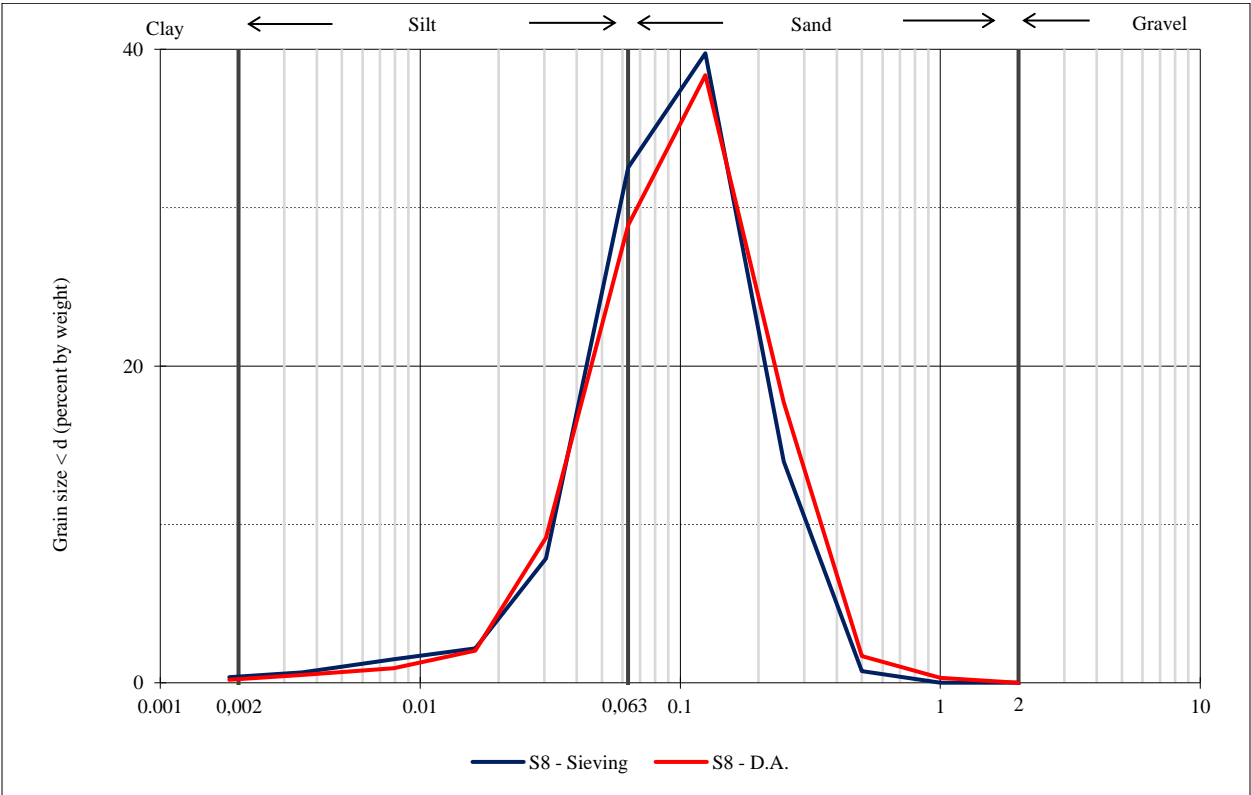
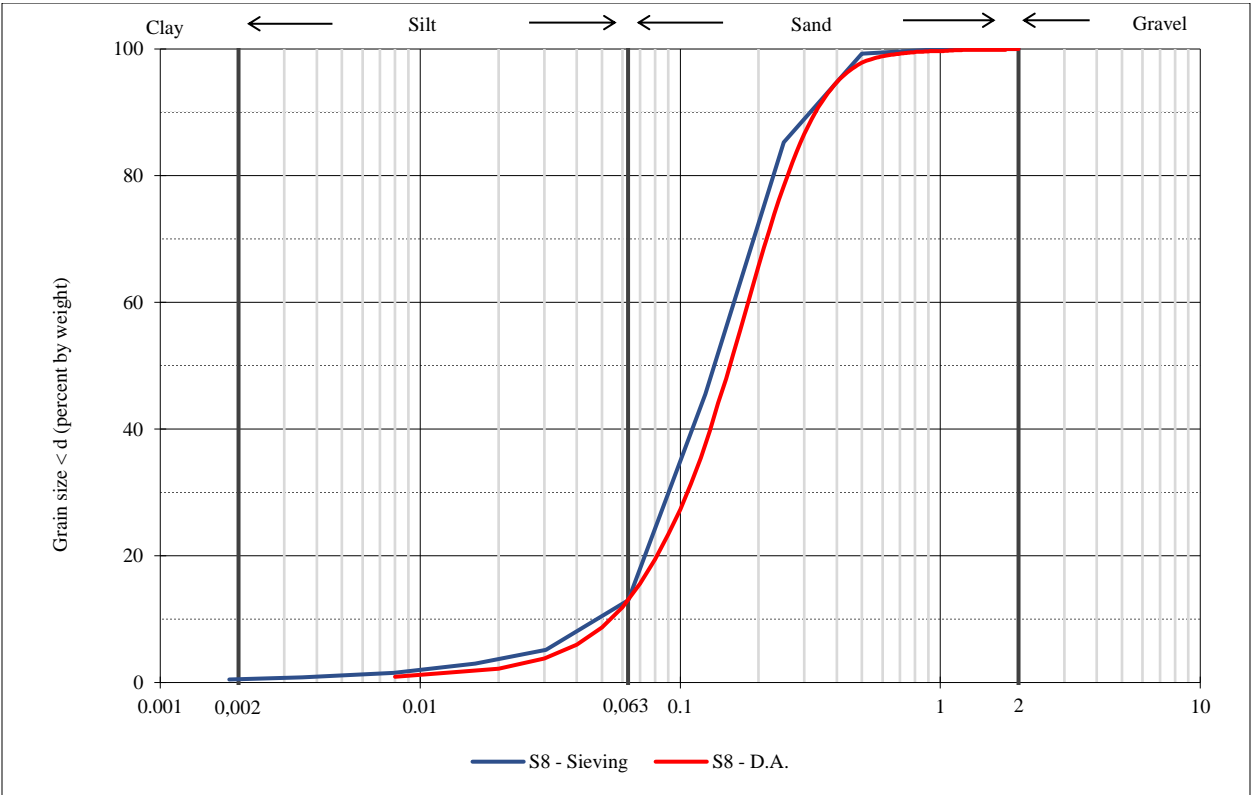
Dynamic Image Analysis Sample S2



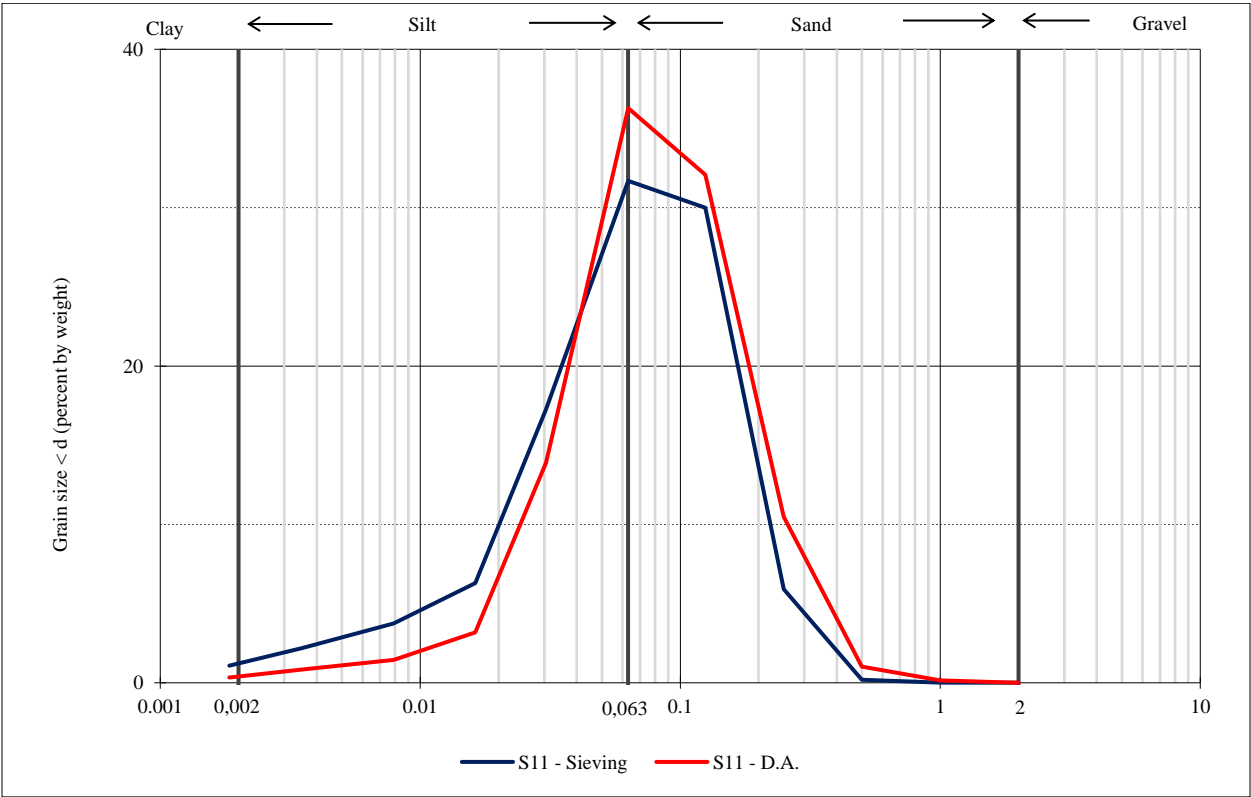
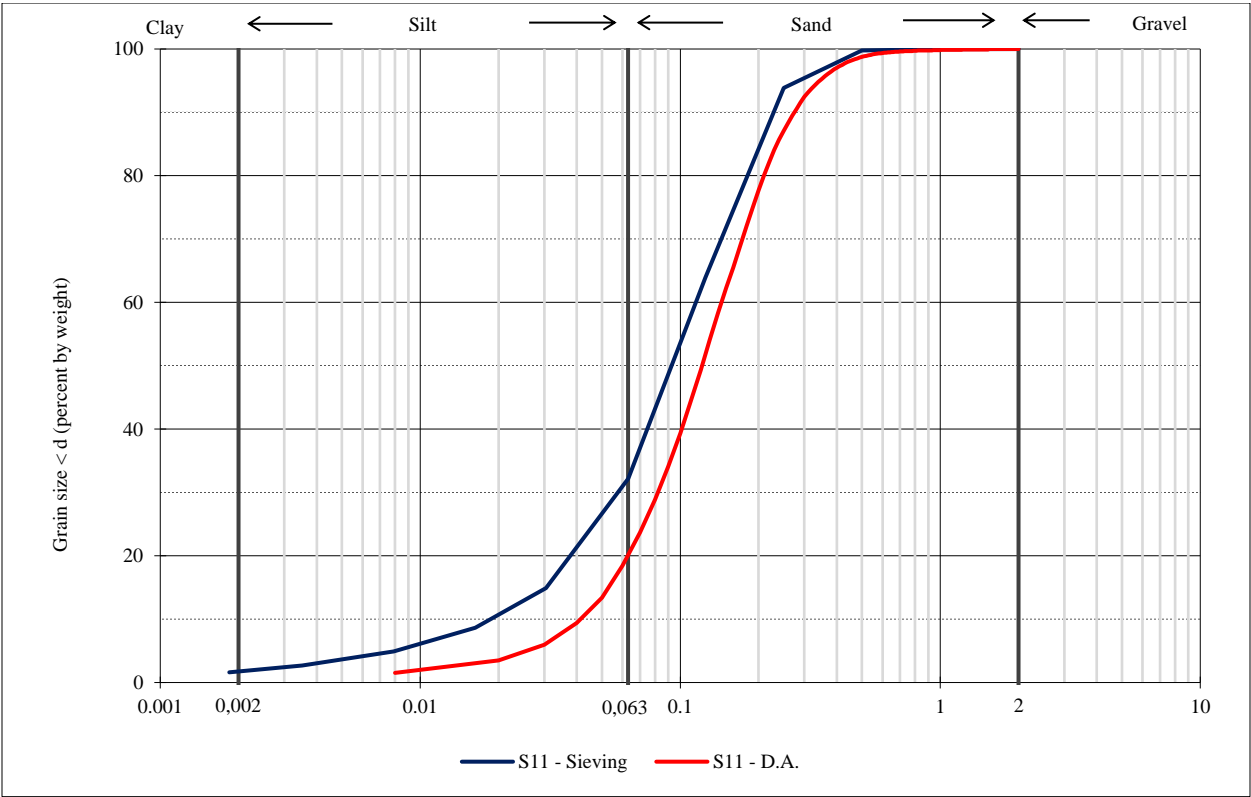
Dynamic Image Analysis Sample S5



Dynamic Image Analysis Sample S8



Dynamic Image Analysis Sample S11



D. Dynamic Image Analysis (Raw Data)

S2 - D.A.		S2 - D.A. OEDOM		S5 - D.A.		S5 - D.A. OEDOM		
x [mm] at Q3 = 10.0 %	0.044		0.044		0.060		0.057	
x [mm] at Q3 = 30.0 %	0.091		0.092		0.123		0.116	
x [mm] at Q3 = 50.0 %	0.140		0.141		0.183		0.174	
x [mm] at Q3 = 60.0 %	0.169		0.171		0.221		0.208	
x [mm] at Q3 = 90.0 %	0.365		0.365		0.575		0.537	
Q3 [%] at x = 0.10 mm	38.204		37.525		25.559		27.674	
Q3 [%] at x = 0.50 mm	95.536		95.590		87.257		88.964	
Q3 [%] at x = 1.00 mm	99.204		99.631		98.948		99.207	
S2 - D.A.		S2 - D.A. OEDOM		S5 - D.A.		S5 - D.A. OEDOM		
Size class	Av. Q3 [%]	Av. p3 [%]	Av. Q3 [%]	Av. p3 [%]	Av. Q3 [%]	Av. p3 [%]	Av. Q3 [%]	Av. p3 [%]
0.008	1.419	1.419	1.496	1.496	0.975	0.975	1.100	1.100
0.01	3.179	1.746	3.292	1.796	2.196	1.221	2.459	1.359
0.02	5.320	2.154	5.385	2.174	3.578	1.382	3.950	1.491
0.03	8.323	3.062	8.457	3.037	5.422	1.819	5.920	1.970
0.04	12.093	3.636	12.093	3.632	7.566	2.122	8.183	2.263
0.05	16.282	4.146	16.267	3.954	10.086	2.534	10.758	2.575
0.06	20.841	4.559	20.828	4.559	12.828	2.826	13.896	3.138
0.07	25.222	4.385	25.222	4.381	15.907	2.934	17.377	3.127
0.08	29.554	4.332	29.369	4.243	18.919	3.010	20.615	3.238
0.09	33.793	4.382	33.384	4.239	22.031	3.229	24.190	3.380
0.1	38.204	4.266	37.525	4.141	25.559	3.416	27.674	3.467
0.11	41.979	4.082	41.791	4.050	29.149	3.585	31.367	3.493
0.12	46.086	4.107	45.706	4.107	32.556	3.495	34.924	3.678
0.13	50.072	3.986	49.534	3.903	35.931	3.375	38.503	3.520
0.14	53.763	3.699	53.168	3.691	39.455	3.470	41.933	3.417
0.15	56.986	3.243	56.436	3.223	42.779	3.324	45.530	3.432
0.16	60.299	3.338	59.726	3.313	46.050	3.271	48.864	3.297
0.17	63.392	3.093	62.853	3.093	49.139	3.104	52.029	3.132
0.18	66.273	2.881	65.809	2.881	52.080	2.971	55.062	2.959
0.19	68.928	2.655	68.496	2.656	54.836	2.767	57.913	2.781
0.2	71.346	2.418	70.925	2.420	57.403	2.567	60.534	2.595
0.21	73.549	2.203	73.149	2.203	59.746	2.362	62.871	2.388
0.22	75.551	1.981	75.186	2.002	61.883	2.145	64.968	2.166
0.23	77.348	1.778	77.039	1.810	63.867	1.989	66.881	1.982
0.24	78.969	1.621	78.728	1.645	65.674	1.833	68.632	1.778
0.25	80.424	1.472	80.260	1.480	67.316	1.662	70.251	1.630
0.26	81.774	1.349	81.626	1.350	68.834	1.518	71.749	1.498
0.27	83.026	1.214	82.872	1.246	70.226	1.412	73.122	1.396
0.28	84.158	1.103	84.027	1.135	71.487	1.318	74.383	1.284
0.29	85.188	1.029	85.073	1.030	72.665	1.237	75.547	1.191
0.3	86.123	0.930	86.038	0.948	73.757	1.166	76.625	1.092

0.31	86.962	0.837	86.927	0.881	74.766	1.076	77.629	1.004
0.32	87.715	0.761	87.715	0.804	75.732	0.990	78.582	0.952
0.33	88.397	0.720	88.397	0.712	76.658	0.926	79.471	0.894
0.34	89.057	0.691	89.057	0.676	77.545	0.887	80.295	0.846
0.35	89.712	0.643	89.712	0.655	78.403	0.858	81.067	0.793
0.36	90.320	0.589	90.320	0.625	79.224	0.821	81.798	0.731
0.37	90.884	0.547	90.884	0.575	79.976	0.752	82.466	0.690
0.38	91.409	0.525	91.409	0.554	80.670	0.700	83.078	0.658
0.39	91.912	0.500	91.912	0.514	81.338	0.674	83.663	0.619
0.4	92.366	0.454	92.366	0.479	81.984	0.646	84.223	0.577
0.41	92.786	0.414	92.786	0.454	82.622	0.638	84.777	0.554
0.42	93.158	0.372	93.158	0.407	83.225	0.602	85.296	0.529
0.43	93.497	0.351	93.523	0.379	83.797	0.564	85.792	0.496
0.44	93.844	0.347	93.883	0.360	84.325	0.528	86.271	0.483
0.45	94.188	0.344	94.210	0.344	84.853	0.519	86.725	0.465
0.46	94.509	0.321	94.509	0.318	85.367	0.481	87.206	0.481
0.47	94.794	0.285	94.794	0.285	85.827	0.474	87.675	0.469
0.48	95.065	0.271	95.065	0.290	86.282	0.493	88.133	0.458
0.49	95.313	0.251	95.330	0.275	86.755	0.473	88.578	0.445
0.5	95.536	0.224	95.590	0.260	87.257	0.453	88.964	0.386
0.51	95.773	0.237	95.854	0.264	87.727	0.423	89.362	0.398
0.52	96.017	0.238	96.115	0.244	88.176	0.413	89.763	0.401
0.53	96.237	0.220	96.341	0.226	88.606	0.414	90.123	0.360
0.54	96.423	0.186	96.544	0.203	88.999	0.411	90.518	0.377
0.55	96.597	0.174	96.753	0.181	89.395	0.396	90.928	0.409
0.56	96.752	0.155	96.972	0.173	89.826	0.397	91.305	0.377
0.57	96.887	0.136	97.185	0.159	90.204	0.363	91.665	0.361
0.58	97.025	0.138	97.357	0.164	90.570	0.366	92.017	0.352
0.59	97.191	0.130	97.521	0.164	90.956	0.364	92.319	0.303
0.6	97.364	0.141	97.708	0.173	91.324	0.368	92.606	0.287
0.61	97.502	0.138	97.893	0.138	91.633	0.364	92.947	0.341
0.62	97.605	0.152	98.080	0.103	91.943	0.374	93.276	0.329
0.63	97.687	0.131	98.180	0.082	92.265	0.352	93.551	0.277
0.64	97.805	0.136	98.265	0.085	92.609	0.344	93.825	0.276
0.65	97.935	0.127	98.347	0.091	92.964	0.318	94.098	0.316
0.66	98.041	0.106	98.451	0.102	93.311	0.291	94.349	0.286
0.67	98.111	0.075	98.578	0.081	93.646	0.288	94.558	0.209
0.68	98.171	0.060	98.691	0.093	93.935	0.289	94.759	0.210
0.69	98.225	0.069	98.790	0.093	94.175	0.282	94.994	0.256
0.7	98.265	0.062	98.870	0.079	94.419	0.256	95.273	0.256
0.71	98.337	0.039	98.910	0.062	94.678	0.259	95.491	0.199
0.72	98.400	0.031	98.961	0.051	94.931	0.253	95.651	0.160
0.73	98.443	0.043	98.987	0.043	95.195	0.261	95.825	0.174
0.74	98.513	0.058	99.017	0.058	95.471	0.252	95.997	0.181

0.75	98.633	0.074	99.074	0.057	95.721	0.225	96.201	0.208
0.76	98.677	0.046	99.127	0.056	95.946	0.225	96.412	0.211
0.77	98.721	0.052	99.145	0.063	96.145	0.199	96.603	0.168
0.78	98.791	0.037	99.184	0.039	96.305	0.166	96.816	0.189
0.79	98.867	0.032	99.245	0.043	96.469	0.176	97.004	0.154
0.8	98.912	0.020	99.274	0.020	96.687	0.208	97.121	0.137
0.81	98.919	0.019	99.291	0.017	96.935	0.248	97.275	0.202
0.82	98.923	0.016	99.334	0.038	97.151	0.191	97.476	0.201
0.83	98.951	0.028	99.376	0.042	97.330	0.153	97.622	0.146
0.84	98.999	0.027	99.399	0.025	97.465	0.153	97.722	0.138
0.85	99.026	0.017	99.424	0.025	97.557	0.137	97.838	0.153
0.86	99.030	0.016	99.463	0.016	97.675	0.118	97.980	0.142
0.87	99.032	0.020	99.483	0.020	97.814	0.131	98.123	0.143
0.88	99.047	0.039	99.487	0.039	97.965	0.117	98.227	0.109
0.89	99.079	0.032	99.498	0.040	98.076	0.102	98.302	0.075
0.9	99.105	0.024	99.520	0.024	98.182	0.121	98.403	0.101
0.91	99.127	0.022	99.528	0.009	98.302	0.120	98.550	0.103
0.92	99.134	0.011	99.528	0.011	98.424	0.122	98.700	0.110
0.93	99.135	0.016	99.528	0.016	98.508	0.091	98.857	0.118
0.94	99.135	0.016	99.528	0.005	98.560	0.099	98.991	0.101
0.95	99.135	0.007	99.528	0.000	98.593	0.113	99.056	0.068
0.96	99.137	0.014	99.535	0.007	98.635	0.129	99.080	0.048
0.97	99.148	0.012	99.562	0.011	98.702	0.096	99.106	0.085
0.98	99.184	0.037	99.591	0.002	98.787	0.085	99.145	0.069
0.99	99.203	0.019	99.620	0.008	98.886	0.073	99.191	0.066
1	99.204	0.002	99.631	0.011	98.948	0.062	99.207	0.049
1.01	99.206	0.000	99.631	0.000	98.980	0.021	99.207	0.050
1.02	99.218	0.001	99.631	0.000	99.015	0.035	99.207	0.032
1.03	99.220	0.003	99.631	0.000	99.059	0.044	99.207	0.002
1.04	99.242	0.023	99.631	0.000	99.107	0.048	99.207	0.000
1.05	99.270	0.026	99.631	0.000	99.140	0.034	99.215	0.008
1.06	99.281	0.005	99.631	0.000	99.201	0.048	99.264	0.028
1.07	99.330	0.006	99.631	0.000	99.271	0.052	99.351	0.021
1.08	99.387	0.053	99.631	0.000	99.347	0.040	99.423	0.011
1.09	99.399	0.012	99.631	0.000	99.377	0.009	99.477	0.043
1.1	99.399	0.000	99.631	0.000	99.379	0.002	99.558	0.049
1.11	99.399	0.000	99.631	0.000	99.382	0.003	99.644	0.009
1.12	99.399	0.000	99.631	0.000	99.414	0.032	99.665	0.003
1.13	99.399	0.000	99.633	0.000	99.478	0.035	99.665	0.016
1.14	99.404	0.000	99.655	0.000	99.503	0.038	99.675	0.033
1.15	99.463	0.000	99.700	0.000	99.505	0.038	99.708	0.033
1.16	99.552	0.009	99.716	0.009	99.505	0.032	99.730	0.022
1.17	99.578	0.026	99.717	0.001	99.505	0.022	99.732	0.002
1.18	99.579	0.025	99.717	0.001	99.505	0.021	99.734	0.002

1.19	99.588	0.009	99.717	0.003	99.512	0.009	99.752	0.008
1.2	99.627	0.000	99.717	0.000	99.547	0.011	99.790	0.000
1.21	99.659	0.000	99.717	0.000	99.617	0.001	99.805	0.000
1.22	99.663	0.000	99.717	0.000	99.696	0.003	99.805	0.000
1.23	99.663	0.000	99.717	0.000	99.756	0.023	99.805	0.000
1.24	99.663	0.000	99.717	0.000	99.769	0.013	99.805	0.004
1.25	99.663	0.000	99.717	0.000	99.769	0.000	99.805	0.016
1.26	99.663	0.000	99.717	0.000	99.772	0.003	99.805	0.001
1.27	99.663	0.000	99.717	0.000	99.797	0.025	99.805	0.000
1.28	99.663	0.000	99.717	0.000	99.833	0.018	99.805	0.000
1.29	99.663	0.000	99.717	0.000	99.844	0.011	99.856	0.000
1.3	99.663	0.000	99.717	0.000	99.861	0.018	99.867	0.000
1.31	99.663	0.000	99.717	0.000	99.861	0.028	99.908	0.000
1.32	99.663	0.000	99.717	0.000	99.861	0.011	100.000	0.000
1.33	99.663	0.000	99.717	0.000	99.861	0.001	100.000	0.000
1.34	99.663	0.000	99.717	0.000	99.861	0.000	100.000	0.000
1.35	99.663	0.000	99.717	0.000	99.868	0.000	100.000	0.000
1.36	99.663	0.000	99.717	0.000	99.900	0.000	100.000	0.000
1.37	99.663	0.000	99.717	0.000	99.909	0.000	100.000	0.000
1.38	99.663	0.000	99.717	0.000	99.909	0.000	100.000	0.000
1.39	99.663	0.000	99.717	0.000	99.909	0.000	100.000	0.000
1.4	99.664	0.001	99.717	0.000	99.909	0.000	100.000	0.000
1.41	99.676	0.012	99.717	0.000	99.909	0.000	100.000	0.000
1.42	99.755	0.079	99.717	0.000	99.909	0.000	100.000	0.000
1.43	99.884	0.038	99.717	0.000	99.912	0.000	100.000	0.000
1.44	100.000	0.003	99.717	0.000	99.940	0.000	100.000	0.000
1.45	100.000	0.000	99.717	0.000	100.000	0.000	100.000	0.000
1.46	100.000	0.000	99.717	0.000	100.000	0.000	100.000	0.000
1.47	100.000	0.000	99.717	0.000	100.000	0.000	100.000	0.000
1.48	100.000	0.000	99.717	0.000	100.000	0.000	100.000	0.000
1.49	100.000	0.000	99.717	0.000	100.000	0.000	100.000	0.000
1.5	100.000	0.000	99.717	0.000	100.000	0.000	100.000	0.000
1.51	100.000	0.000	99.717	0.000	100.000	0.000	100.000	0.000
1.52	100.000	0.000	99.728	0.000	100.000	0.000	100.000	0.000
1.53	100.000	0.000	99.740	0.000	100.000	0.000	100.000	0.000
1.54	100.000	0.000	99.740	0.000	100.000	0.000	100.000	0.000
1.55	100.000	0.000	99.854	0.000	100.000	0.000	100.000	0.000
1.56	100.000	0.000	100.000	0.000	100.000	0.000	100.000	0.000
1.57	100.000	0.000	100.000	0.000	100.000	0.000	100.000	0.000
1.58	100.000	0.000	100.000	0.000	100.000	0.000	100.000	0.000
1.59	100.000	0.000	100.000	0.000	100.000	0.000	100.000	0.000
1.6	100.000	0.000	100.000	0.000	100.000	0.000	100.000	0.000
1.61	100.000	0.000	100.000	0.000	100.000	0.000	100.000	0.000
1.62	100.000	0.000	100.000	0.000	100.000	0.000	100.000	0.000

	S8 - D.A.		S8 - D.A. OEDOM		S11 - D.A.		S11 - D.A. OEDOM		S11.1/2 - D.A. OEDOM.	
x [mm] at Q3 = 10.0 %	0.054		0.051		0.042		0.035		0.039	
x [mm] at Q3 = 30.0 %	0.107		0.103		0.082		0.074		0.079	
x [mm] at Q3 = 50.0 %	0.155		0.151		0.121		0.113		0.120	
x [mm] at Q3 = 60.0 %	0.183		0.178		0.144		0.135		0.144	
x [mm] at Q3 = 90.0 %	0.331		0.324		0.275		0.262		0.271	
Q3 [%] at x = 0.10 mm	31.384		33.150		44.494		48.711		45.240	
Q3 [%] at x = 0.50 mm	98.008		98.298		98.838		99.314		99.216	
Q3 [%] at x = 1.00 mm	99.686		99.937		99.855		100.000		100.000	
	S8 - D.A.		S8 - D.A. OEDOM		S11 - D.A.		S11 - D.A. OEDOM		S11.1/2 - D.A. OEDOM.	
Size class	Av. Q3 [%]	Av. p3 [%]	Av. Q3 [%]	Av. p3 [%]	Av. Q3 [%]	Av. p3 [%]	Av. Q3 [%]	Av. p3 [%]	Av. Q3 [%]	Av. p3 [%]
0.008	0.913	0.913	1.065	1.065	1.524	1.524	2.077	2.077	1.676	1.676
0.01	2.179	1.266	2.490	1.433	3.513	1.989	4.731	2.651	3.901	2.225
0.02	3.774	1.595	4.274	1.784	5.991	2.478	7.930	3.129	6.616	2.716
0.03	5.988	2.215	6.704	2.468	9.384	3.393	11.998	4.088	10.353	3.609
0.04	8.678	2.690	9.541	2.837	13.397	4.013	16.592	4.680	14.629	4.225
0.05	11.904	3.226	12.913	3.375	18.425	5.028	22.146	5.554	19.713	5.109
0.06	15.625	3.721	16.938	4.002	23.719	5.294	27.806	5.660	25.092	5.426
0.07	19.440	3.815	20.938	3.921	28.924	5.205	33.487	5.485	30.456	5.127
0.08	23.382	3.942	25.067	4.129	34.097	5.173	38.648	5.329	35.495	5.107
0.09	27.333	3.952	28.879	3.909	39.375	5.278	43.740	5.014	40.338	5.029
0.1	31.384	4.051	33.150	4.182	44.494	5.119	48.711	4.971	45.240	4.906
0.11	35.468	4.084	37.558	4.242	49.345	4.851	53.132	4.586	49.897	4.766
0.12	39.722	4.254	41.962	4.404	54.179	4.834	57.670	4.616	54.133	4.370
0.13	44.138	4.416	45.992	4.030	58.407	4.228	62.068	4.209	58.328	4.252
0.14	47.953	3.815	49.801	3.809	62.281	3.874	65.621	3.553	62.309	3.850
0.15	51.832	3.879	53.481	3.680	65.471	3.190	68.375	3.140	65.921	3.561
0.16	55.610	3.779	57.203	3.722	68.934	3.463	71.602	3.227	69.266	3.399
0.17	59.171	3.561	60.709	3.506	72.086	3.152	74.572	2.949	72.378	3.087
0.18	62.550	3.379	64.043	3.334	74.982	2.896	77.254	2.682	75.257	2.831
0.19	65.721	3.171	67.171	3.113	77.626	2.644	79.649	2.395	77.861	2.567
0.2	68.663	2.943	70.049	2.878	80.043	2.417	81.767	2.118	80.211	2.317
0.21	71.398	2.735	72.703	2.670	82.190	2.147	83.708	1.903	82.321	2.084
0.22	73.922	2.524	75.145	2.460	84.054	1.864	85.500	1.723	84.194	1.865
0.23	76.228	2.306	77.389	2.244	85.678	1.624	87.091	1.520	85.876	1.671
0.24	78.343	2.115	79.451	2.062	87.110	1.432	88.508	1.326	87.373	1.471
0.25	80.291	1.949	81.344	1.893	88.372	1.262	89.768	1.181	88.710	1.311
0.26	82.099	1.808	83.051	1.707	89.505	1.133	90.877	1.074	89.898	1.171
0.27	83.752	1.653	84.593	1.558	90.544	1.039	91.900	0.965	90.948	1.048
0.28	85.239	1.488	86.022	1.429	91.555	1.011	92.815	0.869	91.886	0.939
0.29	86.572	1.333	87.321	1.302	92.423	0.868	93.605	0.783	92.715	0.829
0.3	87.779	1.207	88.496	1.192	93.137	0.714	94.307	0.673	93.448	0.734
0.31	88.889	1.110	89.572	1.077	93.766	0.629	94.926	0.598	94.137	0.662
0.32	89.898	1.009	90.560	0.988	94.326	0.560	95.491	0.560	94.766	0.607

0.33	90.810	0.913	91.439	0.879	94.818	0.492	95.978	0.487	95.301	0.535
0.34	91.644	0.834	92.225	0.820	95.300	0.482	96.394	0.416	95.770	0.469
0.35	92.385	0.741	92.964	0.764	95.706	0.406	96.771	0.389	96.193	0.423
0.36	93.063	0.679	93.633	0.682	96.087	0.381	97.114	0.353	96.573	0.378
0.37	93.684	0.621	94.204	0.584	96.455	0.368	97.440	0.326	96.924	0.341
0.38	94.246	0.562	94.731	0.527	96.781	0.326	97.701	0.288	97.249	0.312
0.39	94.752	0.506	95.242	0.501	97.066	0.285	97.903	0.233	97.529	0.264
0.4	95.202	0.450	95.692	0.423	97.291	0.225	98.083	0.215	97.770	0.238
0.41	95.617	0.416	96.098	0.398	97.511	0.220	98.259	0.186	97.983	0.222
0.42	96.001	0.384	96.468	0.379	97.727	0.216	98.441	0.177	98.162	0.189
0.43	96.345	0.345	96.784	0.336	97.933	0.206	98.606	0.145	98.349	0.182
0.44	96.649	0.304	97.062	0.287	98.117	0.184	98.731	0.125	98.527	0.168
0.45	96.924	0.275	97.289	0.256	98.259	0.142	98.844	0.113	98.680	0.144
0.46	97.190	0.266	97.517	0.236	98.395	0.136	98.949	0.116	98.814	0.135
0.47	97.429	0.239	97.739	0.222	98.521	0.126	99.058	0.114	98.928	0.112
0.48	97.645	0.216	97.933	0.194	98.638	0.117	99.157	0.100	99.033	0.094
0.49	97.844	0.199	98.121	0.188	98.743	0.105	99.240	0.083	99.128	0.095
0.5	98.008	0.164	98.298	0.177	98.838	0.095	99.314	0.074	99.216	0.082
0.51	98.144	0.137	98.444	0.146	98.921	0.083	99.374	0.060	99.288	0.072
0.52	98.266	0.122	98.577	0.133	99.014	0.093	99.428	0.054	99.347	0.065
0.53	98.372	0.106	98.721	0.133	99.084	0.070	99.488	0.067	99.401	0.060
0.54	98.473	0.101	98.834	0.113	99.144	0.060	99.533	0.045	99.450	0.054
0.55	98.565	0.092	98.913	0.091	99.202	0.058	99.578	0.047	99.509	0.060
0.56	98.648	0.083	98.993	0.103	99.255	0.053	99.632	0.039	99.554	0.053
0.57	98.720	0.073	99.076	0.087	99.299	0.044	99.675	0.023	99.591	0.046
0.58	98.791	0.071	99.145	0.073	99.334	0.035	99.697	0.022	99.631	0.047
0.59	98.847	0.056	99.197	0.052	99.361	0.027	99.706	0.028	99.670	0.041
0.6	98.889	0.042	99.246	0.049	99.394	0.033	99.720	0.020	99.708	0.035
0.61	98.938	0.050	99.292	0.046	99.433	0.039	99.750	0.019	99.749	0.036
0.62	98.992	0.054	99.347	0.055	99.459	0.026	99.786	0.028	99.782	0.032
0.63	99.041	0.050	99.396	0.053	99.484	0.025	99.805	0.023	99.806	0.021
0.64	99.093	0.052	99.445	0.038	99.514	0.030	99.811	0.013	99.834	0.021
0.65	99.133	0.040	99.484	0.033	99.541	0.027	99.819	0.008	99.856	0.015
0.66	99.161	0.028	99.505	0.022	99.556	0.015	99.830	0.016	99.867	0.014
0.67	99.190	0.029	99.520	0.027	99.572	0.016	99.834	0.004	99.872	0.011
0.68	99.223	0.034	99.542	0.029	99.588	0.016	99.834	0.000	99.876	0.008
0.69	99.265	0.042	99.566	0.020	99.599	0.011	99.847	0.000	99.881	0.007
0.7	99.299	0.034	99.592	0.026	99.610	0.011	99.855	0.007	99.894	0.005
0.71	99.321	0.022	99.617	0.025	99.628	0.018	99.862	0.006	99.904	0.008
0.72	99.353	0.033	99.639	0.021	99.648	0.020	99.881	0.011	99.911	0.010
0.73	99.387	0.034	99.661	0.020	99.667	0.019	99.892	0.006	99.918	0.006
0.74	99.410	0.024	99.701	0.029	99.676	0.009	99.899	0.007	99.926	0.003
0.75	99.433	0.023	99.728	0.027	99.678	0.002	99.915	0.006	99.932	0.004
0.76	99.458	0.026	99.734	0.022	99.684	0.006	99.933	0.003	99.936	0.002

0.77	99.472	0.014	99.734	0.011	99.691	0.007	99.938	0.005	99.936	0.000
0.78	99.483	0.011	99.747	0.002	99.704	0.013	99.938	0.000	99.936	0.000
0.79	99.511	0.028	99.766	0.014	99.724	0.020	99.938	0.000	99.936	0.000
0.8	99.547	0.036	99.788	0.022	99.744	0.020	99.941	0.003	99.936	0.000
0.81	99.564	0.018	99.817	0.012	99.757	0.013	99.953	0.006	99.936	0.000
0.82	99.569	0.005	99.844	0.018	99.762	0.005	99.964	0.004	99.936	0.000
0.83	99.578	0.009	99.859	0.023	99.768	0.006	99.965	0.001	99.936	0.000
0.84	99.586	0.008	99.887	0.006	99.770	0.002	99.965	0.000	99.936	0.000
0.85	99.589	0.004	99.893	0.000	99.770	0.000	99.965	0.000	99.936	0.000
0.86	99.595	0.006	99.902	0.000	99.770	0.000	99.965	0.000	99.936	0.000
0.87	99.603	0.009	99.917	0.000	99.770	0.000	99.969	0.000	99.936	0.001
0.88	99.615	0.012	99.932	0.000	99.770	0.000	99.992	0.000	99.936	0.000
0.89	99.632	0.018	99.936	0.000	99.770	0.000	100.000	0.000	99.941	0.001
0.9	99.647	0.015	99.937	0.000	99.770	0.000	100.000	0.000	99.945	0.001
0.91	99.662	0.015	99.937	0.000	99.772	0.002	100.000	0.000	99.960	0.001
0.92	99.671	0.009	99.937	0.002	99.781	0.009	100.000	0.000	99.967	0.003
0.93	99.676	0.005	99.937	0.016	99.809	0.028	100.000	0.000	99.971	0.001
0.94	99.684	0.008	99.937	0.018	99.823	0.014	100.000	0.000	99.983	0.000
0.95	99.686	0.003	99.937	0.000	99.833	0.010	100.000	0.000	99.983	0.000
0.96	99.686	0.000	99.937	0.000	99.836	0.003	100.000	0.000	99.983	0.000
0.97	99.686	0.000	99.937	0.000	99.836	0.000	100.000	0.000	99.983	0.000
0.98	99.686	0.000	99.937	0.000	99.836	0.000	100.000	0.000	99.986	0.000
0.99	99.686	0.000	99.937	0.000	99.843	0.007	100.000	0.000	100.000	0.000
1	99.686	0.000	99.937	0.000	99.855	0.012	100.000	0.000	100.000	0.000
1.01	99.686	0.000	99.937	0.000	99.859	0.004	100.000	0.000	100.000	0.000
1.02	99.690	0.004	99.937	0.000	99.859	0.000	100.000	0.000	100.000	0.000
1.03	99.707	0.017	99.951	0.000	99.859	0.000	100.000	0.000	100.000	0.000
1.04	99.723	0.016	99.953	0.000	99.859	0.000	100.000	0.000	100.000	0.000
1.05	99.726	0.004	99.953	0.000	99.859	0.000	100.000	0.000	100.000	0.000
1.06	99.739	0.013	99.953	0.000	99.859	0.000	100.000	0.000	100.000	0.000
1.07	99.773	0.034	99.953	0.000	99.859	0.000	100.000	0.000	100.000	0.000
1.08	99.783	0.010	99.953	0.000	99.859	0.000	100.000	0.000	100.000	0.000
1.09	99.784	0.001	99.954	0.000	99.859	0.000	100.000	0.000	100.000	0.000
1.1	99.785	0.001	99.961	0.000	99.860	0.001	100.000	0.000	100.000	0.000
1.11	99.790	0.005	100.000	0.000	99.869	0.009	100.000	0.000	100.000	0.000
1.12	99.802	0.013	100.000	0.000	99.888	0.019	100.000	0.000	100.000	0.000
1.13	99.808	0.006	100.000	0.000	99.896	0.008	100.000	0.000	100.000	0.000
1.14	99.809	0.001	100.000	0.000	99.896	0.000	100.000	0.000	100.000	0.000
1.15	99.809	0.000	100.000	0.000	99.896	0.000	100.000	0.000	100.000	0.000
1.16	99.809	0.000	100.000	0.000	99.896	0.000	100.000	0.000	100.000	0.000
1.17	99.809	0.000	100.000	0.000	99.896	0.000	100.000	0.000	100.000	0.000
1.18	99.814	0.006	100.000	0.000	99.896	0.000	100.000	0.000	100.000	0.000
1.19	99.833	0.019	100.000	0.000	99.896	0.000	100.000	0.000	100.000	0.000
1.2	99.845	0.012	100.000	0.000	99.896	0.000	100.000	0.000	100.000	0.000

[illegible]

[illegible]